AD-A156 888 ACOUSTIC CAVITATION AND BUBBLE DYNAMICS(U) MISSISSIPPI 1/2
UNIV UNIVERSITY PHYSICAL ACOUSTICS RESEARCH LAB
A A ATCHLEY ET AL. 15 JUN 85 TR-2-85 N00014-84-C-0193
UNCLASSIFIED F/G 20/1 NL

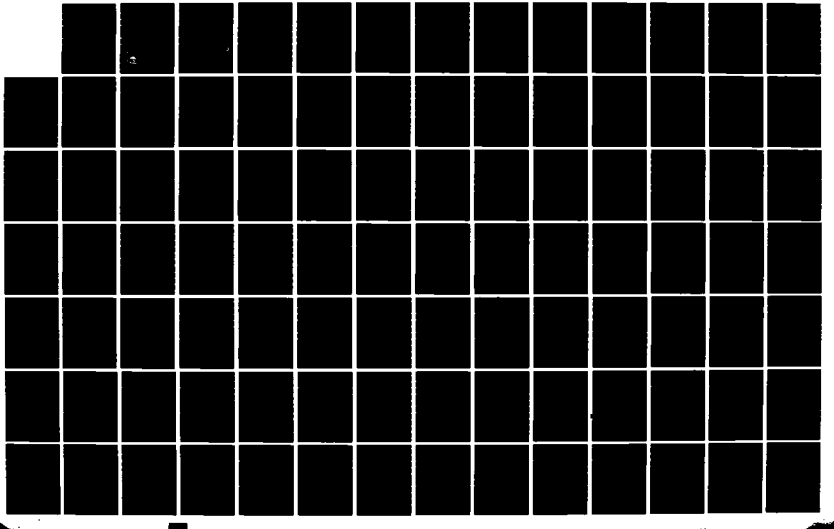

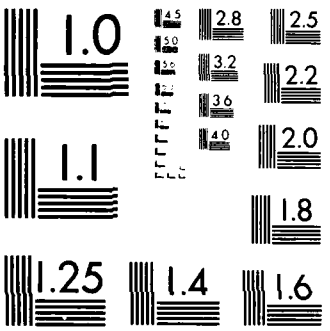

(2)

ACOUSTIC CAVITATION

AND

BUBBLE DYNAMICS

THE UNIVERSITY OF MISSISSIPPI
PHYSICAL ACOUSTICS RESEARCH GROUP
DEPARTMENT OF PHYSICS AND ASTRONOMY

Approved for Public Release

Technical Report
Office of Naval Research
Contract N00014-84-C-0041

ACOUSTIC CAVITATION

AND

BUBBLE DYNAMICS

by

Anthony A. Atchley and Lawrence A. Crum
Physical Acoustics Research Laboratory
Department of Physics and Astronomy
The University of Mississippi
University, MS 38677

June 15, 1985

Unclassified

SECURITY CLASSIFICATION OF THIS PAGE *(When Data Entered)*

REPORT DOCUMENTATION PAGE		READ INSTRUCTIONS BEFORE COMPLETING FORM
1. REPORT NUMBER 2-85	2. GOVT ACCESSION NO. AD-A156888	3. RECIPIENT'S CATALOG NUMBER
4. TITLE *(and Subtitle)* Acoustic Cavitation and Bubble Dynamics		5. TYPE OF REPORT & PERIOD COVERED Technical
		6. PERFORMING ORG. REPORT NUMBER
7. AUTHOR(s) A.A. Atchley and L.A. Crum		8. CONTRACT OR GRANT NUMBER(s) N00014-84-C-0193
9. PERFORMING ORGANIZATION NAME AND ADDRESS Physical Acoustic Research Laboratory Department of Physics University of MS., University, MS 38677		10. PROGRAM ELEMENT, PROJECT, TASK AREA & WORK UNIT NUMBERS
11. CONTROLLING OFFICE NAME AND ADDRESS		12. REPORT DATE June 15, 1985
		13. NUMBER OF PAGES 119
14. MONITORING AGENCY NAME & ADDRESS*(if different from Controlling Office)*		15. SECURITY CLASS. *(of this report)* Unclassified
		15a. DECLASSIFICATION/DOWNGRADING SCHEDULE

16. DISTRIBUTION STATEMENT *(of this Report)*

Approved for Public Release: Distribution Unlimited

17. DISTRIBUTION STATEMENT *(of the abstract entered in Block 20, if different from Report)*

18. SUPPLEMENTARY NOTES

19. KEY WORDS *(Continue on reverse side if necessary and identify by block number)*

Cavitation
Nucleation
Bubbles
Bubble Dynamics
Nonlinear Oscillation

20. ABSTRACT *(Continue on reverse side if necessary and identify by block number)*

This report is a preprint of a chapter to be published in Ultrasound: Chemical, Physical and Biological Effects by Verlag Chemie International, Inc.

DD FORM 1 JAN 73 1473 EDITION OF 1 NOV 65 IS OBSOLETE
S/N 0102-LF-014-6601

Unclassified

SECURITY CLASSIFICATION OF THIS PAGE *(When Data Entered)*

ULTRASOUND: CHEMICAL, PHYSICAL, AND BIOLOGICAL EFFECTS

CHAPTER 1

ACOUSTIC CAVITATION AND BUBBLE DYNAMICS

by

Anthony A. Atchley

and

Lawrence A. Crum

Physical Acoustic Research Group
Department of Physics and Astronomy
University of Mississippi
University, MS 38677

TABLE OF CONTENTS

I. INTRODUCTION

a. Statement of Purpose..... 1

b. Historical Perspective..... 4

II. NUCLEATION AND TRANSIENT CAVITATION INCEPTION

a. Introduction..... 12

b. Homogeneous Nucleation..... 13

c. Heterogeneous Nucleation..... 14

d. Organic Skins..... 17

e. Hydrophobic Ions..... 19

f. Crevices in Solids..... 21

g. Concept of Threshold..... 27

h. Comparison with Theory..... 29

III. EXPERIMENTAL TECHNIQUES FOR INVESTIGATING TRANSIENT CAVITATION

a. Introduction..... 35

b. Know Thy Sound Field..... 36

c. Know Thy Liquid..... 41

d. Know when Something Happens..... 42

e. A Specific Experimental Apparatus..... 45

IV. RECTIFIED DIFFUSION

a. Introduction..... 54

b. The Governing Equations..... 57

c. Experimental Technique..... 63

d. Some Experimental Results..... 65

V. BUBBLE DYNAMICS

a. Introduction..... 67

b. Stable Cavitation..... 67

c. Transient Cavitation..... 72

VI. CONCLUDING REMARKS

a. Cavitation in Biological Tissue..... 74

b. Nonlinear Bubble Dynamics..... 75

c. Cavitation Fields..... 75

VII. LIST OF REFERENCES..... 77

VIII. FIGURE CAPTIONS AND FIGURES..... 81

I. INTRODUCTION

Statement of Purpose and Definition of Terms

Cavitation refers to the formation and the subsequent dynamical life of bubbles in liquids. These bubbles can be either gas-filled or vapor-filled and form in a wide variety of liquids under a wide range of conditions. Cavitation occurs in water, organic solvents, biological fluids, liquid helium, and molten metals as well as many other fluids. It may be hydrodynamic, thermal, or acoustic in origin. The emphasis of this chapter is on acoustic cavitation. One section in particular, however, the one dealing with nucleation, may be applied to cavitation of different origins. It is traditional when describing cavitation to classify it as one of two types - transient or stable. Transient cavitation involves large-scale variations in the bubble's size (relative to its equilibrium size) over a time scale of a few acoustic cycles and this rapid growth usually terminates in a collapse of varying degrees of violence. Stable cavitation, on the other hand, usually involves small (compared to the bubble radius) amplitude oscillations about an equilibrium radius. Stable cavitation in most instances results in little appreciable bubble growth over a time scale of thousands of acoustic cycles. This classification of cavitation is not strict, however. Stable cavitation can lead to transient cavitation and the collapse of a transient cavity can produce smaller bubbles which undergo stable cavitation.

The topic of this chapter, acoustic cavitation, is but one of several possible mechanisms through which ultrasound can interact with a liquid medium. Some of the other mechanisms are the topics of other chapters of this book. Acoustic cavitation can affect a liquid through two possible avenues. The first is the bubble itself. The liquid is disrupted by the

inhomogeneous presence of the bubble. The second avenue through which bubbles affect a fluid is through bubble dynamics. The bubble's interior and the liquid immediately surrounding the bubble are regions which undergo continual change. The bubble-liquid interface continually changes shape and size; liquid molecules diffuse into and out of the bubble; the concentration of gas in the surrounding liquid varies; acoustic streaming occurs in the liquid in the vicinity of the bubble often resulting in severe shear stresses; the interior pressure and temperature fluctuate rapidly; the bubble radiates acoustic energy as it oscillates; thermal and viscous damping hinder the bubble oscillations. Each of these processes manifests itself differently, yet, they all lead to changes in the properties of the liquid, although some of the changes are relatively small. Therefore when one studies the chemical, physical, and biological effects of ultrasound it is wholly appropriate to begin with a general analysis of acoustic cavitation.

The goal of this chapter is to introduce the reader to the broad field of acoustic cavitation. Although considerable information is contained in this chapter, it is by no means complete in either breadth or depth. We refer the reader to numerous books, reviews, and articles for more in depth discussions.

We begin the chapter with a brief historical review of the field of cavitation. The field has a long and colorful history and it has figured prominently in such diverse areas as ship design and elementary particle physics.

The consideration of the physical aspects of cavitation begins with a discussion of the origin of all cavitation processes - the nucleation phase. In terms of liquid properties, cavitation is classified as

resulting either from homogeneous or heterogeneous nucleation. Homogeneous nucleation refers to the formation of a bubble in a liquid free of any inhomogeneities such as solid particulates or organic micelles. Heterogeneous nucleation refers to the growth of a pre-existing gas pocket or microbubble into a macroscopically observable bubble. Models for both kinds of nucleation are discussed and the predictions of these models are compared to experimental results. We also introduce the concept of a cavitation threshold or the minimum pressure amplitude necessary for the onset of either transient or stable cavitation.

Following this discussion, we digress somewhat to consider experimental techniques commonly used in transient cavitation research. This section begins with a brief overview of the basic components of any adequate experimental apparatus. The discussion is intended to inform the researcher of the various aspects of experimental work to which consideration should be given rather than serve as a "complete guide" to experimental techniques (which it certainly is not). The section ends with a description of a versatile experimental apparatus which we have developed in our laboratory.

In the next section, the concept of rectified diffusion is discussed. If a bubble is caused to pulsate by an acoustic field, gas will flow in and out of the bubble during each cycle. There exists a threshold for which more gas flows in than out over an acoustic cycle and the bubble is caused to grow as a result of the sound field. This concept is called "rectified diffusion" and the words are an adequate description of the phenomenon. It is an important concept because it is the commonly observed phenomenon associated with intense sound fields in liquids. Rectified diffusion is a slow process, however, requiring thousands of cycles and if the sound field is sufficiently intense, will play a minor, secondary role to the rapid

growth and collapse of a cavity during a single cycle - termed transient cavitation. However, because of rectified diffusion, bubbles are dynamic systems, changing in size and thus having a variety of comple nonlinear responses to the action of the sound field.

Concluding the chapter, we discuss bubble dynamics. We cover the equations governing stable bubble oscillations and show how they lead to nonlinear effects, noise generation, and chaos. We also discuss the dynamics of a transient cavity, placing emphasis on the collapse phase. Of particular importance to the discussion of transient cavitation are the temperatures and pressures developed within the cavity during collapse. The final part of this chapter is devoted to posing questions about the important topics in cavitation research at the present. The questions not only summarise the material presented in the chapter but also serve to bring the reader up to date with current research activities.

Historical Perspective

Perhaps the first type of cavitation observed was the formation of bubbles in liquids supersaturated with gas. This is familiar to all of those who have ever opened or poured a carbonated beverage. Tomlinson[1] discussed a series of twelve experiments performed with soda-water and various solids. He contended that if the solids were "chemically clean", no bubbles would form on them. He went on to point out that if a solid, initially chemically clean, came into contact with a dirty cloth, unclean air, or dust particles, copious bubbles formed on it when immersed in the soda-water. Tomlinson concluded that chemically clean solids are perfectly wetted, whereas dirty solids are not. From this observation he argued that if a solid were dirty it would have a stronger adhesion force for the gas

than for the liquid and that it was this asymmetry that caused bubble formation. Although this line of reasoning is incorrect, the results of his extensive experimentation with effervescence support the explanation offered by his contemporary M. Gernez.[2] Gernez proposed that the outgassing of supersaturated gaseous solutions was caused by gas pockets, embedded in the fissures found on the surface of every solid, regardless of its degree of finish. (It is therefore Gernez who is the initial proponent of the crevice model of the cavitation nucleus - a model to be discussed extensively here.) Effervescence is a form of cavitation which requires gaseous diffusion to "pump up" gas-containing nuclei until they grow large enough to rise to the surface of the liquid. At about the same time that Tomlinson and Gernez were doing their work, another genre of cavitation was being investigated.

This other kind of cavitation has its origin with the conception and development of hydrodynamics. Not until Daniel Bernoulli[3] set down the guidelines for this new branch of science in 1738 was it understood that a negative pressure could be produced in a liquid. In the following years Euler and d'Alembert debated over the consequences of negative pressures.[4] Euler believed that the application of a negative pressure could result in a rupture of the liquid while d'Alembert refused to accept this view.

The rise of cavitation as a topic for scientific research began with the development of high-powered, high rpm steam turbines in the mid 1800's. With this advance came the means of moving an object (such as a propeller) through a fluid rapidly enough so that the object lost contact with the fluid. The most obvious concern to which this new phenomenon drew attention was that the state-of-the-art propeller design was poor. A second, and as was soon evident, much greater concern was propeller

erosion. In fact, this problem was so critical that in 1915 the British Admiralty appointed a special subcommittee to investigate this phenomenon. In 1917, Lord Rayleigh[5] became involved. His typically straightforward and ingenious solution of the equations governing vapor cavity dynamics is still quite useful today.

Concurrent to this work the first attempts to measure the tensile strengths of liquids were being undertaken. In about 1850, Berthelot began to measure the tensile strength of water and found it to be on the order of 50 bars (maximum)[6]. (Note, in this chapter we shall use the traditional unit of pressure, the bar, which is approximately one atmosphere. In SI units, 1.0 bar = 0.1 MPa. Further, since it has been traditional to use cgs units for the other quantities as well, we shall continue that tradition in this chapter.) His method consisted of heating a liquid, which was sealed in an evacuated glass capillary tube, until the expanding liquid completely filled the tube. The temperature at which the tube was filled was recorded and the liquid was then allowed to cool. Because the liquid adhered to the sides of the tube, this subsequent contraction resulted in the liquid undergoing a tensile stress, eventually ending in the rupture of the liquid. The temperature at which rupture occurred was also recorded. From a knowledge of the filling and rupturing temperatures, along with the thermal expansion coefficient for the liquid being tested, Berthelot was able to calculate a tensile strength. Many other measurements of the tensile strength of water through these static means have been made over the intervening one hundred and thirty-odd years, and their results (ranging from as low as about 5 to as high as about 200 bars) are comparable to Berthelot's. A detailed discussion of these works will not be given here. The point is that for the first time investigators were intentionally putting liquids under stress and considering the

F^- are hydrophobic and will migrate to the surface of an air bubble in water. Other ions such as OH^- are hydrophilic and will not migrate to the surface. Accordingly, one would expect that there would be a dependence of the cavitation threshold on the concentration of such salts as NaCl or NaF, but not of NaOH. Akulichev was able to make measurements of the cavitation threshold of water as a function of the concentration of a number of dissolved salts. His measurements indicate that if the dissolved gas concentration is reduced to below about 40% of saturation, the acoustic cavitation threshold of water is measurably reduced upon addition of the hydrophobic salts NaCl and NaF, but not affected at all by the addition of the hydrophilic salt NaOH.

Atchley[31] has repeated the measurements of Akulichev and also has extended the range of the dissolved ion concentration by two orders of magnitude. In his experiment, he first removed most of the dissolved chemical species that are typically present in distilled water with a series of filters that reduced the dissolved organic content to parts per million and increased the resistivity (reduced the number of dissolved ions) to 1 megaohm. Thus, he was able to measure the cavitation threshold as a function of dissolved ion concentration over four orders of magnitude. Shown in Fig. 1-4 are his measurements for one particular salt, KI; also shown on the figure are the measurements of Akulichev (the dashed line). A true comparison between Atchley's and Akulichev's measurements can not be made in that the dissolved gas concentration ratio used by Akulichev was 0.13 while that of Atchley was 0.30. With this caveat, however, it is seen that the two measurements are consistent.

Fig. 1-4

Atchley's data, however, shows an additional feature: if the water is initially cleansed of most of the dissolved ions, the cavitation threshold

molecules from the skin (or reservoir), resulting in large-scale changes in the radius of the nucleus. Having adjusted the radius in this manner, subsequent "small-scale" changes in radius can occur. These changes involve only the adjustment of the separation of adjacent skin molecules, not a change in the number of molecules.

This model has been applied primarily to compression/decompression studies and in that view is assumed to work as follows: For modest values of overpressure, the skin remains permeable to gas diffusion, though one would suspect that diffusion would be retarded. Thus, the gas within the bubble remains in equilibrium with that in the fluid. As some critical pressure, the skin molecules become so tightly packed that the skin becomes essentially impermeable to diffusion; now no gas can escape the bubble, and it survives compression. When decompression occurs, the bubble can now expand because the surfactant molecules can withstand mechanical compression but not tension.

Yount's so called "varying-permeability" model has been used to explain bubble formation in gelatin exposed to a compression/decompression sequence. It has not yet been applied to acoustic cavitation, although Yount[28] calculates the characteristic times required for surfactant molecules to react to changes in applied pressure and bubble radius and concludes that the molecules could play a role in acoustic cavitation.

Hydrophobic Ions

It has been known for some time that air bubbles in water possess some excess electric charge,[42,43] and thus it seems reasonable to assume that the repulsive nature of like electrical charges on the surface of an air bubble could stabilize it from dissolution. Akulichev[20] has examined this model in some detail and has hypothesized that certain ions such as Cl^- and

sure. Herzfeld[41] subsequently abandoned the hypothesis, but it has been taken up anew by others.

In a modified version of the organic skin hypothesis, Sirotyuk[27] examined the possible stabilization of "microbubbles" by a film of surface-active substances. Detergents and soaps tend to be composed of an oxygen-rich group on one end and a long hydrocarbon tail on the other (see Fig. 1-3a). For a gas bubble in water, the polar end will bond weakly to the water surface and the tail will extend into the gas. This "picket-fence" configuration has an inherent elasticity that may stabilize the microbubble. Sirotyuk has measured the acoustic cavitation threshold of water in a device designed to maintain a high degree of purity, and contends that his experimental measurements support his claim that cavitation nuclei are microbubbles stabilized by surface-active agents. The experimental evidence is extremely weak, however, and subject to different interpretations.

Fig. 1-3a and Fig. 1-3b

A further modification of the organic skin hypothesis has been given by Yount, et al[26,28] In this model, a cavitation nucleus is formed in the following manner: A gas bubble is introduced (the actual mechanism is immaterial) into a liquid and begins to dissolve. While the dissolution takes place, surface-active molecules accumulate on the gas/liquid interface. Eventually, the density of these molecules is sufficient to prevent the collapse of the bubble, presumably through a Coulomb interaction of some sort. Once the critical density is reached, the radius of the nucleus may make "large-scale" changes. The equilibrium condition for this nucleus is that the electrochemical potentials of the skin and the reservoir must be equal. The reservoir is a thin, perhaps monomolecular, layer of non-aligned surfactant molecules which surrounds the skin of aligned molecules. This equilibrium condition can be satisfied by the accretion or deletion of

Fig. 1-2

Figure 1-2 shows a stability curve for gas bubbles at various dissolved gas concentrations. This figure shows that bubbles of very small size (< 5μm) can be made to grow to visible size with only modest dissolved gas concentration ratios. (That's why bubbles appear out of nowhere in a champagne glass.) Note also that very small nuclei or very low supersaturations will not result in bubble growth. (That's why bubbles appear to originate from the same spot, and then stop as the liquid goes flat.)

The important points to be made from the above discussion are (a) that ordinary liquids contain pockets of gas called nuclei that can easily be activated, and (b) that these gas pockets are not free gas bubbles, but must have some mechanism to stabilize the gas pocket from dissolution. We next consider a few of the proposed stabilization mechanisms in cavitation nuclei.

Organic Skins

Since organic molecules are abundant in our environment, and since many of these compounds are surface-active, a number of investigators have proposed that these compounds form "skins" on the surfaces of gas bubbles preventing them from dissolving.

The original suggestion that these organic molecules could stabilize cavitation nuclei was made by Fox and Herzfeld,[15] although it was suggested much earlier[39,40] that these skins influenced the hydrodynamics of gas bubbles rising in a fluid. In the model proposed by Fox and Herzfeld, the skin was rigid and stabilized the gas bubble by preventing gas diffusion. According to this model the cavitation threshold as a function of static pressure should show a discontinuity at the "skin crushing pressure". However, when Strasberg[16] made such measurements, no discontinuity was observed, but rather a gradual rise in threshold with applied static pres-

$$\frac{dR_o}{dt} = \frac{Dd}{R_o}\left[\frac{C_i/C_o - 1}{1 + 4\sigma/3R_o P_\infty}\right]\left(1 + R_o/(\pi Dt)^{\frac{1}{2}}\right) \qquad (1\text{-}2)$$

where D is the diffusion constant, C_i/C_o is the ratio of the dissolved gas concentration to the saturation concentration, P_∞ is the ambient pressure in the liquid far from the bubble, and $d = R_g T C_o/P_\infty$ where R_g is the universal gas constant.

As an example, consider the following table which describes the approximate lifetimes of air bubbles of various sizes present in water.

Table 1-1

Radius (μm)	Dissolution Time (s)
1000	6×10^{6}
100	6×10^{2}
10	6
1	1×10^{-2}

Dissolution times for an air bubble present in water with a surface tension of 70 dyn/cm, a temperature of 20° C and a dissolved gas concentration equal to saturation.

Thus, a liquid containing free gas bubbles that is not supersaturated will rid itself of these bubbles as the small ones dissolve and the large ones rise to the surface. If the liquid is supersaturated (the obvious example is that of a carbonated beverage), bubbles can grow from small stabilized gas pockets on the walls of the vessel to visible size in a short time. There is a threshold size, however, and nuclei below that size will not grow - and they will even dissolve if there is no stabilization mechanism.

tudes - by raising the temperature of the host liquid to near or above the superheat limit of the sample droplet. By "trading" some temperature rise for pressure amplitude, he was able to reach the homogeneous nucleation threshold.

Fig. 1-1

Shown in Fig. 1-1 are Apfel's results for ether immersed in glycerine. The symbols are experimental points indicating homogeneous nucleation has occurred within the liquid and has triggered a droplet explosion; the theoretical curve is Eq. (1-1) with ln C(T) = 53. The excellent agreement between the predicted and measured values indicate that homogeneous nucleation in liquids can occur and can be described rather well analytically.

Heterogeneous Nucleation

Since the cavitation thresholds measured for most liquids is significantly less than the homogeneous nucleation threshold, it is reasonable to assume that most liquids contain foreign substances that stabilize pockets of gas and thus weaken the liquid to stress failure. For the purpose of communication, we shall label these weak spots "nuclei" and assume that they are associated with an inhomogeneity of some sort.

The obvious and simplest model for a nucleus is that of a free bubble. However, due to the "Laplace pressure", an internal pressure due to surface tension and given by $2\sigma/R$ where R is the bubble radius, these bubbles will gradually dissolve as gas is forced out of the interior of the bubble into the liquid.

Epstein and Plesset[38] have theoretically examined the behavior of air bubbles present in liquids and it is of interest to look at some numbers. The differential equation describing the change in equilibrium radius R_o with time is given by

isothermal work to form a vapor cavity of arbitrary size, and then by calculating that value of the size that makes the work an extremum. A vapor cavity of such size, called a "critical" cavity, is in a state of unstable equilibrium and with a slight increase in temperature or decrease in pressure, will grow without bound (at least to observable size).

The right hand side of Eq.(1-1) contains the complex kinetics of the nucleation process through the expression C(T). In order to express this expression precisely, it is necessary to know the evaporation, condensation and accommodation coefficients, and considerable other information about the liquid state. Fortunately, approximate expressions for ln C(T) can be found that differ only by about 25% in a wide variety of liquids; thus, a reasonably good estimate for ln C(T) is 60.[33]

In order to perform measurements of homogeneous nucleation in a liquid, one must ensure that the liquid does not contain any foreign substances that may act as preferential nucleation sites. Early attempts at such measurements failed to sufficiently clean the liquid to remove such substances. Berthelot[4] was able to estimate the tensile strength of water to be in the range of 30 - 50 bars. Briggs[9] and Greenspan and Tschiegg[21] were able to raise that estimate to over 200 bars by systematic attempts to clean the liquid of all "motes" or solid particles. These values are still significantly less than the theoretical value in water of over 1000 bars, however.

Apfel[33] was able to design an experiment that produced a mote-free liquid by injecting small-volume droplets of one liquid into a second host liquid. Because the samples were so small ($<10^{-3}$ cm^3), the chance that a droplet could be produced containing no motes was quite large. Apfel was able to remove a second major obstacle in homogeneous nucleation experiments - the problem of producing extremely large acoustic pressure ampli-

by homogeneous nucleation theory.

We shall briefly discuss nucleation in a homogeneous liquid, and then consider in some detail the various models associated with cavitation inception from something foreign to the pure liquid, or heterogeneous nucleation.

Homogeneous Nucleation

In the bulk of a pure liquid at a given pressure and temperature, density fluctuations cause the rapid formation and destruction of microscopic vapor cavities. The probability that one of these fluctuations can be made to grow to an observable size in a reasonable period of time can be calculated. The pioneering work in this area was performed by Döring[34,35]; subsequent work by Volmer,[36] Fisher[37] and Apfel[33] have redefined Doring's work and permitted us to specify the requirements for homogeneous nucleation with some confidence.

The general form of the transcendental expression that describes the pressure - temperature requirements for the onset of cavitation (here the irreversible growth of a vapor cavity) is given by Apfel[34] as

$$\frac{16\pi\sigma^3(T)/3[P(T) - P_L]^2}{kT} = \ln C(T) \qquad (1\text{-}1)$$

In this expression, T is the absolute temperature, k is Boltzmann's constant, $\sigma(T)$ is the liquid-vapor surface tension, and $[P(T) - P_L]$ is the pressure differential across the cavity interface, P(T) being the pressure of the vapor on the interface and P_L the pressure in the liquid. The function C(T) is discussed below.

The left hand side of Eq. (1-1) represents the energy barrier to nucleation, W_m, divided by kT. W_m is found by calculating the reversible

II. NUCLEATION AND TRANSIENT CAVITATION INCEPTION

Introduction

In one sense, the generation of acoustic cavitation can be described as a measure of the "dynamic tensile strength" of a liquid. The "failure" of the liquid under stress is detected by the presence of a gas (or vapor) phase within the bulk of the fluid. The theoretical tensile strength of both liquids and solids is several orders of magnitude larger than the measured values, unless special circumstances occur. The discrepancy between the experimental and theoretical values is likely due to inhomogeneities in the bulk of the material. These imperfections enable weaker molecular bounding to occur than would be present in a homogeneous material.

In a solid, the inhomogeneities take on the form of dislocations, grain boundaries, etc, and act as initial sites in crystalline plane slippage. If the imperfections are removed, as in the case of metallic whiskers which are essentially single crystals, extremely large tensile strengths can be achieved. (In some cases, of course, imperfections in a solid actually increase the tensile strength.)

In a liquid, pockets of gas serve as the weak points that prevent a liquid from sustaining large tensile strengths. The presence of these sites greatly reduce the tensile strength of the liquid; for example, in water, the theoretical strength is nearly 1000 bars,[6] the measured value, without protracted cleaning, is on the order of one bar.

A novel experiment was performed by Apfel[33] to demonstrate that liquids fail under tensile stress due to the presence of imperfections in the bulk of the liquid. Using extremely small volume samples (by acoustically levitating a small droplet of one fluid within the bulk of a second), he was able to obtain tensile strengths with magnitudes near those predicted

developments in the theory of bubble dynamics. This omission is made for two reasons. Attention will be given to this development in the theoretical portions of this chapter because it is fitting to associate the names of the founders of this field with their theoretical advances. Secondly, the material covered in this review, in general, will not be mentioned elsewhere. The exception to this point is the material dealing with nucleation. The development of nucleation theory is included in the review because it has been a subject of research since the birth of the field of cavitation and is of fundamental concern in the field today.

between two pure liquids. Apfel's crevice model was modified further by Crum[24] who considered the variation of contact angles with surface tension. The crevice model in this latest form was successful in explaining a wide variety of data obtained from acoustic cavitation measurements. Winterton[25] also modified Apfel's model and used it to explain boiling and non-acoustic cavitation.

At about the same time Yount was developing a different type of nucleus.[26] Modifying the organic skin models of Fox and Herzfeld, and Sirotyuk,[27] Yount considered his nucleus to be a bubble surrounded by polar surfactant molecules. This skin has the property of offering a varying permeability to gas, depending upon the ambient conditions. He has applied his model to compression/decompression processes and has been successful in explaining his data. Yount[28] has further developed his model theoretically and experimentally so that there is little doubt that it is plausible. Ward et al[29,30] have done considerable work with the thermodynamics of heterogeneous nucleation in supersaturated systems of constant mass and volume. Among other things, they have predicted the rate of formation and stability of bubbles in a conical pit contained within a system of fixed volume. Their work has been applied to bubble formation in bone cells.

The crevice model has recently been reformulated by Atchley[31] and Atchley and Prosperetti.[32] This reformulation is based upon the mechanical stability of a gas pocket in a conical crevice and the predictions of this new version of the crevice model agree quite well with a broad set of measurements. The model has been applied both to acoustic cavitation and "diffusion" cavitation. Diffusion cavitation is a term for bubble formation driven by gas diffusion such as effervescence of a carbonated beverage.

Conspicuously absent from this historical review is any mention of the

This organic skin model will be discussed further in the next section. An extensive set of measurements was reported by Strasberg.[16] He analyzed his results in terms of the nuclei proposed up to that time and found the crevice model offered the best explanation. Other noteworthy papers of the 1950's are by Connolly and Fox[17] and Galloway[18]; some of their results will be discussed later.

Sette and Wanderlingh[19] were the first to study acoustic cavitation in water induced by cosmic rays. They concluded that the nuclei were recoiling oxygen atoms and their results agreed well with calculations based on Seitz's theory. The Soviet researcher Akulichev[20] proposed another cavitation nucleus based on his measurements of the influence of dissolved ions on cavitation thresholds. His nucleus, similar to that of Fox and Herzfeld, consisted of an ionic skin surrounding a gas bubble. Greenspan and Tschiegg[21] demonstrated that if a liquid was extensively and carefully filtered to remove the nuclei, it could momentarily sustain extrememly high tensile stresses. They also made a valuable contribution to cavitation research by developing a method by which they were able to attain unusually high cavitation thresholds. This method consisted of high-Q resonance chambers that were driven by small tuned ceramic transducers.

In 1970, Apfel[22] developed the crevice model further to include the size of the crevice; he suggested that there existed a "critical" size for the crevice. Crevices larger than and smaller than this critical size exhibit quite different behavior. Apfel published papers on both homogeneous and heterogeneous cavitation. In 1971,[23] he modified a theory for homogeneous nucleation of vapor cavities at the interface between a flat solid and a pure liquid to account for nucleation at the interface

In 1944, Dean[10] suggested that vapor cavities form in the center of small vortices produced by turbulent motion of water around solid objects. In the same year, Harvey[11] suggested that gas pockets stabilized at the bottom of crevices found on dirt particles accounted for the cavitation found in animals. He had concerned himself mainly with cavitation formed by compression/decompression processes in animals (the "bends"); however, he did discuss his model's application to acoustic cavitation. One of the most careful and extensive experiments of the time was performed by Briggs, Johnson, and Mason.[12] They measured cavitation thresholds for a variety of liquids as a function of dissolved gas pressure, viscosity, and pulse length. However, their theoretical explanation of their results was later shown to be incorrect.[6]

The 1950's was a decade of diversification for cavitation research. Perhaps the most important example of this breadth is the invention of the bubble chamber by Glaser. This invention gave rise to the field of radiation-induced cavitation. Seitz[13] gave an explanation for bubble formation in superheated liquids by charged particles. He concluded that the majority of bubbles were "nucleated by moderately-energetic free electrons produced by the incident particles in Coulomb encounters". The bubble chamber was developed as a tool for elementary particle physics while radiation-induced cavitation research took a different avenue. Lieberman[14] measured the threshold for acoustic cavitation in pentane and acetone exposed to neutron and beta sources. He concluded that the cavitation was nucleated by the recoil of carbon ions; these results agreed well with Seitz's theory.

In the field of acoustically induced cavitation, a different type of nucleus was suggested in 1954 by Fox and Herzfeld.[15] This nucleus consisted of a gas bubble surrounded by a rigid skin of organic molecules.

consequences. The application of a tensile stress to a liquid is the basis for present day acoustic cavitation studies, which are actually studies of the "dynamic" tensile strength, as opposed to these earlier "static" measurements.

Acoustic cavitation was first observed during the period from 1915 to 1920 by Langevin and his co-workers while he was pioneering the field of ultrasonics.[7] Söllner[6] was one of the first to observe cavitation in degassed liquids at room temperature and atmospheric pressures (1936). In the 1930's and 1940's a number of other researchers investigated various aspects of ultrasonic cavitation, among them Boyce,[6] Harvey,[6] and Kornfeld and Suvorov.[8]

The fundamental problem of cavitation was by now well formed. Numerous measurements of the cavitation threshold (tensile strength) of water yielded results in the range of 1-25 bars (using the most careful and painstaking procedures thresholds of up to 300 bars have been obtained,[9] but they are unusual) and yet, theoretical predictions of the homogeneous (pure liquid) threshold of water are thousands of bars.[6] What accounts for this order-of-magnitude (best case) discrepancy? Failure in solids under tension is usually attributed to an imperfection in the solid. The same logic (ie, imperfections in the liquid) was applied to the failure of liquids.

In the remainder of this section different types of cavitation will be mentioned in an overview of the field in the last half-century. The investigators of these branches of cavitation research sought these imperfections (cavitation nuclei) to explain the various aspects of the particular cavitation process. Cavitation nucleated by these inhomogeneities is termed heterogeneous cavitation.

increases with addition of hydrophobic ions to a relative maximum and then subsequently decreases in a similar manner to that discovered earlier by Akulichev. Note that the relative increase in the threshold is nearly a factor of 3. These data indicate quite clearly that the dissolved ion concentration is an important aspect of the stabilization process.

Crevices in Solids

One of the earliest models proposed for microbubble stabilization was that attributed to Harvey et al[11] in which gas is trapped in a conical crevice in a solid inhomogeneity present in the liquid. (It appears that Gernez considerably preceded Harvey in the suggestion of crevices in solids as possible nucleation sites, but Harvey's extensive studies in this area have resulted in this model often being referred to as the Harvey model). This model has received considerable attention, due to its plausibility and its success in explaining available data, and has been examined by many researchers, including Strasberg,[16] Apfel,[22] Winterton,[25] Crum[24] and most recently by Atchley[31] and Atchley and Prosperetti,[32] whose analysis will now be used to describe this model in some detail.

Liquids such as water are known to contain numerous small solids (Apfel[44] estimates this number to be as high as 100,000/cm^3) that remain in suspension due to Brownian motion. If one has ever observed the boiling of water in a pot, or the effervescence of bubbles from a carbonated beverage contained in a glass, it is soon apparent that there are nucleation sites on the walls from which the bubbles appear to form (and reform). Apparently, the cracks and crevices of the walls are imperfectly wetted by the liquid and thus contain gas pockets that act as the sites of bubble growth.

As mentioned above, the crevice model assumes that gas pockets are

stabilized at the bottom of cracks or crevices found on hydrophobic solid impurities present in the liquid. For simplicity these crevices are assumed to be conical. The essential features of the model are depicted in Fig. 1-3b. Whereas skin-type nucleation models require the effect of surface tension be neutralized for the stability of the nucleus, the crevice model uses the effect of surface tension for stabilization. In order to understand the stabilization mechanism of the crevice model, one must first understand the relationships of the various pressures involved. Consider a system consisting of a closed container partially filled with a liquid, as illustrated in Fig. 1-5. The space above the liquid is filled with the liquid vapor and a gas. The total pressure in this space is equal to the partial pressure of the gas plus the vapor pressure. That is, the total ambient pressure is $P_G + P_v$. Assuming that the gas is soluble in the liquid, some gas diffuses into it. The equilibrium concentration of the gas in the liquid is found by Henry's law,

Fig. 1-5

$$C = K(T)P_G \tag{1-3}$$

where C is the concentration and K(T) is a function of temperature only. Through Henry's law we can establish the concept of gas tension, G, which is the gas pressure required for the liquid to have a given gas concentration at a given temperature.

Within the liquid there exists a solid impurity which contains a gas and vapor-filled crevice. We call the gas pocket a cavitation nucleus. Diffusion of gas across the interface of this nucleus maintains the partial pressure of the gas inside the nucleus, P_g, equal to the gas tension of the liquid in the neighborhood of the interface. If the entire system is in equilibrium then $G = P_G$ and $G = P_g$, so $P_G = P_g$. The pressure within the

nucleus is $P_g + P_v$. The pressure balance equation for the nucleus is

$$P_L + \frac{2\sigma}{R} = P_g + P_v \qquad (1\text{-}4)$$

where P_L is the total pressure which the liquid exerts on the interface. If hydrostatic effects are neglicted, then $P_L = P_G + P_v$. Since at equilibrium $P_G = P_g$, we have $P_L = P_g + P_v$. This requires that the Laplace pressure ($2\sigma/R$) be zero or, in other words, $R = \infty$. Thus at equilibrium and when the liquid is saturated, the interface is flat.

Now assume that the liquid is undersaturated with respect to the "atmosphere", that is, $G < P_G$. Since diffusion maintains the equality of the gas tension and the gas pressure inside the nucleus we have $P_L > P_g + P_v$. In order to satisfy Eq. (1-4), the Laplace pressure must act so as to oppose P_L. This condition requires that the interface be bowed toward the apex. When equilibrium is established, the Laplace pressure exactly equals $P_L - P_g - P_v$ and the nucleus is stabilized against dissolution.

Suppose we have a degassed (undersaturated) liquid and the liquid pressure is increased. In response to this condition, the interface bows inward more, until it reaches the advancing contact angle. At this point any subsequent motion of the interface involves the entire interface advancing toward the apex. As it advances, the radius of curvature necessarily becomes smaller, since the angle that the interface makes with the crevice wall is now fixed at the advancing contact angle. As the radius of curvature decreases, the Laplace pressure increases. Eventually equilibrium is reestablished. It is readily seen that in small crevices (and thus small radii of curvature) significant levels of applied hydrostatic pressure can be withstood without destroying the nucleus. Indeed, Hayward[45] has shown that the gas pockets stabilized in solid,

hydrophobic particles added to water can sustain applied pressures of 140 bars before they are deactivated.

Having established the stabilization mechanism for a gas pocket in a crevice (a Harvey nucleus), we turn our attention to the process by which such a nucleus forms a free bubble in a liquid, in other words the nucleation process.

Assume there exists a stabilized Harvey nucleus in a degassed liquid. At this point, an acoustic field of pressure amplitude P_A is applied such that the liquid pressure exerted on the interface is $P_o + P_A$. Assume P_A is such that $P_v > P_o - P_A$. During the negative half-cycle, the interface bows outward and the nucleus attains a maximum volume. This process will be isothermal if the thermal diffusion length is large compared to crevice dimensions, and this condition is easily met.

A bubble will be nucleated from this new position only if two nucleation criteria are met. The first is that the angle of contact between the interface and the crevice wall reach the receding contact angle. The second criterion is that the radius of curvature of the interface exceed a critical value R_c. This criterion, first imposed by Atchley and Prosperetti,[32] insures that the nucleus is mechanically unstable and will grow in an unbounded manner. This point is crucial to any nucleation theory and is deserving of a brief digression.

Consider a gas filled bubble of radius R surrounded by a liquid which exerts a pressure P_L on the bubble. Assume the bubble is in equilibrium so that the pressure inside equals the liquid pressure plus the Laplace pressure :

$$P_v + P_g = P_L + \frac{2\sigma}{R} \quad . \tag{1-5}$$

If the gas is ideal then rearranging (1-5) gives

$$P_L + \frac{2\sigma}{R} = \frac{3nR_gT}{4\pi R^3} + P_v, \qquad (1\text{-}6)$$

where n is the number of moles of the gas inside the bubble, R_g is the universal gas constant, and T is the absolute temperature. To examine the stability of this system, consider the effect of a small increase in the bubble radius, R. For the bubble to be stable, the pressure which tends to collapse it, which is given by the left-hand side of equation (1-6), must increase more than the pressure which tends to make it grow, given by the right-hand side of equation (1-6). This will always be true if $P_L \geq P_v$, because the gas pressure varies as R^{-3} while the Laplace pressure varies as R^{-1}. If, however, $P_L < P_v$ then the situation is different.

The stability criterion can be expressed, in general, as

$$\partial/\partial R(P_L + 2\sigma/R) > \partial/\partial R(3nR_gT/4\pi R^3 + P_v). \qquad (1\text{-}7)$$

Performing the differentiation and solving for R gives

$$R < 4\sigma/3(P_v - P_L). \qquad (1\text{-}8)$$

In other words, when $P_L < P_v$, the bubble will be stable against spontaneous growth only if R is less than the critical radius given by

$$R_c = 4\sigma/3(P_v - P_L). \qquad (1\text{-}9)$$

Taking another view, a bubble will grow in a spontaneous unbounded manner when the liquid pressure is less than the vapor pressure only if $R \geq R_c$. A bubble that grows in this way will be mostly vapor-filled.

Equation (1-9) was derived for a spherical bubble, yet it will be applied to a different geometry, namely a gas filled crevice. However, this application leads to no loss of generality. It can be shown that the

critical radius of any nucleus whose volume can be written as fR^3, such as a spherical bubble or a Harvey nucleus, is given by Eq. (1-9).

The acoustic pressure amplitude which must be applied to a liquid in order to meet both of the nucleation criteria is given by[32]

$$P_A = P_o - P_v + (2/3^{3/2})P_g \left[\left(\frac{P_o - P_v - P_c}{P_g}\right)^3 \left|\frac{\cos(\alpha_p - \beta)}{\cos(\alpha_i - \beta)}\right|^3 \left(\frac{\cot\beta + \eta_p}{\cot\beta - \eta_i}\right)\right]^{1/2}, \quad (1\text{-}10)$$

where

$$\eta_i = \frac{2}{\delta_i^3} - \left(\frac{2}{\delta_i^2} + 1\right)\left(\frac{1}{\delta_i^2} - 1\right)^{1/2}, \quad (1\text{-}11)$$

and

$$\delta_i = |\cos(\alpha_i - \beta)|. \quad (1\text{-}12)$$

(The subscript i denotes one of two conditions. If i = A, the interface is at the advancing contact angle. If i = 1, the interface is at some angle greater than the advancing contact angle.)

Apfel[22] defines crevices of larger than or smaller than critical size. A crevice is larger than citical size if the angle of contact of the interface in a degassed liquid, α_i, is equal to the advancing contact angle. A crevice is smaller than critical size if it is not. Therefore, if a crevice is larger than critical size, η_i and δ_i in Eq. (1-10) may be replaced with η_A and δ_A. For crevices smaller than critical size, such a substitution is not possible and η_i and δ_i are functions of P_g and the radius of the crevice at the point of contact between the crevice wall and the interface, a_1. Crevices larger and smaller than critical size behave differently, in terms of cavitation threshold. We will return to this point later.

Concept of Threshold

The investigation of cavitation nucleation mechanisms historically is linked with measurements of the transient cavitation threshold. The process through which a nucleus produces a detectable bubble is somewhat as follows: A stabilized nucleus is exposed to an acoustic field. If the amplitude of the field is sufficiently low, the nucleus undergoes no appreciable change in size. When the field reaches a sufficient amplitude the nucleus becomes unstable and rapidly (within a few acoustic cycles) grows into a mostly vapor-filled bubble. This vaporous cavity eventually reaches a size sufficiently large to be detected. (Methods of detection are discussed later.) In theory, the cavitation threshold is the value of the acoustic pressure amplitude necessary for the nucleus to become unstable. In practice, the cavitation threshold is the value of the acoustic pressure amplitude to which the liquid is exposed when an "event" is detected. Idealistically the two thresholds are the same.

By measuring the cavitation threshold as a function of various liquid properties, information can be gained about the cavitation nucleus. In this section we briefly summarize the results of a number of cavitation threshold measuremets on water. The summary is the compilation of the results of the research reported in references [15-18,20-24 and 31].

Dissolved Gas Tension

Liquids saturated with gas have transient cavitation threshold near one or two bars, provided that they have not been "cleaned" in any appreciable way. The type of cavitation that is detected in saturated (or near saturated) liquids is not the "crisp" transient cavitation one would expect to observe when vaporous cavities collapse. "Crisp" cavitation is

that in which a clearly distinguishable audible snap or pop is heard indicating the violent collapse of an individual cavity. Rather, the cavitation in a saturated liquid indicates that the bubbles contain an appreciable amount of gas which cushions the collapse. In this case, cavitation is associated with the presence of numerous gas bubbles that gradually appear in the bulk of the liquid. Often "streamers" or relatively long lines of bubbles will be present. If any sound is heard, it will be a contenual hissing or frying noise. As the gas tension is reduced from saturation to about 25% of saturation, the threshold increases almost linearly to about seven bars and the cavitation becomes crisper. For gas tensions below about 25%, the threshold increases much more rapidly.

Hydrostatic Pressure

The cavitation threshold is directly proportional to the hydrostatic pressure applied to the liquid. The threshold of a liquid can be increased permanently if the hydrostatic pressure is maintained long enough for gas to diffuse out of the nucleus.

Surface Tension

The cavitation threshold varies inversely with surface tension. This behavior is somewhat suprising since the Laplace pressure varies directly with surface tension.

Temperature

The cavitation threshold varies inversly with temperature. The decrease in threshold with increasing temperature is roughly linear except for liquids near the boiling point. Near the boiling point the threshold

drops to zero.

Solid Contaminants

The cavitation threshold increases with decreasing number and size of solid contaminants (dirt).

Dissolved Ion Concentration

The behavior of the cavitation threshold as a function of dissolved ion concentration is unusual. However, in general as the concentration increases, the threshold, relative to extremely low concentrations, also increases.

Comparison with Theoretical Predictions

Of the nucleation models discussed previously, the crevice model has been the most extensively, and most successfully, applied to acoustic cavitation. In this section we compare the predictions of the crevice model to measurements of the cavitation threshold of degassed and distilled water. We use the Atchley and Prosperetti version of the crevice model for our analysis, except where noted.

Dissolved Gas Tension

Fig. 1-6a and Fig. 1-6b

Figures 1-6a and 1-6b are two graphs of the cavitation threshold versus gas tension. Plotted are the predictions of Eq. (1-10) as well as the experimental thresholds measured by Strasberg[16], Connolly and Fox[17], and Galloway.[18] No attempt has been made to normalize any of the data, although the calibrations of the various experimental systems were based on different standards. Three comparisons are evident. If the "lone" data

point at a gas tension of about 0.1 bar were eliminated, there would appear to be a linear dependence on gas tension. However, the "lone" data point is not actually "lone". Figure 1-6b is an expanded version of Fig. 1-6a which includes Galloway's data for gas tensions below 0.1 bar. (These are the only data available for these extreme values of gas tension.) Emphasis should not be placed on the absolute values of his data; thresholds of those magnitudes are uncommon and there has been no effort made to fit the theory to the data. The trend of the data, however, is important and in good agreement with the crevice model prediction.

Referring to Fig. 1-6a, it is seen that the experimental thresholds tend to be about 2 bars for saturated solutions while the crevice model predicts a threshold of about 1 bar. This discrepancy may result from the fact that the theoretical model does not strictly reproduce the experimental procedure. That is, the line on the graph represents the acoustic pressure amplitude necessary for the nucleus to become mechanically unstable. The experimental thresholds are measured values of the acoustic pressure amplitude within the liquid at the time a bubble was detected. It should not be assumed that these two pressure amplitudes are always the same. The process by which a nucleated bubble (or nucleate) becomes a detected bubble is indeed complex. One factor which can complicate the evolution of a nucleate is gas diffusion into the expanding bubble. This factor is ignored in the theoretical threshold predictions. However, the effects of gas diffusion should diminish as the gas content of the system decreases. This conclusion is consistent with the results shown in Fig. 1-6a; there is better agreement between theory and experiment at gas tensions below about 0.5 bar.

If the crevice is smaller than critical size, the threshold is predicted by Eq. (1-10) with $\eta_i = \eta_l$ and $\delta_i = \delta_l$. Theoretical predictions

Fig. 1-7

of the threshold as a function of gas tension are presented in Fig. 1-7. The different lines correspond to different values of a_1, ranging from 10 nm to 50 nm. It is seen that for crevices smaller than critical size, the threshold at saturation in no longer equal to $P_o - P_v$. On the contrary, the threshold can assume large values since it is now a function of a_1. Although there is a threshold dependence on gas tension, it is not as strong as in the case of crevices larger than critical size. In order to see this difference, we normalize the predictions presented in Figs. 1-6a and 1-7 to their values at saturation. These normalized thresholds are

Fig. 1-8

reproduced in Fig. 1-8. It is clear from the figure that the dependence on dissolved gas concentration is less for crevices smaller than critical size. This result is consistent with the observations of Greenspan and Tschiegg.[21] They found that after water had undergone protracted filtration through 0.2 μm filters, the cavitation threshold was about 160 bars if they waited one minute for cavitation to occur or 210 bars if they waited only a few seconds for it to occur. In addition, the threshold was independent of gas tension; their range of gas tensions was from about 0.15 to 0.85 bars. Referring to Fig. 1-8, over this range of gas tensions the threshold for crevices smaller than critical size varies by about a factor of two, while that of crevices larger than critical size varies by about a factor of nine. It should be pointed out that the curve for the smaller crevices was calculated for a_1 = 15 nm, but the results are essentially the same for all values of a_1.

Surface Tension

The functional dependence of the cavitation threshold on the liquid-gas surface tension is not as obvious as with the case of gas tension. To

understand this dependence, we follow the lead of Crum,[24] who used an empirical relationship discovered by Bargeman and Van Voorst Vader,[46] viz.,

$$\cos \alpha_E = C/\sigma - 1 \qquad (1\text{-}13)$$

where α_E is the equilibrium contact angle and C is a constant. For many nonpolar solids C has a value of about 50 dyn/cm. This relationship is valid for surface tensions greater than about 10 dyn/cm. In the analysis given by Crum as well as the one to follow, it is assumed that $\alpha_E = \alpha_A$ and that $\alpha_R = \alpha_A - \alpha_H$, where α_H is the hysteresis contact angle. (Hysteresis is what gives rise to the asymmetrical shape of droplets sliding down windows.) Using these relationships, the crevice model becomes a model with two adjustable parameters: α_H and β. In the analysis of this model, the sum of these two parameters ($\phi = \alpha_H + \beta$) was held constant. Fig. 1-9 is a graph of threshold versus surface tension. Two sets of data are shown corresponding to two different values of gas tension. The data are Crum's[24]. It is seen that the agreement between theory and experiment is quite good.

Fig. 1-9

Temperature

Temperature variations affect the cavitation threshold through three measureable parameters: gas tension, surface tension, and vapor pressure. The largest variation is associated with the temperature dependence of the dissolved gas tension; however, all of the dependencies are taken into account in the analysis, using data from standard references.[47-49]

The cavitation threshold is plotted as a function of temperature for a range of dissolved gas tensions in Fig. 1-10. The open squares represent Galloway's data[18] and the solid squares represent Crum's data.[24] The solid lines represent the threshold as predicted by Eq. (1-10) for $\beta = 12.85^\circ$ and

Fig. 1-10

$\beta + \alpha_H = 35^\circ$. The data have been normalized to fit the theory at room temperature ($23^\circ C$). The variation with temperature is predicted well by the crevice model. Although there are no data to test the theory above $50^\circ C$, the threshold must approach the vapor pressure at the boiling point. This behavior is suggested by the "tail" at high temperatures.

Hydrostatic Pressure

Crum[24] has applied Apfel's[22] version of the crevice model to Strasberg's[16] measurements of the threshold dependence on applied hydrostatic pressure. His results are shown in Fig. 1-11. It is seen the overall theoretical trend is in good agreement with the measured trend.

Fig 1-11.

Dissolved Ion Concentration

As of now, no model has been able to predict the dependence of the threshold on dissolved ion concentration.

In summary, then, it is seen that for carefully controlled measurements in distilled water, a standard crevice model gives reasonably good predictions of the dependence of the cavitation threshold on a variety of physical parameters. It can not explain all the dependences, however, and is thus still incomplete in the current version. To have an adequate model, one must somehow introduce the obvious influences of dissolved ion concentration and surface-active materials. This problem is a difficult one but also interesting and important and awaits the ingenuity of a future investigator.

A final caveat: currently, nucleation is of considerable interest to those examining the biological effects of ultrasound, and specifically - cavitation in tissue. It is important to note that the nuclei present

there may be entirely different in character, and that the successful results obtained for water may not apply to those situations.

μm in radius.

Akulichev[20] has reported that the cavitation threshold has an important dependence on the concentration of dissolved ions, particularly certain alkaline salts. We desired to reproduce and extend these measurements. In order to determine the dependence of the threshold on the ionic concentration, it was necessary to remove as many chemical impurities from the liquid as possible, so that the desired ions could be added at low concentrations. In a method similar to removing the physical impurities by filtration, the chemical impurities were removed by circulating the liquid through Sybron Barnstead organic and ionic removal columns. The manufacturer contends that the content of high molecular weight organics is lowered to a few parts/million and the resistivity of the water is raised to 1 megaohm/cm.

Crum[24,56,57] and others [54] have also discovered that small additions of surface-active agents can greatly influence the threshold. These agents can be easily added to the liquid with our apparatus, but their removal is more difficult. It is possible to remove most organic surfactants from the liquid by irradiation with an intense ultraviolet source though a quartz window. Although we have not yet introduced this modification, it is easily done and in our plans for the immediate future. The surface tension of water can be changed from its maximum (near 72 dyn/cm) to about 30 dyn/cm.

Cavitation Generation System

The generation of acoustic cavitation in a liquid such as water is relatively simple. One needs only a function generator, a power amplifier, and an appropriate transducer. To determine the threshold, one merely

volumetric Van Slyke apparatus. This system permits an examination of this ratio from about 0.3 to 1.0.

In order to fully automate the threshold measurement system, we found it necessary to build a resonance tracking system to lock onto a resonant mode of the sphere. Since energy dissipation would tend to raise the temperature of the sphere-transducer combination, a constant-temperature control system was required to hold the resonance frequency of the sphere to within permissible limits. Within the light-tight box containing the cavitation flask and the photomultiplier tube, the temperature change could be held to within a degree Celsius.

One of the motivations for the construction of this system was to determine information about the nature of cavitation nuclei. In particular, we were interested in the dependence of the cavitation threshold on the size of solid particulate matter, and thus to a certain extent, the size of the nuclei. Nuclei size control was achieved via extensive filtration; the filter size thus determined, in a sense, the nuclei size. Implicit in this statement is the assumption that the filter remains relatively clean. During the filtration process, the filters were replaced frequently and visual inspections revealed little or no observable deposits on the surface. The measured fluid flow rates during the filtrations were about 1 liter per minute. Since the total quantity of water in the system was about 2 liters, one could reasonably assume that the entire bulk of the fluid would have made a pass through the filter in 5 minutes. Prior to each run, the sample underwent simultaneous filtration and "argonation" for 45 minutes through filters that remain as clean as possible. We therefore assume that the nuclei size distribution had an upper bound that was approximately equal to, or slightly less than, the filter pore size. Filter sizes used in this study ranged from 10 μm to 0.5

We now briefly describe specific details of the experimental apparatus. For a detailed description, see Ref. [55].

Fluid Management System

The cavitation threshold depends upon the liquid "properties" such as dissolved gas content, surface tension, temperature, ionic content particulate contamination, and chemical impurity. Accordingly, we wished to control these parameters as much as possible so that we could study the properties of the nuclei that give rise to cavitation. Figure 1-12 shows the fluid management system that we have devised for this purpose.

Fig. 1-12

It was determined by Greenspan and Tschiegg[21] in their careful study of cavitation inception that one needed a closed system that permitted the liquid to be continuously circulated before adequate degrees of cleanliness could be achieved. They discovered that squeezing pliable tubing or exposing the liquid briefly to the air would "re-seed" the liquid with nuclei. Accordingly our system is a closed one, with the liquid only exposed to glass, teflon, and stainless steel. Although the figure is reasonably self-explanatory, a few special features are noted below.

We found it desirable to remove the dissolved air from the liquid and replace it with argon, which gives a more intense sonoluminescent response than air (due to the differences in thermal conductivities). We did this by simultaneously evacuating the reservoir, circulating the liquid and bubbling argon through the liquid within the reservoir. By an appropriate selection of gas pressures and circulation rates and times, a predetermined "dissolved argon concentration ratio" (the amount of dissolved argon compared to that at saturation) could be roughly achieved. The actual value was determined by measurement of a sample of the liquid by a

of cavitation and is generally termed chemiluminescence.) Optical methods of cavitation detection place a stringent requirement on the liquid and its container - they must be optically transparent. (This requirement makes optical detection of cavitation within biological systems difficult.)

In general, there are many different ways of detecting the various types of cavitation that exists. The choice of the detection scheme must be based upon the specific type of cavitation to be detected and the experimental limitations placed upon the detection system. The cardinal rule in detection is still "know when something happens".

Description of a Specific Experimental Apparatus

We have developed an apparatus that incorporates some of the ideas presented above. It is perhaps useful to describe it here as an example of a versatile, yet precise, system which can be used to measure cavitation thresholds.

Control over the liquid composition is best attained when there are few interfaces between different materials that require potentially contaminating adhesives and seals. An obvious configuration with several advantages is a spherical glass flask, in which the liquid is contained inside with the transducers mounted to the outside wall, and driven so as to excite a standing wave pattern within the liquid. The spherical focusing generates a high intensity region at the center of the flask that is well removed from the walls. Further, the system can be easily cleaned, provides high optical visibility, and is simple in construction. This configuration was suggested by Blake,[6] perhaps first utilized by Galloway,[18] and employed later with great success by Strasberg,[16] Barger,[53] and Vaughan.[54] The major disadvantages of the spherical flask configuration is that the maximum acoustic pressure attainable is about 25 bars (2.5 MPa).

cavitation. This method does however provide a way of determining the sizes of bubbles. The absorption of ultrasound of a given frequency depends upon the radius of the bubbles. Therefore, by transmitting a band of frequencies and noting which frequency components are attenuated the most can enable one to determine the size of the bubbles formed.

Bubbles can also be detected optically. The eye can be used to detect the presence of bubbles in a liquid. However, the eye has only limited usefulness as a detector because of the small sizes and short lifetimes of some cavitation events. The problem of subjectivity arises as well. Photographic methods have been employed to detect cavitation but because of the delay associated with processing, this method is more useful for "capturing" an event than for threshold measurements. Real time detection is usually preferable. The detection of light scattered from bubbles is also a means of detecting cavitation but this method requires precise alignment of components and the cavitation must be generated in the path of the light beam.

The production of sonoluminescence provides another criterion for a cavitation threshold, one which we have found quite successful. Sonoluminescence is radiated light whose production is associated with bubble activity. (Since sonoluminescence is the topic of a later chapter, we will attempt no further discussion of its origin.) This light may be detected with a dark adapted eye, photographic plates, or with electronic light detectors (photomultiplier tubes, single photon counters, etc). The intensity of the sonoluminescence can be enhanced by changing the gas composition of the liquid sample or by altering the chemical properties of the liquid. The latter method usually involves the addition of light "enhancers" to the liquid. (The light produced is then a secondary result

criterion, although useful for cavitation produced by continuous wave ultrasound in the kilohertz frequency region, is essentially useless when one observes pulsed cavitation in the megahertz region. A second commonly used criterion, the presence of free gas bubbles in the insonified region, may only indicate growth by rectified diffusion. Such bubble growth may occur without any associated violent effects such as free radical production or shock wave generation.

Cavitation can be detected chemically through a variety of reactions that most likely involve free radical production. This method has the advantage that it can measure the field and can be extremely sensitive, the disadvantage is that it can not be done in real time and that some reasonably difficult assaying must be performed.

Another threshold criterion is the detection of subharmonics of the driving frequency produced by oscillating bubbles. Bubbles radiate subharmonics only when oscillating violently. Thus, bubbles which oscillate not-so-violently are not observed. Likewise, if one is interested in strictly transient cavitation (that is, in detecting the transient collapse of cavity) this criterion may not be appropriate. The detection of subharmonics indicates the presence of violently - oscillating bubbles and not, necessarily, transient cavitation. Its use is more appropriate when stable cavitation is of interest.

Another method of detection which indicates the presence of bubbles is based upon the fact that bubbles are efficient absorbers of ultrasound. The cavitation threshold is marked by the excessive absorption of a reference acoustic pulse (not related to the field which generates the cavitation) which is transmitted through the fluid. The onset of absorption indicates the presence of bubbles in the liquid. Again, however, this method does not distinguish between stable and transient

situations, a resonance system may be ideal because the resonator serves as the sample container. However, the use of a resonance system eliminates the possibility of using a short duration pulsed ultrasound, as discussed previously. The type of detection system employed depends upon the nature of the liquid as well. For example, a system that detects cavitation optically would be useless if the liquid (or container) is opaque.

Know When Something Happens

The measured value of the cavitation threshold depends to a great extent on how one "looks" for the cavitation event. In fact, the entire concept of a threshold is strongly dependent upon the phenomenon one is trying to detect - the threshold for the onset of free radical production may be vastly different and unrelated to the threshold for the rectified diffusion of gas within a pulsating gas bubble. Also, a detection method that is useful in one mode of operation (eg, continuous, low frequency ultrasound) may not be at all useful in a different mode (eg, pulsed, high frequency ultrasound). Likewise, if two different detection schemes are employed simultaneously, "the" threshold detected by one may be quite different than "the" threshold detected by another. Obviously, before one designs a detection system, one should know as much as possible about the phenomenon that one expects to observe and the method by which this phenomenon will be generated.

Since the result of a threshold measurement depends upon the criteria which constitute the onset of cavitation, it is useful to review some of the threshold criteria used in the past. Perhaps the most common threshold criterion is the detection of the audible "click" associated with the shock wave produced in the host liquid by a collapsing transient cavity. This

upon which we have not touched has to do with sound field calibration. Calibration in a resonance system is most commonly accomplished with a probe hydrophone having small dimensions. The aim of calibration is to be able to ascertain the properties of the sound field (peak pressure amplitude, field geometry, etc) from a knowledge of the signal supplied to the transducer and usually must be performed with a sound field having a pressure amplitude lower than it will have during actual measurements. This precaution is necessary to prevent damage to the probe by the formation of cavitation on it. We will not attempt any discussion of calibration techniques. Standard techniques for calibration have been devised by various scientific groups (AIUM[52] for example).

Know Thy Liquid

The properties of the liquid dictate the outcome of cavitation threshold measurements. Therefore, in order to correctly interpret the results of threshold measurements one must know as much about the liquid as possible. This knowledge consists not only of the liquid properties at the time of the measurement but the history of the liquid as well. However, a simple knowledge of liquid properties is not adequate for most experimental systems. In order to test the range of validity of any theory, it is necessary to be able to vary the liquid properties as well. It is also necessary to control the properties of the liquid so that they remain unchanged during the period over which the measurements extend. Depending upon the nature of the individual experiment, this time period may be anywhere from a few minutes to several hours.

The nature of the liquid must also be considered when choosing a transducer. When ultrapurity is required or when dealing with a corrosive liquid, the transducer and the liquid should not be in contact. In such

to visually observe when cavitation occurs.

Another disadvantage of these systems is that the resonance frequency is strongly temperature dependent. Thus, when measurements extend over long periods of time, the system must continually be retuned to keep it operating at resonance. The resonance frequency is also dependent upon the nature of the liquid sample. For example, a flask filled with water will have a different resonance frequency then when it is filled with glycerine.

One advantage of resonance systems is that they can have high Q's. The Q of an oscillator is a measure of the sharpness of the resonance or the time required for the system to dissipate energy. Generally speaking, the greater the Q, the higher the pressure produced at the focus. Q's of 10,000 are not uncommon for resonance systems.[21] It should be pointed out, however, that this property of resonance systems makes them unacceptable for measurements involving short pulses of ultrasound. The lower limit of the duration of the pulse that can be produced by a transducer is dictated by how quickly the oscillation of the transducer damps out. The damping time is directly related to the Q. Therefore, for short pulse durations, the transducer must have a low Q.

Generation of cavitation by a focused sound field offers a significant advantage over that produced by an unfocused, or uniform, sound field. This advantage is that the researcher knows more or less where the cavitation is going to occur. Whereas cavitation generated by a uniform sound field is equally likely to occur anywhere within the sound field, cavitation generated by a focused sound field can be made to occur only in the focal region. This knowledge can be quite useful especially when one attempts to detect the cavitation.

One aspect of experimental systems which is exceedingly important and

Consider a spherical flask filled with a liquid, and having one or more transducers affixed to its side. When the transducers are driven, the entire flask vibrates and, if the transducer - flask system is driven at one of its resonance frequencies, the oscillation amplitude of the flask wall can be relatively large. In this manner the effective surface area of the transducer beomes that of the entire flask. As the flask oscillates radially, the acoustic field is focused at the center of the sphere. Resonance systems having different geometries have been used and although the pattern of the acoustic field may be more complex than that produced by a spherical system, they all work on the same principle.

Resonance systems such as this have disadvantages, one being the often difficult problem of permanently mounting the transducers to the flask. The transducer is usually epoxied to the flask. During operation, however, there invariably exists relative motion between the transducer and the flask, thereby generating stress in the adhesive. Over a period of time this stress weakens the adhesive. The weakening is accelerated by larger driving amplitudes. The stress can be minimized if extreme care is taken to retune the transducer to match the resonance frequency of the flask. (The retuning of a transducer is a fine art!). However, it is virtually impossible to eliminate failure of the adhesive and in fact this failure usually dictates the upper limit to pressure amplitudes that can be achieved with these systems. A way of avoiding the adhesive-failure problem is to make the entire containment vessel from transducer material. In fact, cylindrical transducers made from piezoelectric ceramics, with thin glass windows on the ends, make excellent cavitation cells. In this case, however, the quality factor, or Q, of the system is determined by the ceramic, which is typically more lossy than glass, or stainless steel, which thus have higher Q's. Ceramics are also opaque and it is difficult

salt (potassium sodium tartrate), and barium titanate ($BaTiO_2$ is actually electrostrictive rather than piezoelectric but can be made to behave as a piezoelectric if permanetly polarized); ceramics such as lead zirconate titanate (PZT); polar polymer films such a polyvinyl chloride (PVC), polyvinyl flouride (PVF), and polyvinylidene flouride (PVDF); and even biological substances such as the dried Achilles tendon of a cow.[51] Presently ceramic piezoelectrics are widely used to generate ultrasonic signals, as they are relatively inexpensive and can be cast in various shapes to fit various experimental requirements.

Most focused transducers are spherical or parabolic sections and are quite analogous to converging optical lenses. However, since piezoelectric ceramics can be manufactured in almost any configuration, they can be easily adapted to fit an experimental situation. One example of such a transducer is a hollow cylindrical tranducer. When driven in a radial mode, the acoustic field is focused inward along the cylindrical axis and, if closed on the ends, also develop standing waves along the axis. Thus, a region of intense sound can be generated in the center of a cylindrical container. This type of transducer has been used in various cavitation studies, some of which will be discussed later.

For a given pressure amplitude at the transducer face, a transducer having a larger surface area will produce a higher pressure amplitude at the focus than one having a smaller surface area. However, the cost of a transducer is very dependent upon surface area. In addition to higher costs, larger transducers naturally take up more space and are harder to manipulate. There is a method of effectively increasing the surface area of a transducer. This method involves resonance systems and we will briefly describe such a system now.

acoustical impedance vastly different than that of liquids, the formation of bubbles on the transducer creates an impedance mismatch between the transducer and the liquid, thereby diminishing the efficiency of the sound generation system. Bubbles are also good absorbers of ultrasound. If bubbles form in the region in front of the transducer, the ultrasound will be highly attenuated as it passes through this region and the insonification of the bulk of the liquid is greatly reduced.

In order to diminish the chances of bubble formation at the transducer, the pressure amplitude near the face must be kept to a minimum. However, high pressure amplitudes must still be produced in the bulk of the liquid in order to generate cavitation there. Both of these requirements can be met if the sound field is focused. One early method of focusing was accomplished by reflecting the acoustic field generated by a flat radiator off a curved surface. Willard[50] was one of the first to employ a curved transducer to focus a sound field so as to remove the effect of boundaries. He used a concave, spherically focused, piezoelectric transducer, driven in the megahertz frequency region. Today, this focusing technique is quite common.

Perhaps it is worthwhile to digress momentarily on the subject of piezoelectric transducers. Piezoelectric materials develop an electric polarization when mechanically stressed and, conversely, they become deformed when electrically polarized. The extent of the deformation (polarization) depends upon the extent of the polarization (deformation). If the polarization alternates, first p sitive and then negative, the deformation alternates; that is, the thickness of the material changes at the frequency at which the polarization alternates. Many different materials exhibit piezoelectric properties: crystals such as quartz, tourmaline, Rochelle

In order to understand the basic aspects of any experimental system, it is useful to give a brief description of transient cavitation. Transient cavitation is produced by a high amplitude acoustic field (usually), the threshold for its inception is strongly dependent upon the nature of the liquid, and it is short-lived (a transient cavity has a life time of one, or at most a few, acoustic cycles). This characterization suggests that an experimental system must consist of three components: 1) a method of generating the cavitation, i.e., a method of producing a sound field; 2) a method of preparing the liquid and controlling its properties; and 3) a method of detecting the cavitation when it occurs. Apfel[44] ascribes to each of these components a golden rule for threshold measurements: 1) Know thy sound field, 2) Know thy liquid, and 3) Know when something happens.

Know Thy Sound Field

There has been a tremendous variety of experimental systems that have been used to generate acoustic cavitation. In an early comprehensive review by Blake,[6] many of these systems are described. These early devices commonly employed a flat acoustic radiator, or transducer, to produce the sound field. These systems have one major disadvantage. Flat transducers produce high amplitude fields in the immediate vicinity of the transducer face, as well as in the bulk of the liquid. Therefore, since solid-liquid interfaces serve as preferential sites for bubble formation, the end result of most early attempts at generating acoustic cavitation was the formation of bubbles on the transducer face. Thus, the cavitation was as much a property of the transducer material as it was of the liquid. Cavitation generation on or near the transducer is undersirable for other reasons as well. First, the violence of the collapse of a transient cavity can cause erosion of the transducer material. In addition, since gas bubbles have an

III. EXPERIMENTAL TECHNIQUES FOR INVESTIGATING TRANSIENT CAVITATION

Introduction

The origin of bubbles in liquids was considered in the previous section. It was implied that cavitation nucleation and the inception of transient cavitation were closely linked. Measurements of the transient cavitation threshold were compared to the theoretical instability of a Harvey nucleus. It was seen that, in general, the agreement between measurement and calculation was quite good, except when the liquids under consideration were near saturation. In this region of gas concentration, the theoretical prediction underestimated the experimental result. This discrepency is not unexpected. In liquids near saturation, the diffusion of gas into and out of the bubble has a large effect on its growth and, especially, collapse. It is commonly known by researchers in transient cavitation, that "truly" transient cavitation rarely occurs in gassy liquids. However, in regions of lower gas concentration there clearly exists a correlation between the instability of the nucleus and the inception of transient cavitation. Thus, in order to investigate nucleation processes, it is appropriate to measure the transient cavitation threshold. Measurements of the transient cavitation threshold are also made to investigate the violent side effects of transient cavitation such as material erosion and free radical production.

In this section we consider various aspects of the experimental investigation of transient cavitation. We begin the discussion with a brief overview of some general concerns of experimental system design and end the discussion with a description of an apparatus which we have developed in our laboratory.

increases the gain of the oscillator (at a rate determined by the operator) until there is audible or visual evidence that cavitation has occurred. One then repeats the operation after waiting for a short interval for the liquid to equilibrate. It is rather obvious that this technique involves a considerable amount of subjectivity that would ideally be avoided. We have attempted to automate the system so that completely objective measurements can be made. Although we haven't entirely succeeded, the following procedure is a significant advance toward operator independence.

Fig. 1-13

Figure 1-13 shows a block diagram of the cavitation generation system. The heart of the system is a ramp generator (our design) that drives both the amplitude modulation input of a function generator and a strip chart recorder. The DC voltage level of the strip chart record is linearly related to the peak to peak output amplitude of the function generator. This signal passes through a precision attentuator, is amplified by a power amplifier, which in turn supplies the driving voltage to two PZT-4 cylindrical transducers that are mounted on a one liter fused quartz resonance sphere. The sphere was custom made for us with a slightly flattened bottom (to mount the photomultiplier tube) and smaller neck (to reduce its effect on the resonant modes). The transducers are stock items, 2.54 cm long, with an i.d. of 1.91 cm, an o.d. of 2.54 cm, and a resonance frequency of about 50 kHz. Also epoxied to the cell are a miniature PZT-5 pill transducer (to monitor the sound field) and a linear thermistor (to monitor the temperature). The entire sphere assembly is cradled in a monofilament line harness to reduce damping. The signal generated by the pill transducer drives the vertical input of a storage oscilloscope as well as the input of a digital resonance tracking circuit (our design). This device maximizes the RMS output of the cell by adjusting the frequency of the function generator (via the VCO input) to lay on resonance. A

universal counter monitors the frequency.

Since the acoustic pressure amplitude is essentially determined by the DC modulation signal, a "shutting down" of the sound field is tantamount to resetting the ramp generator to its quiescent "no ramp" state. The ramp generator exercises total control over the sound field while the strip chart recorder keeps a running record, in hard copy, of the pressure amplitude in the cell.

The essential nature of the cavitation generation system is that the sound field within the cavitation cell is increased linearly with time, at reproducible rates, until cavitation occurs. The system then resets into a predetermined quiescent state, and remains there until the timer restarts the ramp (the actual sequence of events that determine a measurement will be given later).

Cavitation Detection System

One of the most subjective aspects of cavitation threshold measurements is the decision as to what constitutes a threshold. The appearance of bubbles has been used by some observers[58] (sometimes called "quasicavitation," because what is observed is normally rectified diffusion, rather than rapid growth and violent collapse), the presence of subharmonics by others[59] (primarily nonlinear oscillations of stable gas bubbles), audible clicks and pops[60] (at least a shock wave involved), as well as a variety of other chemical and physical mechanisms. Because we would like to consider only violent cavitation, for the time being, we use the presence of a significant level of radiated electromagnetic energy (sonoluminescence) as an indication of cavitation inception. Thus, with this constraint, we are considering the "transient-violent cavitation threshold".[61]

Fig. 1-14

Figure 1-14 shows the cavitation detection apparatus together with the gating, timing and triggering circuitry. Once cavitation has been initiated in the spherical resonator by the ramping voltage, the sonoluminescent flash is observed by the photomultiplier tube. The anode pulse from the photomultiplier tube base, upon amplification by three stages of a preamplifier, feeds into a pulse height discriminator. The discriminator level, which determines the sensitivity of the apparatus, is set to 600 mV, a value that is well above the electrical background level (~ 150 mV) but which lies below the typical sonoluminescence pulse height (~1.0 V). If the anode pulse survives discrimination, it then passes through a "noise gating" network (described below) followed by a linear gate and finally results in the "trigger" pulse that subsequently resets the system. A "system reset" refers to a reduction in the sound pressure amplitude to a minimal quiescent level for a predetermined length of time. An Ortec model 776 timer provides the necessary control signals.

As an example of how the system works in a typical run, consider the system to be in its quiescent state where the sound field is off and the timer is counting. The timer disables both the linear gate and the ramp generator via the "busy" output, which is active whenever the timer is counting. At the end of the timing sequence, the busy signal goes low which opens the linear gate and engages the ramp generator. The ramp proceeds until a transient event generates a pair of light pulses which, provided they survive amplitude discrimination and "noise" gating, reset the timer and the whole process starts over. The linear gate prevents any stray noise pulses from resetting the timer before the quiescent period is over. In the event that a transient collapse does not generate a sufficient quantity of light to trigger the reset, the operator, who is monitoring the situation with headphones, can manually reset the system

simply by pressing a button. This system override is to prevent an unlimited ramp that could damage the cell transducers. Shown in Fig. 1-15 is a sketch of raw data from a typical run.

Fig. 1-15

Sonoluminescence is not the only source of light one encounters in this configuration. It is found that a background "light noise" level of about 5 pulses per minute exists, probably due to Cerenkov radiation. We desire a slow ramp rate; however, with stray noise signals occurring every 12 seconds or so, one cannot wait too long for cavitation to occur. Pulse height discrimination proves only partially effective since the brightest noise pulses are more intense that the weakest sonoluminescence events. We observe that in this system transient collapses almost always occur in bunches, some of the catastrophic events generating hundreds of pulses in a matter of milliseconds. This fact, of considerable interest in itself, inspired a "noise gating" scheme in which the criteria for the generation of a trigger pulse is the occurrence of <u>two</u> discriminator pulses separated by no more than 100 ms. The pulse height discriminator has two outputs, one of which is connected directly to the "B" input of a Lecroy model 465 coincidence unit. The other undergoes a 20 ns delay (via a Tennelec model TC410A gate and delay module) and then activates the trigger of a BNC model model 8010 pulser. This device produces a 100 ms gate signal that drives the "A" input of the coincidence unit. The time delay insures that the discriminator pulse, which is about 15 ns in width, reaches the coincidence unit <u>before</u> the gate signal. Thus, to establish coincidence, a second discriminator pulse must follow within 100 ms. The output of the coincidence unit generates the trigger signal that resets the system. This technique allows us to halve the discriminator level while increasing the noise immunity by a factor of seven.

The system just described is a relatively complex system for generating and detecting cavitation. However, cavitation is a very complex phenomenon, subject to a variety of misinterpretations. Unless one controls the liquid and the sound field applied, and knows what to detect and how to determine if a valid detection has occurred, then the information obtained may be essentially useless.

IV. RECTIFIED DIFFUSION

Introduction

When one visually examines the effect of the direct application of a sound field to a liquid such as water, one often sees streamers of bubbles produced by the action of the sound field. In certain configurations, one can see gas bubbles rising from the field of acoustic activity. The process by which dissolved gas in the liquid is converted into free gas in the form of bubbles by the action of the sound field is called "rectified diffusion". This "rectification of mass" is a direct consequence of the applied sound field and can be of importance whenever the applied acoustic pressure amplitude exceeds the threshold for rectified diffusion (on the order of a bar or less for typical values of the acoustic frequency and bubble radius.) For liquids that are not supersaturated with gas, a definable threshold exists due to the Laplace pressure exerted on the gas contained within a bubble by the force of surface tension. The value of this pressure is given by $P_i = 2\sigma/R_o$, where P_i is the internal pressure, and R_o is the equilibrium radius of the bubble.

For relatively large gas bubbles, on the order of 1 cm in diameter, this pressure is quite small (<0.001 bar). However, for bubbles on the order of 1 μm in diameter, this pressure can be quite significant (>1.0 bar). Thus, when one considers the stability of free gas bubbles in a liquid with a surface tension similar to that for water, they must be stabilized in some manner as described earlier, or they will dissolve rapidly.

With the application of a sound field, however, a bubble can be made to oscillate about an equilibrium radius and caused to grow in size because of the following effects.

The first effect is an "area" effect. When the bubble contracts, the concentration of gas (moles l^{-1}) in the interior of the bubble increases, and gas diffuses from the bubble. Similarly, when the bubble expands, the concentration of gas decreases, and gas diffuses into the bubble. Since the diffusion rate is proportional to the area, more gas will enter during expansion than will leave during the contraction of the bubble; therefore, over a complete cycle, there will be a net increase in the amount of gas in the bubble.

The second effect is the "shell" effect. The diffusion rate of gas in a liquid is proportional to the gradient of the concentration of dissolved gas. Consider a spherical shell of liquid surrounding the bubble. When the bubble contracts, this shell expands, and the concentration of gas near the bubble wall is reduced. Thus, the rate of diffusion of gas away from the bubble is greater than when the bubble is at its equilibrium radius. Conversely, when the bubble expands, the shell contracts, the concentration of gas near the bubble is increased, and the rate of gas diffusion toward the bubble is greater than average. The net effect of this convection is to enhance the rectified diffusion. It has been shown that both the area and the shell effects are necessary for an adequate description of the phenomenon.

Apparently, rectified diffusion was first recognized by Harvey,[11] who considered the biological implications of the effect as early as 1944. Blake[62] was probably the first to attempt a theoretical explanation and his predictions were nearly an order of magnitude too small, because he considered only the area effect. An adequate theory was first presented by Hsieh and Plesset[63] who were the first to include the effect of convection. Strasberg,[64] who had made some experimental measurements, showed

that the theory of Hsieh and Plesset[63] generally agreed with his measurements. Eller and Flynn[65] extended the analysis to include nonlinear or large amplitude effects by treating the boundary condition of the moving wall in a slightly different way. Safar[66] showed that the Hsieh-Plesset results were essentially equivalent to those of Eller and Flynn[65] when inertial effects were added to the Hsieh-Plesset approach.

The few measurements obtained by Strasberg were extended by Eller[67] to include both the threshold and the growth rate. He found that the theory was adequate in predicting the thresholds for growth by rectified diffusion but was unable to account for some large growth rates that he observed. He suggested that acoustic streaming (rotational liquid movement due to asymmetrical bubble pulsations) may be the cause of the larger-than-predicted rates of growth. Gould[68] was able to directly observe gas bubble growth by rectified diffusion through a microscope and discovered that growth rates could be greatly enhanced by the onset of surface oscillations of the bubble, which in turn seemed to induce significant acoustic microstreaming. Attempts by Gould[68] to apply the acoustic streaming theories of Davidson[69] and of Kapustina and Statnikov[70] to explain his results were not successful. Extended theoretical treatments were presented by Skinner[71] and Eller[72] to account for growth through resonance.

Additional measurement of the growth of gas bubbles by rectified diffusion were later obtained by Crum[73] who made both threshold and growth rate measurements for a variety of conditions. He extended the theory to include effects associated with the thermodynamic behavior of the bubble interior and found excellent agreement between theory and experiment for both the rectified diffusion threshold and the growth rate for air bubbles in pure water. Anomalous results were obtained, however, when a small amount of surfactant was added to the water. The rate of growth of bubbles

by rectified diffusion increased by a factor of about five when the surface tension was lowered by a factor of about two, with no discernible surface wave activity. Although some increase is predicted, the observed growth rates were much higher. A slight reduction in the threshold with reduced surface tension was also observed. Some explanations offered by Crum[61] for this anomalous behavior were that there was some rectification of mass due to the surfactant on the surface of the bubble and/or there was microstreaming occurring even in the absence of surface oscillations.

To bring our limited review of the literature up to date, it is noted that there have been recent applications of the equations of rectified diffusion to studies of the threshold for growth of microbubbles in biological media,[74] the threshold for cavitation inception,[61] and as a possible explanation for the appearance of gas bubbles in insonified guinea pigs.[75] Finally, a comprehensive paper on rectified diffusion was recently published by Crum[76] and can be referred to for details.

The Governing Equations

A brief outline of the theory is now given, complete with the detailed equations to be used to make calculations of the threshold and the growth rate of bubbles by rectified diffusion. A complete mathematical description of the growth of a gas bubble by rectified diffusion would require an equation of motion for the bubble, diffusion equations for the liquid and the interior of the bubble, and heat conduction equations for both the liquid and the bubble. Continuity relations at the bubble wall would be required, and the situation is further complicated by the fact that these equations are coupled. Since this general approach presents a very formidable mathematical problem, various simplifications are required

to obtain a solution.

The approach used by Hsieh and Plesset[63] and by Eller and Flynn[65] is to separate the general problem into an equation for the motion of the bubble wall, and a diffusion equation for the concentration of gas dissolved in the liquid alone. We will use as the equation of motion for the gas bubble the well-known Rayleigh-Plesset[77] equation, given here by

$$R\ddot{R} + \frac{3}{2}\dot{R}^2 + \frac{1}{\rho}\{P_o[1-(R_o/R)^{3\eta}]\} \\ -P_A \cos \omega t + \rho R_o \omega_o b\dot{R}\} = 0, \tag{1-14}$$

where R and R_o are the instantaneous and equilibrium values of the bubble radius respectively, ρ is the liquid density, η the polytropic exponent of the gas contained within the bubble, P_A the acoustic pressure amplitude, ω the angular frequency, ω_o the small-amplitude resonance frequency and b is a damping term applied to the bubble pulsations. It is assumed that the damping is only important near bubble resonance and thus the expressions for the specific damping terms are only applicable near resonance.

Further, $P_o = P_\infty + 2\sigma/R_o$ where P_∞ is the ambient pressure. The small amplitude (linear) resonance frequency of the bubble, ω_o, is given by

$$\omega_o^2 = (1/\rho R_o^2)(3\eta P_o - 2\sigma/R_o). \tag{1-15}$$

The diffusion equation for the gas in the liquid is Fick's law of mass transfer and is given by

$$dC/dt = \partial C/\partial t + \underline{v} \cdot \nabla C = D\nabla^2 C, \tag{1-16}$$

where C is the concentration of gas in the liquid, $\underline{v}$ is the velocity of the liquid at a point, and D is the diffusion constant. The coupling between Eqs. (1-14) and (1-16) is through the convective term $\underline{v} \cdot \nabla C$, and

represents a major difficulty in the solution. This term was neglected by Blake[62] and resulted in a prediction for the threshold that was an order of magnitude too small. The problem with the moving boundary has been solved in two slightly different ways by Hsieh and Plesset[63] and by Eller and Flynn.[65] The details of their solutions can be found in their respective works; the solution of the latter will be used here.

It is shown by Eller and Flynn[65] that the time rate of change in the number of moles n of gas in a bubble is given by

$$dn/dt = 4\pi DR_o C_o \cdot \left[\langle R/R_o \rangle + R_o \left(\frac{\langle (R/R_o)^4 \rangle}{\pi Dt} \right)^{\frac{1}{2}} \right] H, \tag{1-17}$$

where C_o is the 'equilibrium' or 'saturation' concentration of the gas in the liquid in moles (unit volume)$^{-1}$, the pointed brackets imply time average, t is the time, and H is defined by

$$H = C_i/C_o - \langle (R/R_o)^4 \, (P_g/P_\infty) \rangle / \langle (R/R_o)^4 \rangle. \tag{1-18}$$

Here C_i is the concentration of dissolved gas in the liquid far from the bubble and P_g, the instantaneous pressure of the gas in the bubble, is given by

$$P_g = P_o (R_o/R)^{3\eta}. \tag{1-19}$$

As seen by the above equation, a polytropic exponent assumption is made for the pressure of the gas in the interior of the bubble. This assumption is commonly made and has been shown to be reasonably accurate for small-amplitude pulsations. There is evidence that it needs to be modified for moderate to large amplitude oscillations, however.

The values of R/R_o to be used in the equations above are obtained

by an expansion solution of Eq. (1-14) in the form

$$R/R_o = 1 + \alpha(P_A/P_\infty)\cos(\omega t + \delta) + \alpha^2 K(P_A/P_\infty)^2 + \ldots \tag{1-20}$$

where it has been determined that

$$\alpha^{-1} = (\rho R_o^2/P_\infty)[(\omega^2 - \omega_o^2)^2 + (\omega\omega_o b)^2]^{\frac{1}{2}} , \tag{1-21}$$

$$K = \frac{(3n + 1 - \beta^2)/4 + (\sigma/4R_oP_\infty)(6n + 2 - 4/3n)}{1 + (2\sigma/R_oP_\infty)(1 - 1/3n)} , \tag{1-22}$$

$$\delta = \tan^{-1}[\omega\omega_o b/(\omega^2 - \omega_o^2)] , \tag{1-23}$$

and

$$\beta^2 = \rho\omega^2 R_o^2/3nP_\infty . \tag{1-24}$$

It is necessary to know the damping of the bubble pulsations when the bubble is driven near resonance. This damping has been calculated by Eller[78] using the expressions of Devin;[79] a similar but not identical value for the damping term has also been obtained by Prosperetti.[77]

Because the pressure in the interior of the bubble is assumed to be given through the polytropic exponent approach, an accurate expression for the thermal damping cannot be given. Prosperetti[77] has shown that an estimate of this damping can be expressed through an "effective viscosity". Since the damping is only important near resonance (or at harmonics and subharmonics of the resonance frequency), and since the rectified diffusion equations are probably not accurate near resonance anyway, this nonrigorous approach will be followed for the present time.

The total damping constant, b, is assumed to be able to be written

as a sum of contributions due to the three common damping mechanisms, viz., thermal, viscous, and radiation:

$$b = b_t + b_v + b_r, \tag{1-25}$$

where

$$b_t = 3(\gamma-1)\left[\frac{X(\sinh X + \sin X) - 2(\cosh X - \cos X)}{X^2(\cosh X - \cos X) + 3(\gamma-1)X(\sinh X - \sin X)}\right] \tag{1-26}$$

with

$$X = R_o\,(2\omega/D_l)^{\frac{1}{2}}, \tag{1-27}$$

and

$$b_v = 4\omega\mu/3\eta P_\infty, \tag{1-28}$$

$$b_r = \rho R_o^3 \omega^3/3\eta P_\infty c, \tag{1-29}$$

with

$$\eta = \gamma(1 + b_t^2)^{-1}\left[1 + \frac{3(\gamma-1)}{X}\left(\frac{\sinh X - \sin X}{\cosh X - \cos X}\right)\right]^{-1} \tag{1-30}$$

In these equations γ is the ratio of specific heats and $D_l = K_l/\rho_l C_{pl}$, where K_l is the thermal conductivity of the gas in the bubble, ρ_l is the density of gas, C_{pl} is the specific heat at constant pressure for the gas, and μ is the viscosity and c is the speed of sound, both in the liquid. To obtain a usable expression for the growth-rate equation, the time averages $\langle R/R_o\rangle$, $\langle(R/R_o)^4\rangle$, and $\langle(R/R_o)^4\,(P_g/P_\infty)\rangle$ are required. It is found that

$$\langle R/R_o\rangle = 1 + K\alpha^2(P_A/P_\infty)^2 \tag{1-31}$$

$$\langle(R/R_o)^4\rangle = 1 + (3 + 4K)\alpha^2\,(P_A/P_\infty)^2 \tag{1-32}$$

and

$$\langle(R/R_o)^4(P_g/P_\infty)\rangle = \left[1 + \frac{3(\kappa-1)(3\kappa-4)}{4}\alpha^2(P_A/P_\infty)^2\right.$$

$$\left. + (4-3\kappa)K\alpha^2(P_A/P_\infty)^2\right]\left(1 + \frac{2\sigma}{R_o P_\infty}\right). \tag{1-33}$$

By assuming an ideal gas behavior, we can relate the equilibrium radius to the number of moles of gas by the equation

$$P_o = 3R_g T/(4\pi R_o^3) \quad , \tag{1-34}$$

where R_g is the universal gas constant and T is the absolute temperature. This equation should be a good approximation for small acoustic pressure amplitudes, so that the density fluctuations do not become excessive, and for low host-liquid temperatures, so that the ratio of vapor/gas within the bubble remains low. Such conditions would be met for normal experimental situations.

By combining Eqs. (1-17), (1-18) and (1-34), an expression is obtained for the rate of change of the equilibrium bubble radius with time:

$$\frac{dR_o}{dt} = \frac{Dd}{R_o}\left[\langle R/R_o \rangle + R_o\left(\frac{\langle (R/R_o)^4 \rangle}{\pi Dt}\right)^{1/2} \right] \cdot \left(1 + \frac{4\sigma}{3R_o P_\infty}\right)^{-1}\left(\frac{C_i}{C_o} - \frac{(R/R_o)^4 (P_g/P_\infty)}{\langle (R/R_o)^4 \rangle}\right) \quad , \tag{1-35}$$

where $d = R_g TC_o/P_\infty$.

In Eq. (1-35), the time averages $\langle R/R_o \rangle$, $\langle (R/R_o)^4 \rangle$ and $\langle (R/R_o)^4 (P_g/P_\infty) \rangle$ are given by Eqs. (1-31), (1-32) and (1-33), respectively. The threshold acoustic pressure for growth of a gas bubble is obtained by setting $dR_o/dt = 0$, and results in the equation

$$P_A^2 = \frac{(\rho R_o^2 \omega_o^2)\left[(1-\omega^2/\omega_o^2)^2 + b^2(\omega^2/\omega_o^2)\right](1 + 2\sigma/R_o P_\infty - C_i/C_o)}{(3+nK)(C_i/C_o) - \{[3(n-1)(3n-4)/4] + (4-3n)K\}(1 + 2\sigma/R_o P_\infty)} \quad . \tag{1-36}$$

Some questions of interest are:

i. bubble-bubble interactions. What is the nature of the interactions between bubbles? Is it governed by simple Bjerknes forces or is it more complex? Can a cloud of bubbles give rise to stronger efects than individual bubbles?

ii. propagation of sound through bubble mixtures. How is the propagation of sound affected by a bubbly mixture? At what concentration of bubbles does a saturation effect set in? What theoretical approaches are necessary to examine these phenomena?

stabilization mechanisms on cavitation inception by pulsed ultrasound? Are there frequency bandwidths to be avoided?

Nonlinear Bubble Dynamics

This area may seem esoteric and mathematically complex, but most sound fields of interest in sonochemistry are larger than 0.50 bar, a pressure amplitude above which nonlinear effects in bubble dynamics must be taken into account. Some areas that are as yet unexplained are:

i. damping mechanisms. What evidence is there that the damping at relatively large bubble pulsation amplitudes is properly accounted for by linear theories? How important is the discrepancy?

ii. noise production. What correlation exists between spectral components of the radius-time curve of a bubble and the radiated acoustic signals? Can the noise radiated by a cavitation field be related to the pulsations of individual gas bubbles?

iii. acoustic chaos. What relationships exist between the concept of deterministic chaos in nonlinear mechanics and the oscillation of a single gas bubble as it is driven at higher and higher amplitudes? Can this systematic approach to chaos be observed experimentally with a single bubble?

Cavitation Fields

This area was not discussed in this chapter. It refers to the fact that most cavitation utilized in sonochemistry is not due to isolated single bubbles but due to a collection of clouds of bubbles. These bubbles interact with each other and behave as a group, rather than individually.

VI. CONCLUDING REMARKS

The authors wish to take this opportunity to point out some of the phenomena of acoustic cavitation that they believe will be worthy of future investigation and that have promise of meaningful contributions to the advancement of science.

Cavitation Produced In Biological Tissue

High intensity ultrasound was once thought to be perfectly safe for widespread clinical use (and still is by perhaps the majority of investigators). However, there is an increasingly large body of information that suggests that cavitation is produced by both therapeutic and diagnostic ultrasound and that there may be risks associated with its use. Some areas that need future study are:

i. microbubble nucleation and stabilization. What are the nature of stabilized microbubbles in tissue? What is the stabilization mechanism? In what ways can they be activated? What is their anatomical distribution?

ii. biological effects. What are the damage mechanisms for cavitation in tissue: shock waves, high velocity jets, free radical production? Are the effects observable on a short-term macroscopic level, or only on a cellular or long-term level?

iii. continuous wave studies. Can the cavitation nuclei present in tissue be made to grow by rectified diffusion? Will the stable bubbles generate sufficiently high temperatures so as to produce free radicals? What are the requirements for growth in tissue?

iv. pulsed studies. Can one make the translation from cavitation in water to cavitation in tissue? What are the effects of nuclei

Apfel's numerical study enables one to obtain an estimate of the thresholds for cavitation inception and what type of cavitation is to be expected. Flynn has examined also the case of short-pulse excitation. In Flynn's study, the response of a small microbubble to a Gaussian acoustic pulse is examined. The wholly expected but vitally important result is that violent transient cavitation can be expected from acoustic pulses similar to those used in clinical diagnostic ultrasound devices. Figure 1-29 shows some typical results obtained by Flynn.

Fig 1-29

Recently, some experimental confirmation of these predictions have been obtained by Crum and Fowlkes.[94] In their study, they irradiated a liquid containing luminol, a light enhancing chemical, and observed light emission indicative of chemiluminescence for acoustic pluses as short as 1.0 μs. Shown in Fig. 1-30 are measurements of the cavitation threshold, as determined by sufficient levels of emitted light, as a function of pulse width for approximately 1.0 μs pulses of 1.0 MHz ultrasound. For this case the duty cycle was 1:10. Since there was some concern that the cavitation nuclei may be responding to the pulse repetition frequency rather than the individual pulses, an examination of the threshold as a function of duty cycle was made. Shown in Fig. 1-31 is the variation of the threshold with duty cycle and there are indications that a limiting threshold is expected.

Fig. 1-30

Fig. 1-31

These data give strong evidence that an extensive risk-assessment of diagnostic ultrasound should be carried out in the immediate future. Cavitation is a violent phenomenon, and at high frequencies, hard to detect. Further research in this area is greatly needed and promises exciting rewards.

resonance. Such a cavity could quite conceivably maintain its integrity (not break up) and would probably also radiate light by sonoluminescence. Fig. 1-27 Figure 1-27 describes sonoluminscence observed by an image intensifier camera from a cavitation field that in the view of the investigator contained stable cavities rather than transient ones.

Some important points can be made from these observations of the violent behavior exhibited by stable bubbles: if the bubbles oscillate with pulsation amplitudes sufficient to produce sonoluminescence, then there must be free radicals produced. If the free radicals are produced each cycle, then an enormous number of these highly reactive species could be produced as a result of the ultrasound. In fact, a larger number would be produced by "stable" bubbles that created free radicals each cycle than by transient events that destroyed themselves after each cycle. The authors believe that these results have important implications in the biological effects of therapeutic ultrasound in the light of the recent discovery that individual gas bubbles have been observed in the insonified region of living tissue.[58,90]

Transient Cavitation

A small gas bubble subject to an acoustic pressure amplitude of more than a few atmospheres will experience such violent radial pulsations that the wall velocity of the collapsing bubble will approach the velocity of sound. At this point, the likelihood is small that the bubble can maintain its physical integrity and will most probably shatter upon collapse. Apfel[91,92] and Flynn[93] have recently examined this problem in some detail and have published theoretical threshold curves for transient cavitation inception. Fig. 1-28 Figure 1-28 shows regions where transient cavitation is to be expected for insonification of water with high intensity ultrasound.

the large amplitude oscillations of a gas bubble to observe the spectral content of these pulsations. Figure 1-23 shows that when a bubble of 50 μm is driven at an amplitude of 1.05 bars of acoustic pressure amplitude, the bubble radius repeats itself with the same period as the driving frequency. This is called "period one" behavior and the Fourier spectrum shows only harmonics of the driving frequency. Figure 1-24 shows that when the amplitude is increased slightly to 1.15 bars, the radius now repeats itself after <u>two</u> cycles of the driving frequency. This is called "period two" behavior and the spectrum now indicates the presence of a strong subharmonic. Because the presence of the subharmonic is easily detected and because it is somewhat indicative of violent bubble behavior, it is often used as a criterion for cavitation inception. These figures indicate to us that such a definition of cavitation inception is arbitrary, at best.

Fig. 1-23

Fig. 1-24

As an interesting sidelight of bubble oscillations, one can follow this bifurcation sequence from period one to period two, from two to four, from four to eight, etc, until the bubble exhibits chaotic behavior that has some inherent determinism. Figure 1-25 shows a plot of a systematic progression to chaos following the bifurcation scheme described above. This new area of nonlinear mechanics is of considerable current interest and activity.

Fig. 1-25

Finally, Prosperetti et al [89] have recently obtained a more precise formulation of the bubble-oscillation problem enabling one to numerically estimate the temporal and spatial dependence of the temperature and pressure within a "stable" oscillating bubble. Figure 1-26, for example, shows that a bubble of 50 μm driven at a relatively modest acoustic pressure amplitude of 0.5 bars can reach an internal temperature of nearly 3000°K when driven at a driving frequency that is near its second harmonic

Fig. 1-26

required to introduce these nonlinear effects was on the order of 0.25 bar (0.025 MPa).

Fig 1-21

To follow up on this point, Consider Fig. 1-21 which is a plot of the relative pulsation amplitude, $X_m = (R_{max} - R_o)/R_o$, versus the ratio of the driving frequency to the resonance frequency for a 1.0 μm bubble in water. The figure shows the results of a numerical calculation by Lauterborn and an approximate analytical solution by Prosperetti[88] of the Rayleigh - Plesset equation. Note that a smooth linear resonance curve is not observed; there is, in fact, considerable nonlinear structure in the form of higher harmonics. The amplitude of these higher harmonics can be quite considerable. Some experimental confirmation of these results are shown in

Fig. 1-22

Fig. 1-22. This plot shows the variation of the Levitation Number, a useful nondimensional number that is quite similar to the X_m of Lauterborn and Prosperetti, plotted versus the ratio of the measured radius to the resonance radius (approximately equal to ω/ω_o) for an air bubble in a glycerine/water mixture. The experimental points show that this nonlinear behavior is easily observed; the solid curves are theoretical calculations that indicate that there is not good agreement between the calculated and measured values. The dashed curve shows the analytical result that one would expect if one assumes a polytropic approximation; the solid curve is a numerical result in which the internal pressure is calculated directly, and the thermal damping obtained from this result. It is seen that the damping is still overestimated and further work needs to be done in this area.

If one examines the oscillations of a stable gas bubble driven at higher and higher amplitudes, it is seen that not only are a wide spectrum of harmonics generated by the pulsating bubble, but also a series of subharmonics and ultraharmonics. We have examined in a numerical manner

this form of damping. On the other hand, retaining the internal pressure as a spatially and temporally varying quantity introduces a nearly intractable complication. The damping problem was circumvented somewhat by Prosperetti who introduced an "effective viscosity" that could account for the additional contributions of thermal and radiation damping. Thus, one can obtain a linearized solution to the Rayleigh - Plesset equation that gives a first-order approximation to the behavior of a pulsating gas bubble in a liquid.

The linear or first-order approach to this problem is to assume the internal pressure is given by the polytropic approximation and the radius of the bubble can be written as

$$R = R_o (1 + x) \qquad (1\text{-}42)$$

where x is given by Eqs. (1-20) through (1-24). This approach enables one to obtain an analytical expression that closely approximates the threshold and growth rate for rectified diffusion, as shown earlier in Figs. 1-17 and 1-18, and enables one to indirectly measure the variation of the polytropic exponent with bubble radius, as shown in Fig. 1-20. This figure shows that the linear approximation described above gives a general description of the variation of the polytropic exponent with bubble radius until the ratio of bubble size to resonance size approaches the value 0.5. At this point, the second harmonic resonance of the bubble is excited and the agreement between the linear theory and the experimental measurements fails.

Fig. 1-20

This failure demonstrates an important caveat that must be acknowledged when dealing with the oscillations of a gas bubble in a liquid: a pulsating gas bubble is a highly nonlinear system and its nonlinear behavior can be activated at very low values of the acoustic pressure amplitude. For example, the average acoustic pressure amplitude

specific heat at constant volume, and K is the thermal conductivity of the fluid.

It would be a formidable task indeed to solve these coupled equations for the variables of interest within the bubble: the temporally and spatially dependent pressure and temperature, the radial displacement and the velocity of the bubble interface. A great deal of effort has been expended to approximate these equations in such a way as to obtain results that can be compared with the limited experimental results presently available. It is beyond the scope of this chapter to describe these approaches in any detail; rather, we refer the reader to the classic papers of Rayleigh,[5] Plesset,[82] Noltingk and Neppiras,[83] and Poritsky.[84] Further, some recent reviews by Neppiras,[85] Apfel,[44] Flynn,[86] and Prosperetti[87] provide a wealth of information on this topic.

In order to describe some results applicable to this study, we shall examine perhaps the most widely-used equation, the Rayleigh - Plesset equation, given earlier as Eq. (1-14) and repeated below in a somewhat different form

$$\rho(R\ddot{R} + 3\dot{R}^2/2) = [P_i(R,t) - P_A(t) - 2\sigma/R - 4\mu\dot{R}/R], \qquad (1\text{-}40)$$

where in this case we have not made the polytropic approximation

$$P_i = P_\infty (R_o/R)^{3n}, \qquad (1\text{-}41)$$

although in some cases we shall wish to do so. The problem with applying Eq. (1-41) above to realistic situations is that if one makes the polytropic approximation, then unless one considers very small bubbles or very high frequencies, the viscous damping term inadequately accounts for the damping. For regions of common interest, the principle damping mechanism is thermal in origin; however, introducing the internal pressure via the polytropic exponent removes the phase information that accounts for

V. BUBBLE DYNAMICS

Introduction

In order to examine the effect of an acoustic field on a liquid it is desirable to first understand the response of a single bubble to an oscillating pressure field. In this section we present the general equations of bubble dynamics and examine in a restricted way the theoretical and experimental behavior of a pulsating bubble in a liquid.

Stable Cavitation

We consider a spherical bubble containing gas and vapor present in a liquid that extends to infinity. To adequately account for the motion of the bubble interface, it is necessary to solve the equations of conservation of mass, momentum, and energy for both the gas and liquid phases, and, as a boundary condition, match these equations at the interface between the gas and the liquid. These equations are:

conservation of mass

$$\frac{1}{\rho}\left[\frac{\partial p}{\partial t} + u\frac{\partial p}{\partial r}\right] = -\left[\frac{\partial u}{\partial r} + \frac{2u}{r}\right] \tag{1-37}$$

conservation of momentum

$$\frac{\partial u}{\partial t} + u\frac{\partial u}{\partial r} = -\frac{1}{\rho}\frac{\partial \rho}{\partial r} \tag{1-38}$$

conservation of energy

$$\rho c_v\left[\frac{\partial T}{\partial t} + u\frac{\partial T}{\partial r}\right] = K\nabla^2 T - p\nabla\cdot u \tag{1-39}$$

In these equations, ρ is the density, u is the radial velocity, r is the radial distance, p is the pressure, T is the temperature, c_v is the

So far, our analysis in this section has been limited to the rectified diffusion threshold. It is in order also to examine the rate of growth by rectified diffuion when the acoustic pressure amplitude exceeds the threshold. An examination of the growth (or decay) of a bubble is shown in Fig. 1-18. The symbols are experimental measurements; the curves were obtained by numerical integration of Eq. (1-36). It was observed by Eller[67] that his measurements of the growth rate were considerably larger than predicted by theory. Gould[68] later confirmed the excessive growth rates but also noticed that surface oscillations, with their associated acoustic streaming, were probably the explanation for the increased growth rates that he observed.

Fig. 1-18

Shown in Fig. 1-19 are some observations of growth rates made by Crum.[73] He observed an agreement between the measured and predicted rates provided surface oscillations were avoided, and provided that the water was relatively pure and free of surface-active contaminants. When surface-active agents were added to the water, growth rates much higher than predicted were observed. Among the explanations offered for this effect were that (a) the surface active agents were behaving as a rectifying agent, permitting more diffusion in than out, and (b) acoustic streaming was occurring in the absence of surface oscillations, induced somehow by the surface contamination. This interesting anomaly has not yet been explained.

Fig. 1-19

In general, then, one can say that except for region of low surface tension, the concept of rectified diffusion is rather well understood and can be described with considerable accuracy by a straight-forward analytical theory, provided, of course, that one drives the bubble in its linear range of pulsation amplitudes.

Some Experimental Results

In this section a graphical representation of the equations is presented as a function of the various physical parameters that are applicable. Some measurements of thresholds and bubble growth rates are also given for comparison. In these figures, unless specific mention is made otherwise, it is assumed that we are considering an air bubble in water with the following set of experimental conditions: $P_\infty = 1.01 \times 10^6$ dyn cm^{-2}, $\sigma = 68$ dyn cm^{-1}, $\rho = 1.0$ g cm^{-3}, $D_1 = 0.20$ cm^2 s^{-1}, $\mu = 1.0 \times 10^{-2}$ g cm^{-1} s^{-1}, $c = 1.48 \times 10^6$ cm s^{-1}, $\gamma = 1.4$, $T = 293$ K, $D = 2.4 \times 10^{-5}$ cm^2 s^{-1} and $d = 2.0 \times 10^{-2}$.

Central to the study of rectified diffusion are measurements of the acoustic pressure amplitude required for bubble growth and the agreement between these measurements and the applicable theory. Shown in Fig.1-17 are measurements of the threshold for a frequency of 22.1 kHz along with the theoretical calculations. The solid curve is the prediction of Eq. (1-36); the dashed line is a simplified version of the threshold. (See reference [75]).

Fig. 1-17

The agreement between theory and experiment (for this limited range of bubble radii) is seen to be rather good and within the range of experimental error. This bubble range is particularly important at this frequency because it partially bridges the gap between isothermal behavior (for $R_o = 20$ μm, $n = 1.01$) and adiabatic behavior (for $R_o = 80$ μm, $n = 1.23$) of the bubble pulsations. The gradual reduction in the threshold as the bubble radius increases is mostly due to the fact that as the bubble grows toward resonance size its pulsation amplitude increases, which results in more rectified mass transfer per cycle.

driven at its $(r, \theta, z) = (2, 0, 2)$ mode at a frequency of 22.1 kHz.

When a standing wave exists in the liquid, an acoustic radiation pressure force, commonly called the primary Bjerknes force[80] is exerted on air bubbles that draw them toward a pressure antinode if they are less than resonance size and force them toward the nodes if they are larger than resonance size. Because of gravity, there is also a constant (essentially) force of buoyancy on a gas bubble in a liquid, and this force is always directed upward. Since the primary Bjerknes force[81] is proportional to the acoustic pressure, which varies with position, there exist positions of stable equilibrium for the bubble in the "levitation chamber" somewhat above the position of the pressure antinode. With a little practice, one can easily position a bubble within the field and monitor this position with a cathetometer.

The normal approach is then to establish a fixed acoustic pressure amplitude within the chamber, which essentially fixes the position of the bubble (the position is independent of the radius if the bubble is sufficiently smaller than resonance size). The radius is then measured with some technique (such as permitting the bubble to rise at its terminal velocity, measuring this velocity, and then determining the radius from an applicable drag law) as a function of time. For threshold measurements, the acoustic pressure amplitude is constantly adjusted to ascertain the value for which a bubble of measured size neither grows nor dissolves.

With this technique it appears that rectified diffusion threshold measurements can be made to within an accuracy of approximately 5%. The radii measurements depend upon the applicability of the drag law, and its specific accuracy, but are probably good to within a few percent also.

These expressions in Eqs. (1-35) and (1-36) are the governing equations for rectified diffusion and enable one to obtain the threshold for inception of growth and the rate of this growth. The growth rate equation (1-35), also applies below the threshold, and with $P_A = 0$, describes the case for diffusion in the absence of an applied sound field. Reference [76] shows that these equations can be considerably reduced in complexity when one examines restricted ranges of bubble size, acoustic frequency, etc. The reader is referred to these equations if Eqs. (1-35) and (1-36) appear too formidable. However, the authors have found that the equations need to be evaluated with a computer anyway, and one might just as well put in the general forms that are applicable over a wide range of parameters.

Experimental Technique for Examining Rectified Diffusion

In this section is presented a brief description of the principal experimental technique used to make measurements of growth of bubbles by rectified diffusion. This technique was first utilized by Strasberg[64] with some modifications by Eller[67] and Gould.[68]

The main feature of the technique is the isolation of a single gas bubble in an acoustic stationary wave, with the ability to determine the bubble radius accurately and quickly. The specific description of the technique used by Crum is now given. Refer to Fig. 1-16 for a diagram of the experimental apparatus.

Fig. 1-16

The stationary wave system was constructed by cementing a hollow glass cylinder between two matched hollow cylindrical transducers, fitted with a flexible pressure release diaphragm on one end and open at the other. The composite system was approximately 7.5 cm in diameter by 10 cm in height, with the width of the glass in the middle about 2.5 cm. This system was

REFERENCES

1. Tomlinson, C. Phil. Mag. 1867, 34, 136, 220.

2. Gernez, M. Phil. Mag. 1867, 33, 379.

3. Bernoulli, D. Hydrodynamica, sive de viribus et motibus fluidorum comentarii Strasbourg, 1738.

4. Freed D.; Walker, W.F. "Notes on the history of cavitation", in Cavitation and Multiphase Flow Forum — 1984 Hoyt, J.W. Ed.; 1, 1984.

5. Lord Rayleigh. Phil. Mag. 1917, 34, 94.

6. Blake, F.G. "The tensile strength of liquids: A review of the literature", Tech. Memo No. 9 Harvard Acoustics Research Laboratory, 1949.

7. Klein, E. J. Acoust. Soc. Am. 1948 20, 601.

8. Kornfeld, M.; Suvorov, L. J. Appl. Phys. 1944 15, 495.

9. Briggs, L.J. J. Appl. Phys. 1950, 21, 721.

10. Dean, R.B. J. Appl. Phys. 1944 15, 446.

11. Harvey, E.N., Barnes, K.K; McElroy, W.D; Whitely, A.H; Pease, D.C.; Cooper, K.W; J. Cell. Comp. Physiol. 1944 24 1.

12. Briggs, H.B.; Johnson, J.B.; Mason, W.P. J. Acous. Soc. Am. 1947, 19, 664.

13. Seitz, F. Phys. Fluids. 1958, 1, 2.

14. Lieberman, D. Phys. Fluids. 1959, 2, 466.

15. Fox, F.; Herzfeld, K. J. Acoust. Soc. Am. 1954, 26, 984.

16. Strasberg, M. J. Acoust. Soc. Am. 1959, 31, 163.

17. Connolly, W.; Fox, F. J. Acoust. Soc. Am. 1954, 26, 843.

18. Galloway, W. J. Acoust. Soc. Am. 1954 26k, 849.

19. Sette, D.; Wanderlingh, F. Phys. Rev;. 1962, 125, 409.

20. Akulichev, V. Sov. Phys. Acoust. 1966, 12, 144.

21. Greenspan, M.; Tschiegg, C. J. Res. Nat. Bur. Stds. 1967, 71C, 299.

22. Apfel, R. J. Acoust. Soc. Am. 1970, 48, 1179.

23. Apfel, R. J. Chem Phys. 1971, 54, 62.

24. Crum, L. Nature. 1979, 278, 148.

25. Winterton, R. J. Phys. D: Appl. Phys. 1977, 10, 2041.

26. Yount, D. J. Acoust. Soc. Am. 1979, 65, 1429.

27. Sirotyuk, M. Sov. Phys. Acoust. 1970 16, 237.

28. Yount, D. J. Acoust. Soc. Am. 1982, 71, 1473.

29. Ward, C.A.; Balakrishnav. A.; Hooper, F.C. J. Basic Engr. 1970, 92, 695.

30. Tikuisis, P; Ward, C.A.; Venter, R.D. J. Appl. Phys. 1983, 54, 1833.

31. Atchley, A.A. Ph.D. Dissertation. The University of Mississippi, 1984.

32. Atchley, A. A.; Prosperetti, A. Submitted for publication to J. Acoust. Soc. Am. 1985.

33. Apfel, R. J. Acoust. Soc. Am. 1971, 49, 145.

34. Döring, W. Z. Phys. Chem. 1937, B36, 371.

35. Döring, W. Z. Phys. Chem. 1936, B38, 292.

36. Volmer, M. "Kinetik der Phasenbildung" in Die Chemische Reaktion Band IV. 1939, Verlag von Theodor Steinkopff, Dresden and Leipzig.

37. Fisher, J. J. Appl. Phys. 1948, 19, 1062.

38. Epstein, P.; Plesset, M. J. Chem. Phys. 1950, 18, 1505.

39. Arnold, H.D. Phil. Mag. 1911, 22, 755.

40. Langmuir, I. J. Am. Chem. Soc. 1917, 39, 1848.

41. Herzfeld, K. "Proc. First Sympos. Naval Hydrodynamics", F.S. Sherman, Ed.; 1957, 319.

42. Alty, T. Proc. Roy. Soc.. 1924, A106, 315.

43. Alty, T. Proc. Roy. Soc. 1926, A112, 235.

44. Apfel, R. In "Ultrasonics" Edmonds, P. Ed; Academic Press: New York, 1981, Vol. 19, Chapter 7, pp. 355-441.

45. Hayward, A. J. Phys. D: Appl. Phys. 1970, 3, 574.

46. Bargeman, D.; Van Voorst Vader, F. J. Colloid and Interf. Sci. 1973, 42, 467.

47. Washburn, E.W. Ed. International Critical Tables, McGraw-Hill: New York, 1928, Vol. 3, 257.

48. Weast, R. C. Ed. Handbook of Chemistry and Physics, CRC Press: Cleveland, 1975, 56th Edition, F-43.

49. Eisenberg, D.; Kauzmann, W.; The Structure and Properties of Water. Oxford University Press: Oxford, 1969, 61-62.

50. Willard, G.W. J. Acoust. Soc. Am. 1953, 25, 669.

51. Meyer, E.; Newmann, E. "Physical and Applied Acoustics-An Introduction". Academic Press: New York, 1972.

52. J. Ultrasound. Med. 1983, 2, No. 4, S7.

53. Barger, J. "Thresholds of Acoustic Cavitation in Water", Tech. Memo. No 57 Harvard Acoustics Research Laboratory, 1964.

54. Vaughn, P.W.; Graham, E.; Leeman, S. App.Sci. Res. 1982, 38, 45.

55. Roy, R. A.; Atchley, A.A; Crum, L.A.; Fowlkes, J.B.; Reidy, J.J. "A Precise Technique for the Measurement of Acoustic Cavitation Thresholds and Some Preliminary Results" Accepted for Publication in J. Acoust. Soc. Am.

56. Crum, L.A. In "Cavitation and Inhomogeneities in Underwater Acoustics", Lauterborn, W. Ed.; Springer - Verlag: New York, 1980, p.84.

57. Crum, L.A.; Brosey, J.E. J. Fluid Engr. 1984, 106, 99.

58. ter Haar, G.; Daniels, S. Phys. Med. Biol 1981, 26, 1145.

59. Sommer, F.G.; Pounds, D. Med Phys. 1982, 9, 1.

60. Neppiras, E.A.; Coakley, W.T. J. Sound Vib. 1970, 45, 341.

61. Apfel, R. E. J. Acoust. Soc. Am. 1981, 69, 1624.

62. Blake, F.G. "The Onset of Cavitation in Liquids", Tech. Memo. No. 12 Harvard Acoustics Research Laboratory, 1949.

63. Hsieh, D.Y.; Plesset, M.D. J. Acoust. Soc. Am. 1961, 33, 206.

64. Strasberg, M. J. Acoust. Soc. Am. 1961, 33, 359,

65. Eller, A. I.; Flynn, H.G. J. Acoust. Soc. Am. 1965, 37, 493.

66. Safar, M.H. J. Acoust. Soc. Am. 1968, 43, 1188.

67. Eller, A.I. J. Acoust. Soc. Am. 1969, 46, 1246.

68. Gould, R. K. J. Acoust. Soc. Am. 1974, 56, 1740.

69. Davison, B.J. J. Sound Vib. 1971, 17, 261.

70. Kapustina, O. A.; Statnikov, V.G. Sov. Phys. Acoust. 1968, 13, 327.

71. Skinner, L.A. J. Acoust. Soc. Am. 1972, 51, 378.

72. Eller, A.I. J. Acoust. Soc. Am. 1975, 57, 1374.

73. Crum, L.A. J. Acoust. Soc. Am. 1980, 68, 203.

74. Lewin, P. A.; Bjorno, L. J. Acoust. Soc. Am. 1981, 69, 1624.

75. Crum, L.A.; Hansen, G.M. Phys. Med. Biol. 1982, 27, 413.

76. Crum, L.A. Ultrasonics 1984, 22, 215.

77. Prosperetti, A. J. Acoust. Soc. Am. 1977, 61, 17.

78. Eller, A.I. J. Acoust. Soc. Am. 1970, 47, 1469.

79. Devin, C. J. Acoust. Soc. Am. 1959, 31, 1654.

80. Bjerknes, V.F.K. Die Kraftfelder 1909, Vieweg and Sohn: Braunschweig.

81. Crum, L.A. J. Acoust. Soc. Am. 1975, 57, 1363.

82. Plesset, M. In "Cavitation in Real Liquids", Davies, R. Ed.; American Elsevier: New York, 1, 1964

83. Noltingk, B.E.; Neppiras, E.A.; Proc. Phys. Soc. London 1951, B64, 1032.

84. Poritsky, H. In "Proc. First. U.S. Naval Congress. Appl. Mechj." Sternberg, E. Ed.; Am. Soc. Mech. Engr.: New York, 1952, 813.

85. Neppiras, E.A. Phys. Rep. 1980, 61, 159.

86. Flynn, H.G. In "Physical Acoustics" Mason, W.P. Ed.; Academic Press: New York, 1964, Vol. IB, Chapter 9, pp. 57-172.

87. Prosperetti, A. Ultrasonics 1984, 22, 77.

88. Prosperetti, A. J. Acoust. Soc. Am. 1974, 56, 878.

89. Prosperetti, A.; Commander, K.; Crum, L.A. to be published.

90. ter Haar, G.; Daniels, S.; Eastaugh, K.C.; Hill, C.R.; Br. J. Cancer 1983, 45 Supp 5.

91. Apfel, R., Br. J. Cancer. 1982, 45. Supp 5, 140.

92. Apfel, R. In "Cavitation and Inhomogeneities in Underwater Acoustics", Lauterborn, W. Ed.; Springer - Verlag: New York, 1980, p. 79.

93. Flynn, H. G., J. Acoust. Soc. Am. 1982, 72, 1926.

94. Crum, L.A.; Fowlkes, J.B. to be published.

FIGURE CAPTIONS

1-1. Graph of liquid pressure at vaporization versus temperature for ether droplets in glycerine. (Reproduced with permission, Ref. [33].)

1-2. Stability curves for gas bubbles in water at various dissolved gas concentrations and surface tensions. If a gas bubble lies above the appropriate line, it will grow by diffusion at zero acoustic pressure amplitude; if it lies below, it will dissolve.

1-3. Illustration of two possible cavitation nuclei. a) This drawing illustrates an organic skin nucleus, ie, a bubble stabilized by a skin of polar surfactant molecules. The nucleus is surrounded by a thin layer of nonaligned molecules in a reservoir. (Ref. [28]) b) This drawing illustrates the stabilization of a gas pocket in a crack in a hydrophobic solid. (Ref. [24])

1-4. Graph of cavitation threshold versus dissolved ion concentration of KI in water with a gas tension of 0.30 bar. The data points are Atchley's (Ref. [31]). The dash line indicates the trend of Akulichev's measurements (Ref. [20]) made in water with gas a tension of 0.13 bar.

1-5. Diagram of a closed system illustrating the identification of the various pressures involved in cavitation nucleation. The system consists of a gas and vapor filled space above a liquid in which exists a hydrophobic solid containing a gas and vapor filled crevice.

1-6. Graph of cavitation threshold versus gas tension for crevices larger than critical size. The solid line is the prediction of Eq. (1-10) with $\beta = 12.85^{\circ}$, $\alpha_H = 22.15^{\circ}$ and $\sigma = 70$ dyn/cm. The data are Strasberg's (□) (Ref. [16]), Galloway's (◇) (Ref. [18]), and Connolly and Fox's (◆) (Ref. [17]). In Fig. 1-6a, G ranges from zero to one bar, while in Fig. 1-6b, G ranges from zero to 0.1 bar.

1-7. Graph of cavitation threshold versus gas tension for crevices smaller than critical size. The lines are the predictions of Eq. (1-10) for $\beta = 12.85^{\circ}$, $\alpha_H = 22.15^{\circ}$, $\sigma = 70$ dyn/cm and various values of a_1.

1-8. Graph of normalized cavitation threshold versus gas tension. The upper curve is the predicted threshold from Fig. 1-6a and the lower curve is the predicted threshold from Fig. 1-7 for $a_1 = 15$nm.

1-9. Graph of cavitation threshold versus surface tension for water for different values of gas tension. The data are Crum's (Ref. [24]) and the curves are the predictions of Eq. (1-10) using $\beta = 12.85^{\circ}$ and $\alpha_H = 22.15^{\circ}$ for G = 0.47 bar and $\beta = 10.8^{\circ}$ and $\alpha_H = 24.2^{\circ}$ for G = 0.19 bar.

1-10. Graph of cavitation threshold versus temperature for water. The data are Galloway's (□) (Ref. [18]) and Crum's (■) (Ref. [24]) and have been normalized to fit the theory at room temperature. The curves are the predictions of Eq. (1-10) with $\beta = 12.85^{\circ}$ and $\alpha_H = 22.15^{\circ}$ for the indicated values of G.

1-11. Graph of cavitation threshold versus applied static pressure. The arrow indicates the direction of the change in static pressure

(After Crum, Ref [56].).

1-12. Schematic diagram of the fluid management system of the experimental apparatus developed by Roy, et al (Ref. [55]).

1-13. Schematic diagram of the cavitation generation system of the experimental apparatus developed by Roy, et al (Ref. [55]).

1-14. Schematic diagram of the cavitation detection system of the experimental apparatus developed by Roy, et al (Ref. [55]).

1-15. Reproduction of a strip chart record illustrating the technique for threshold measurements and the reproducibility of the data. The liquid was distilled water having a gas tension of 0.50 bar, a surface tension of 71.3 dyn/cm, a temperature of 23.0^{o}C and circulated through a 20 μm filter. (Ref. [55])

1-16. Diagram of experimental apparatus for use in rectified diffusion measurements.

1-17. Variation of the threshold for growth by rectified diffusion of an air bubble in water as a function of the bubble radius for a frequency of 22.1 kHz, a surface tension of 68 dyn/cm and a gas tension of 1 bar. The data are experimental measurements; the solid line is calculated from Eq. (1-36); the dashed line is from a less complicated expression from Ref. [76].

1-18. Variation of bubble radius with time for a liquid surface tension of 68 dyn/cm and an acoustic pressure of 0.27 bar. The liquid has a gas tension of 1.0 bar. The solid lines are calculated by numerical integration of Eq. (1-35).

1-19. Dependence of bubble radius on time for an air bubble undergoing rectified diffusion in water. The curves are the result of numerical integration of Eq. (1-35). The lower two curves are for distilled water having a surface tension of 68 dyn/cm and different values of the acoustic pressure amplitude. The upper curve is for water containing surfactants.

1-20. Variation of the polytropic exponent with bubble radius for air bubbles in water. The symbols are experimental measurements and the solid line is the theoretical prediction.

1-21. Variation of the relative pulsation amplitude with normalized frequency for 1.0 μm radius air bubble in water indicating the analytical and numerical response of the bubble to a pressure amplitude of 0.9 bar. Note the highly nonlinear behavior.

1-22. Variation of the levitation number with normalized bubble radius for an air bubble in a glycerine/water mixture. The solid line represents a numerical solution of Eq. (1-14) using a polytropic approximation and an "effective viscosity" used to account for thermal damping. The broken line is a result from Ref. [88] which calculates thermal damping directly from internal pressure. The driving frequency was 22.2 kHz and the resonance radius of the bubble was 138 μm.

1-23. Radius-time curves and frequency spectrum plots for a gas bubble oscillating under the stated conditions.

1-24. Radius-time curves and frequency spectrum plots for a gas bubble oscillating under the stated conditions.

1-25. Graph of maximum bubble radius at zero pressure amplitude. The pattern, or Feigenbaum "tree", shows the systematic sequence of bifurcations leading to chaos for a gas bubble of 50 μm driven at approximately half its resonance frequency.

1-26. Variation of the temperature inside a pulsating gas bubble as a function of time for different values of the driving frequency. The bubble has a radius of 50 μm and the acoustic pressure amplitude is 0.6 bars.

1-27. Photographs taken from a video monitor of sonoluminescence activity viewed by an image intensifier tube for increasing levels of acoustic pressure amplitude. The horn is driven at its lowest level in (a) and at its highest level in (f), where the standing wave pattern is disrupted by violent cavitation on the horn tip. The "layers" of activity are due to bubbles trapped near antinodal planes separated by approximately a half wavelength.

Switch caption numbers

1-28. Graph of acoustic pressure amplitude (upper curve) and relative bubble radius (lower curve) versus nondimensional time. The acoustic pulse has a frequency of 2.25 MHz, a maximum pressure amplitude of 4.75 bars, and a width of 1 μs. The bubble has an equilibrium radius of 1 μm. (Reproduced with permission, Ref. [93].)

1-29. Cavitation prediction chart for a frequency of 1.0 MHz, a gas tension of 1.0 bar, and a bubble of resonance frequency 3.25 μm. The ordinate is the threshold radius divided by the resonance radius and the abscissa is the normalized acoustic pressure. The hatched areas indicate regions of different cavitation behavior: In region

A, growth is by rectified diffusion. In region C, bubbles will become transient. In region B, growth by rectified diffusion is dominant; however, transient cavitation can occur if bubbles grow to resonance size by rectified diffusion. The curves labeled R_D, R_B, R_I, and R_T denote limits for bubbles to grow by rectified diffusion, mechanical instability (Blake threshold), inertial processes, or by becoming transient, respectively. (Reproduced by permission, Ref. [92].)

1-30. Graph of cavitation threshold versus pulse length for a duty cycle of 1:10. The points are from Ref. [94]; the error bars indicate $\pm$ one standard deviation. The acoustic frequency was 1.0 MHz and the liquid was water containing luminol and saturated with argon.

1-31. Variation of the cavitation threshold of water containing luminol with duty cycle for a pulse length of approximately 1 μs. The acoustic frequency was 1.0 MHz and the data are from Ref. [94].

Figure 1-1

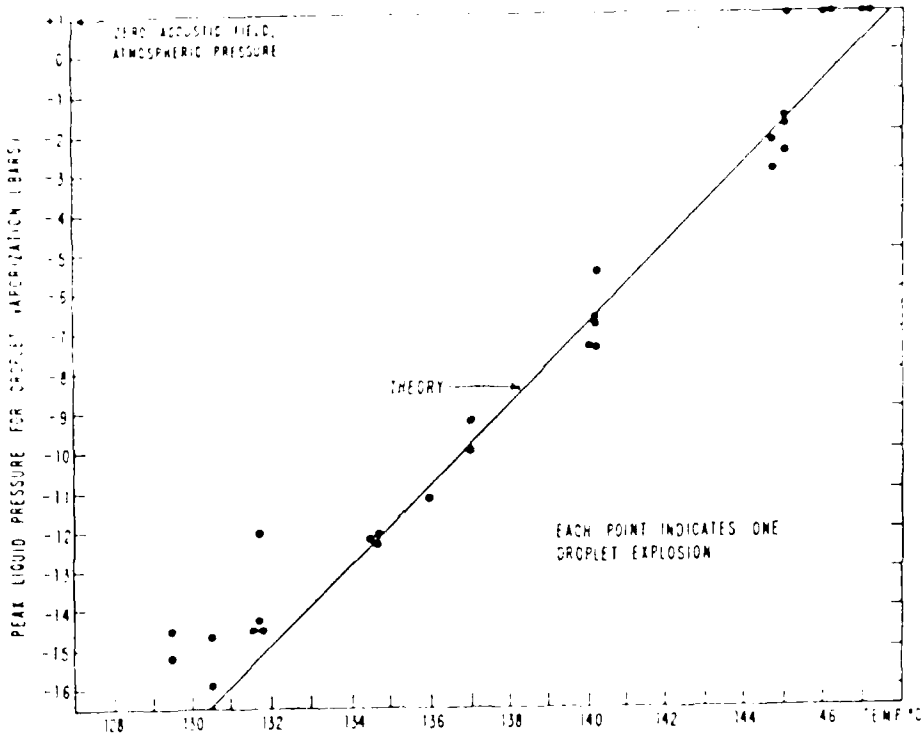
ZERO ACOUSTIC FIELD,
ATMOSPHERIC PRESSURE
THEORY
EACH POINT INDICATES ONE
DROPLET EXPLOSION
0
-1
-2
-3
-4
-5
-6
-7
-8
-9
-10
-11
-12
-13
-14
-15
-16
128
130
132
134
136
138
140
142
144
146

Figure 1-2

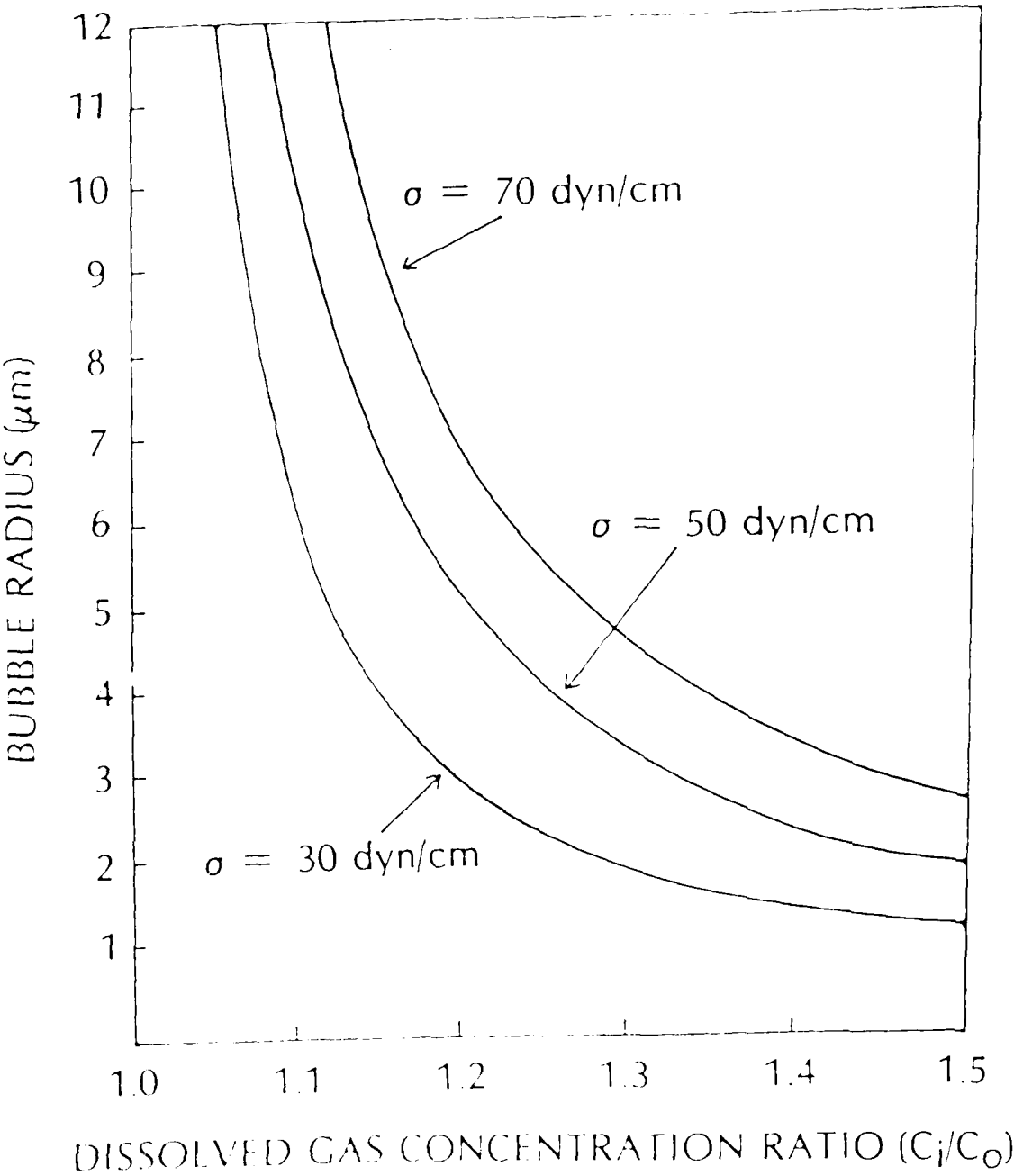
12
11
10
9
8
7
6
5
4
3
2
1
BUBBLE RADIUS (μm)
σ = 70 dyn/cm
σ = 50 dyn/cm
σ = 30 dyn/cm
1.0
1.1
1.2
1.3
1.4
1.5
DISSOLVED GAS CONCENTRATION RATIO (Ci/Co)

Figure 1-3a

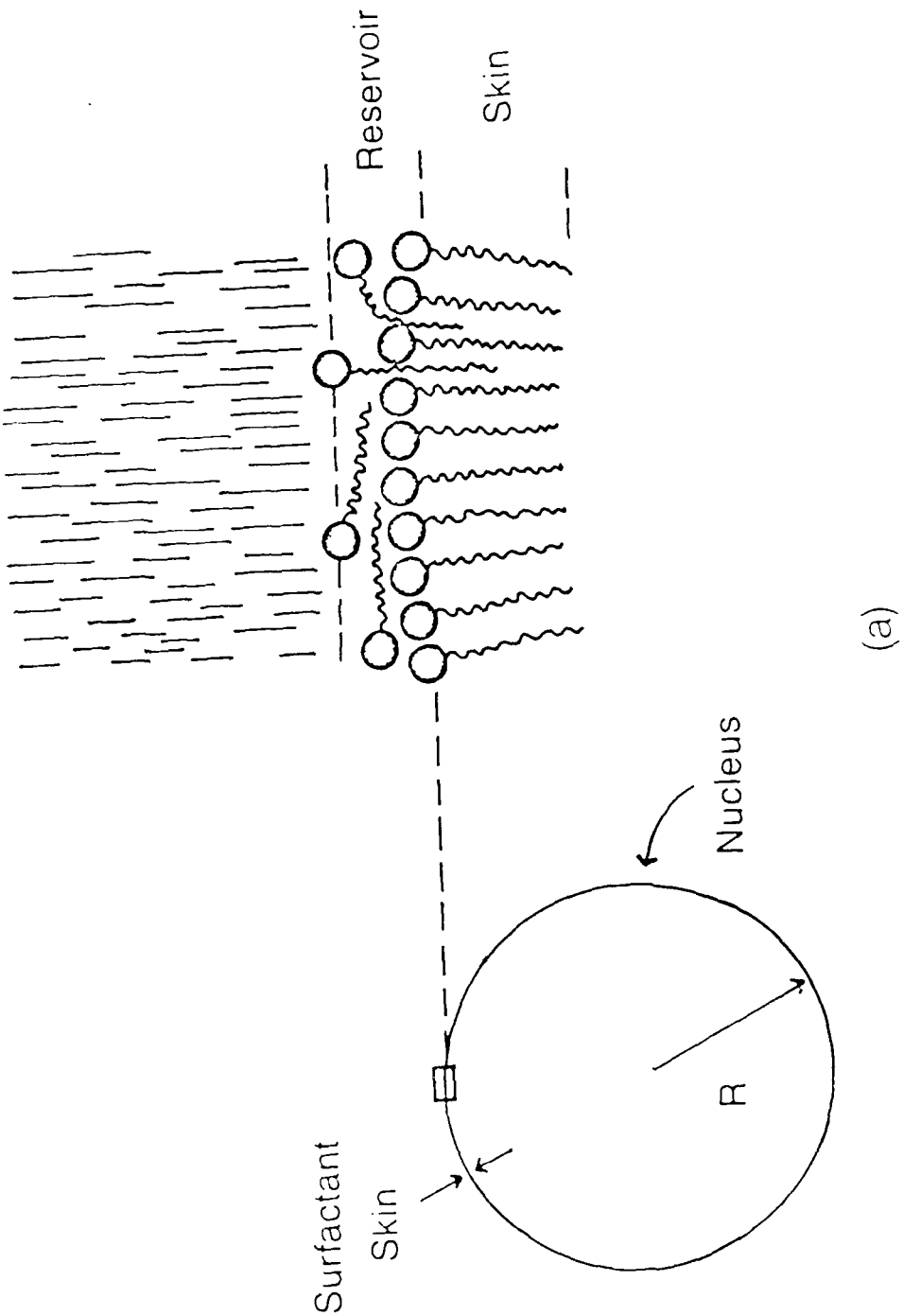

Figure 1-3b

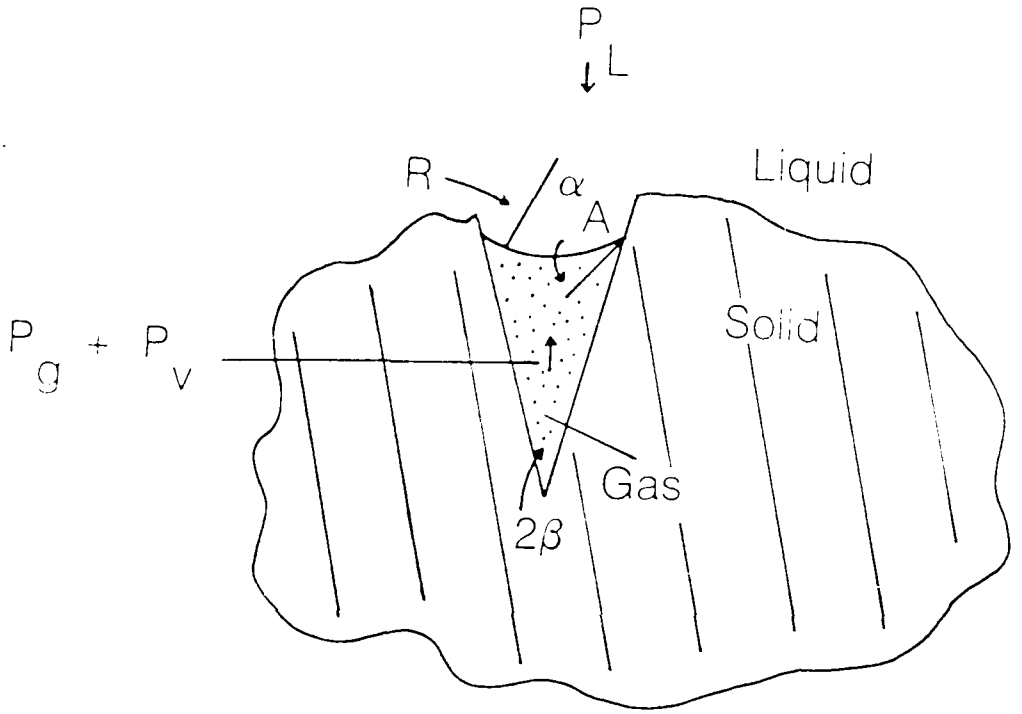

(b)

AD-A156 888 ACOUSTIC CAVITATION AND BUBBLE DYNAMICS(U) MISSISSIPPI 2/2
UNIV UNIVERSITY PHYSICAL ACOUSTICS RESEARCH LAB
A A ATCHLEY ET AL. 15 JUN 85 TR-2-85 N00014-84-C-0193
UNCLASSIFIED F/G 20/1 NL

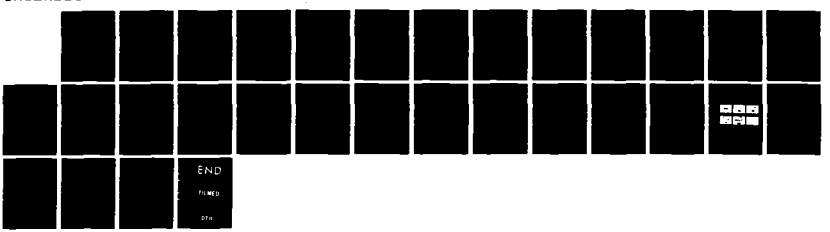

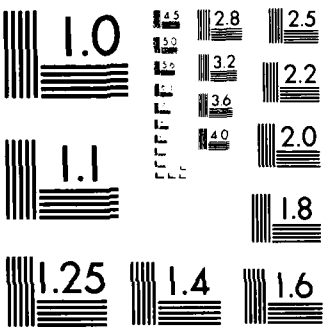

MICROCOPY RESOLUTION TEST CHART

NATIONAL BUREAU OF STANDARDS 1963-A

Figure 1-4

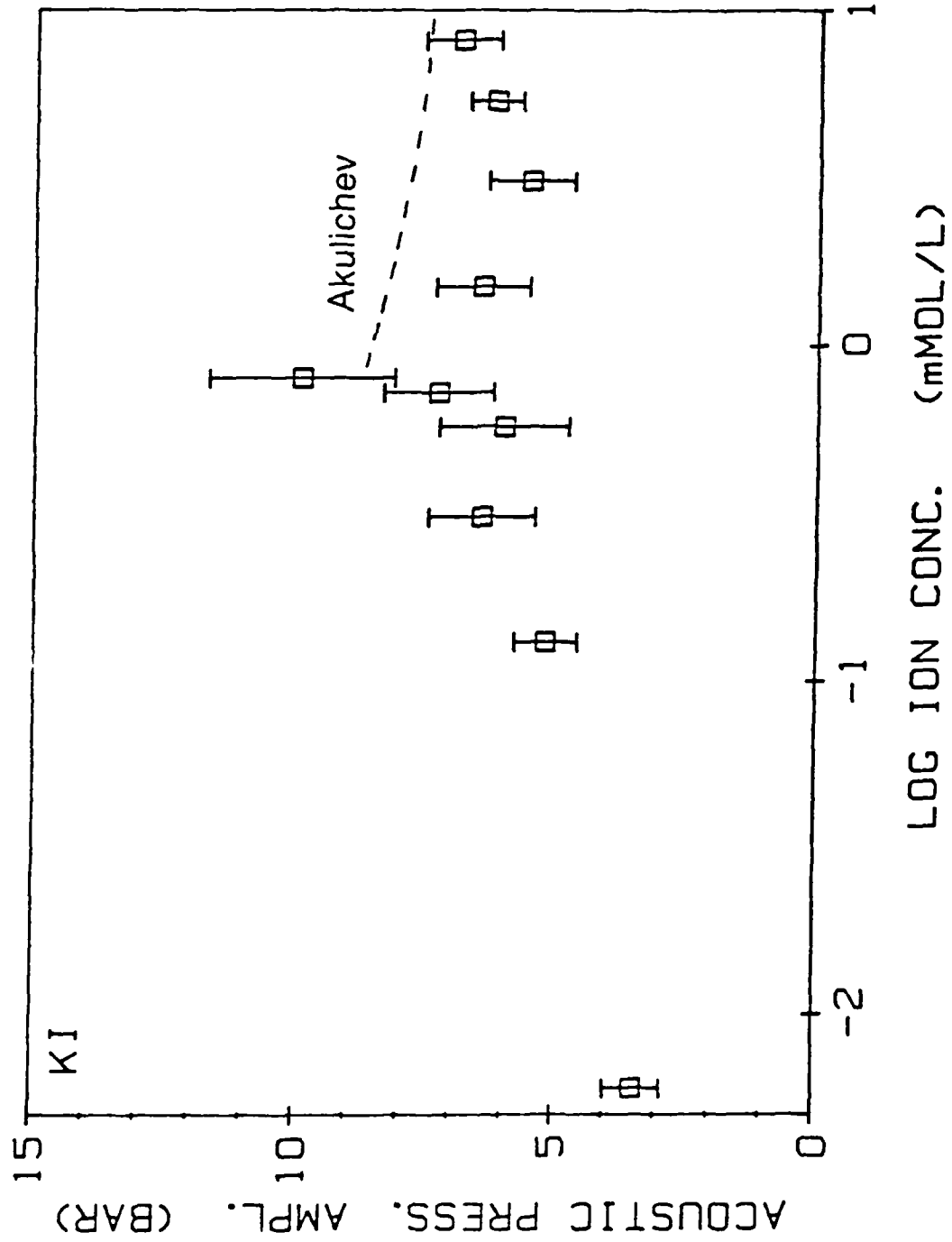
KI
Akulichev
ACOUSTIC PRESS. AMPL. (BAR)
15
10
5
0
1
0
-1
-2
LOG ION CONC. (mMOL/L)

Figure 1-5

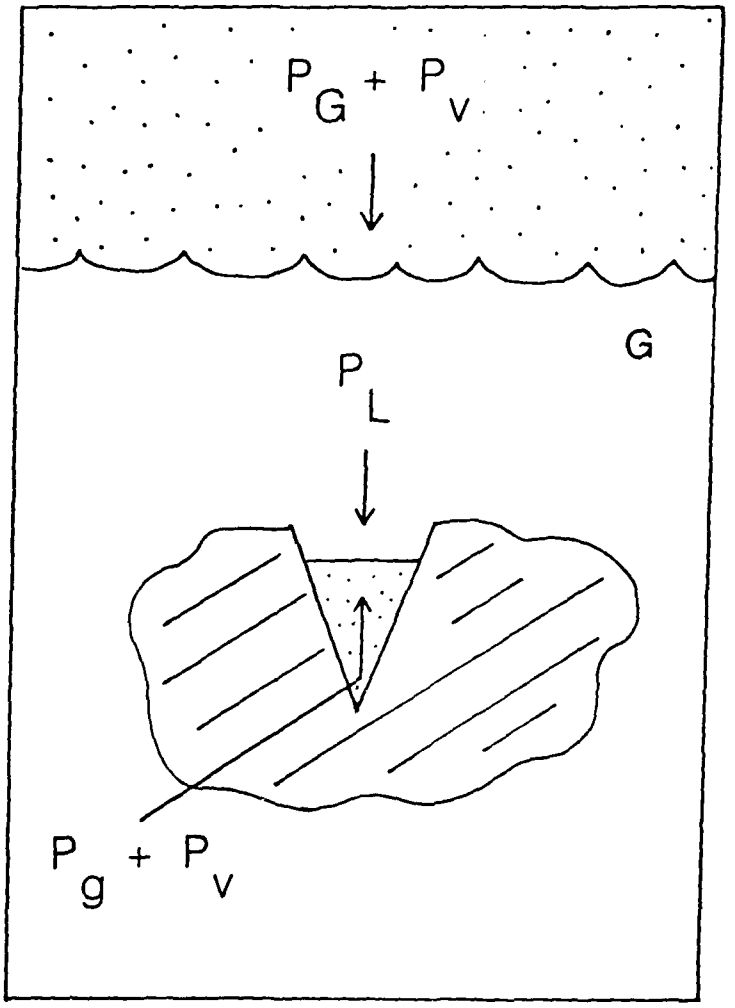

Figure 1-6a

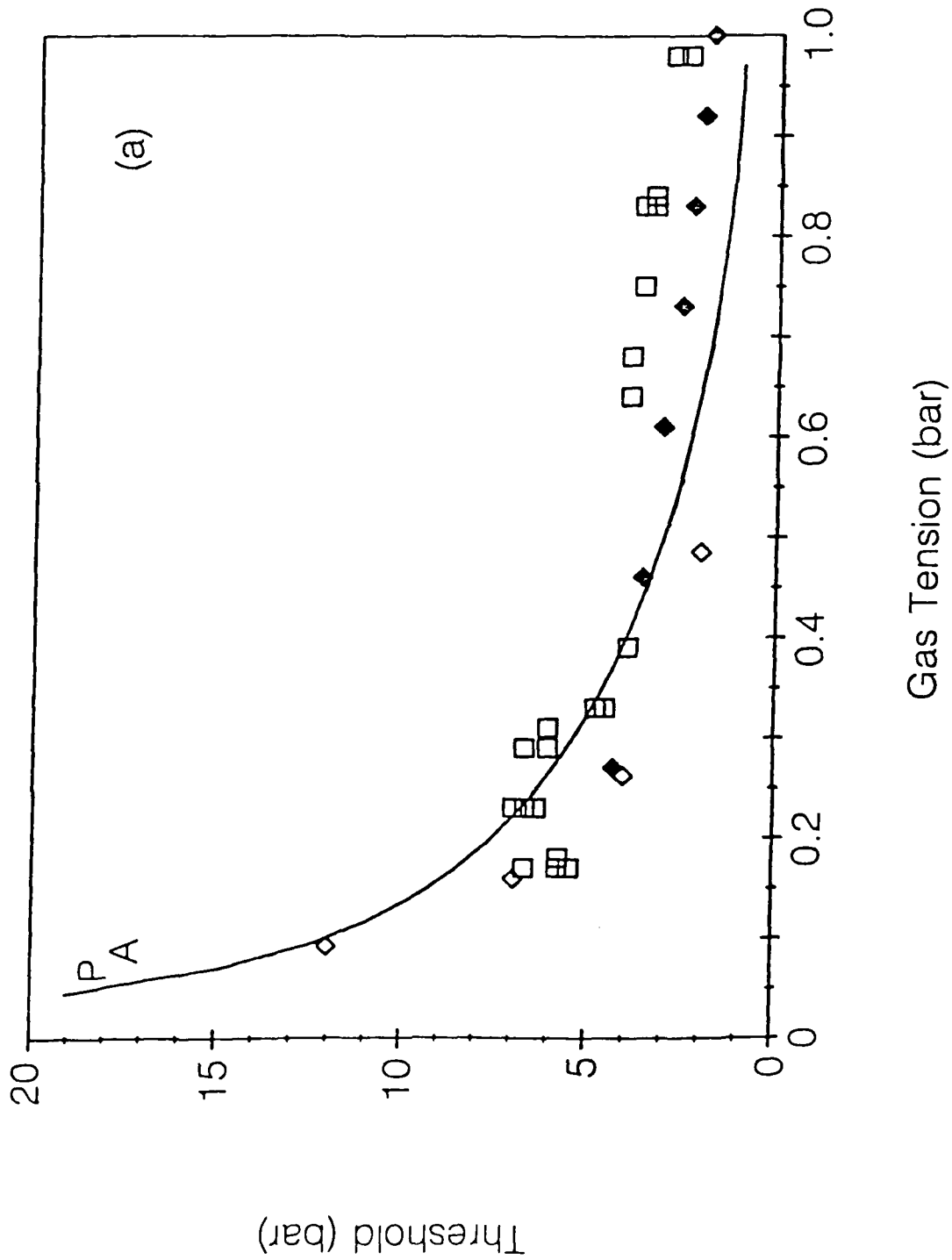

Figure 1-6b

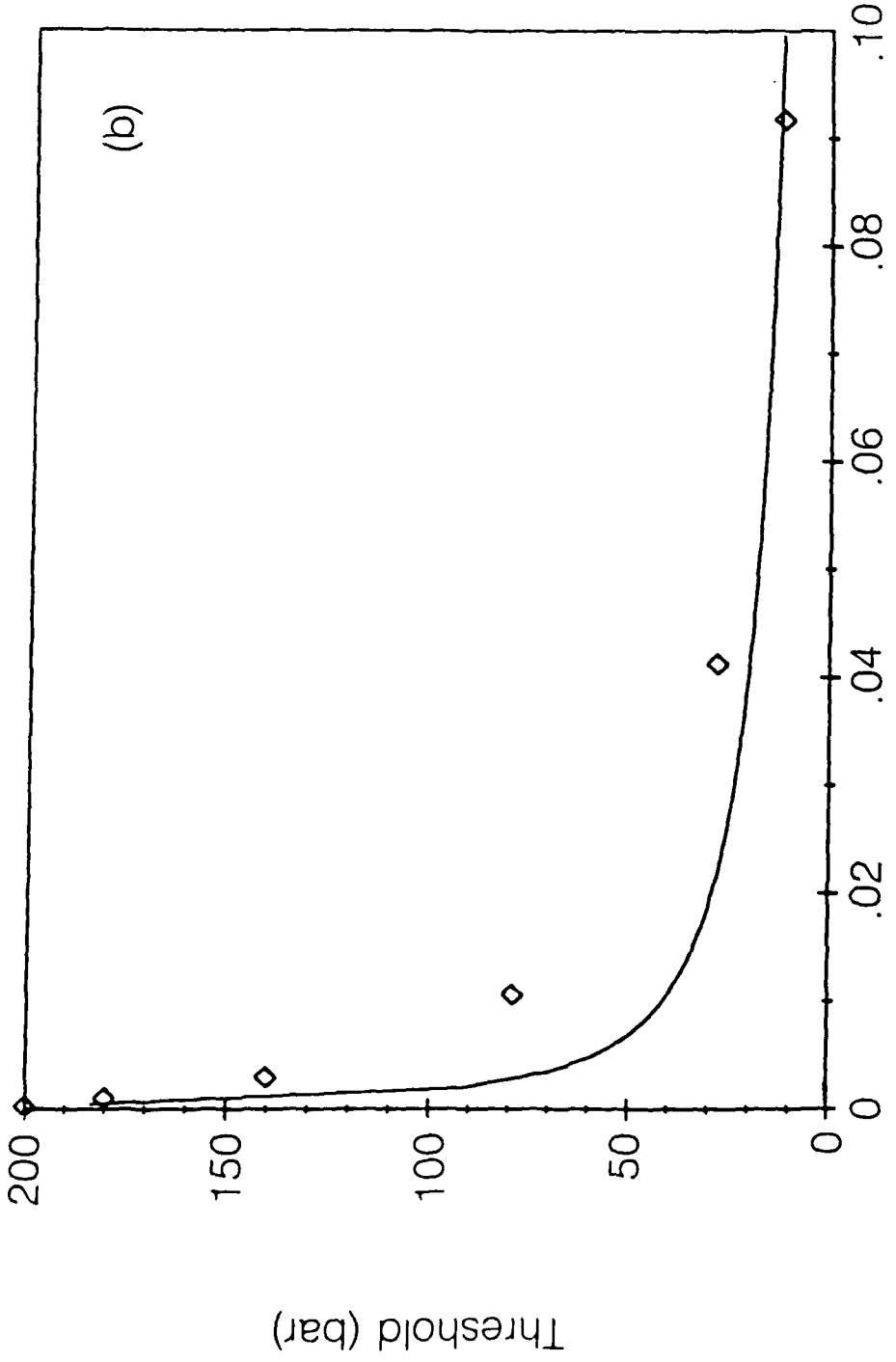

Figure 1-7

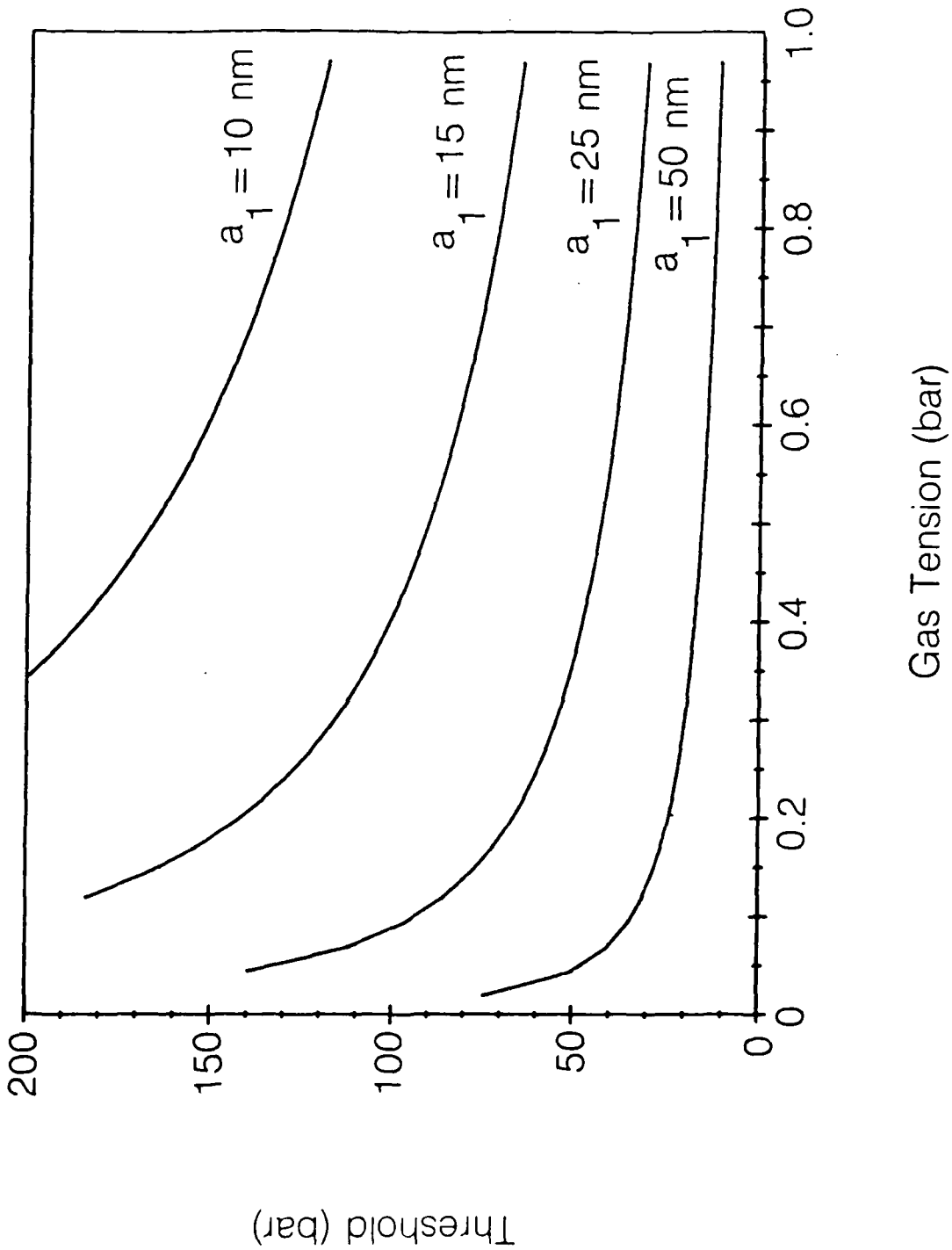
Threshold (bar)
200
150
100
50
0
0
0.2
0.4
0.6
0.8
1.0
Gas Tension (bar)
$a_1 = 10$ nm
$a_1 = 15$ nm
$a_1 = 25$ nm
$a_1 = 50$ nm

Figure 1-8

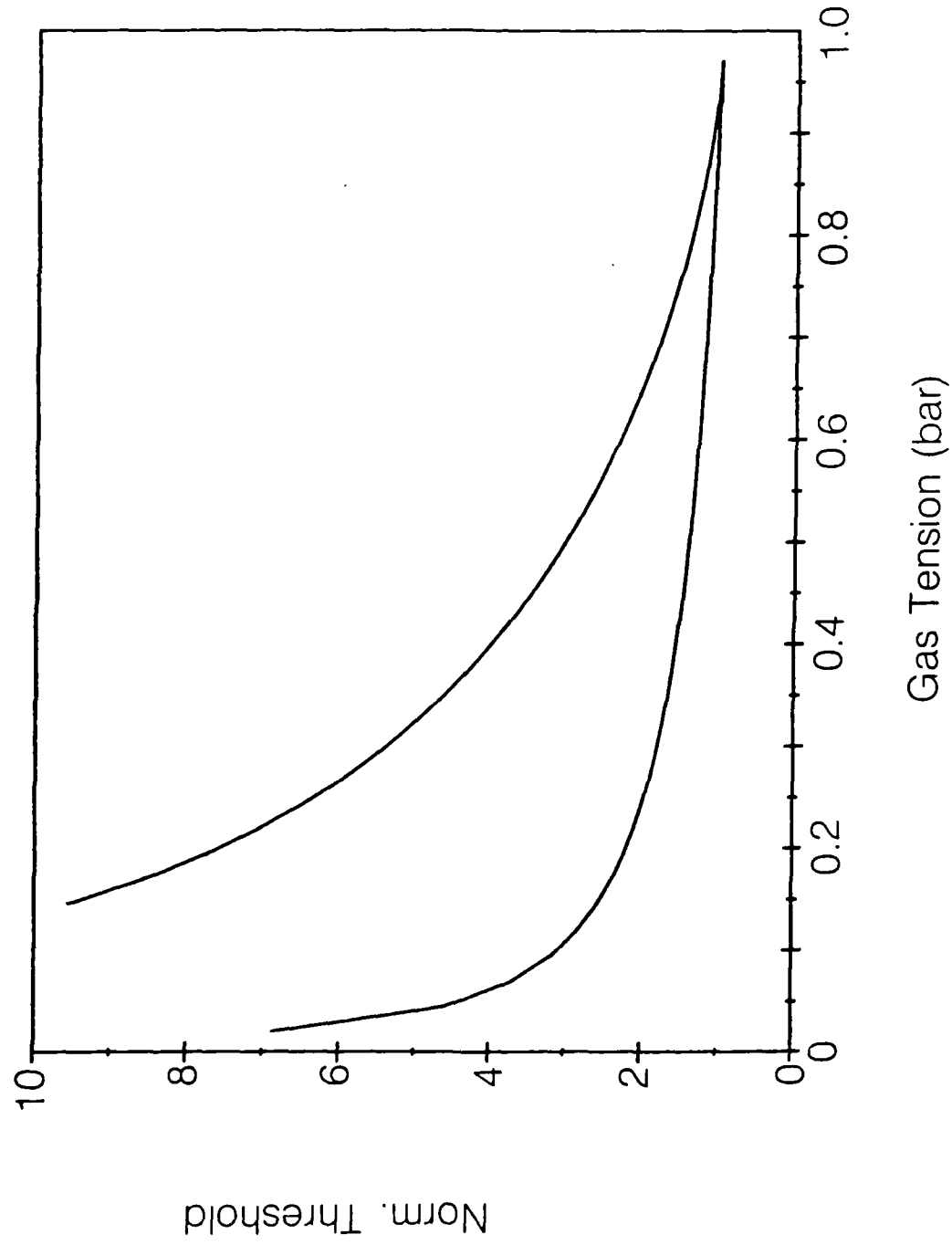

Figure 1-9

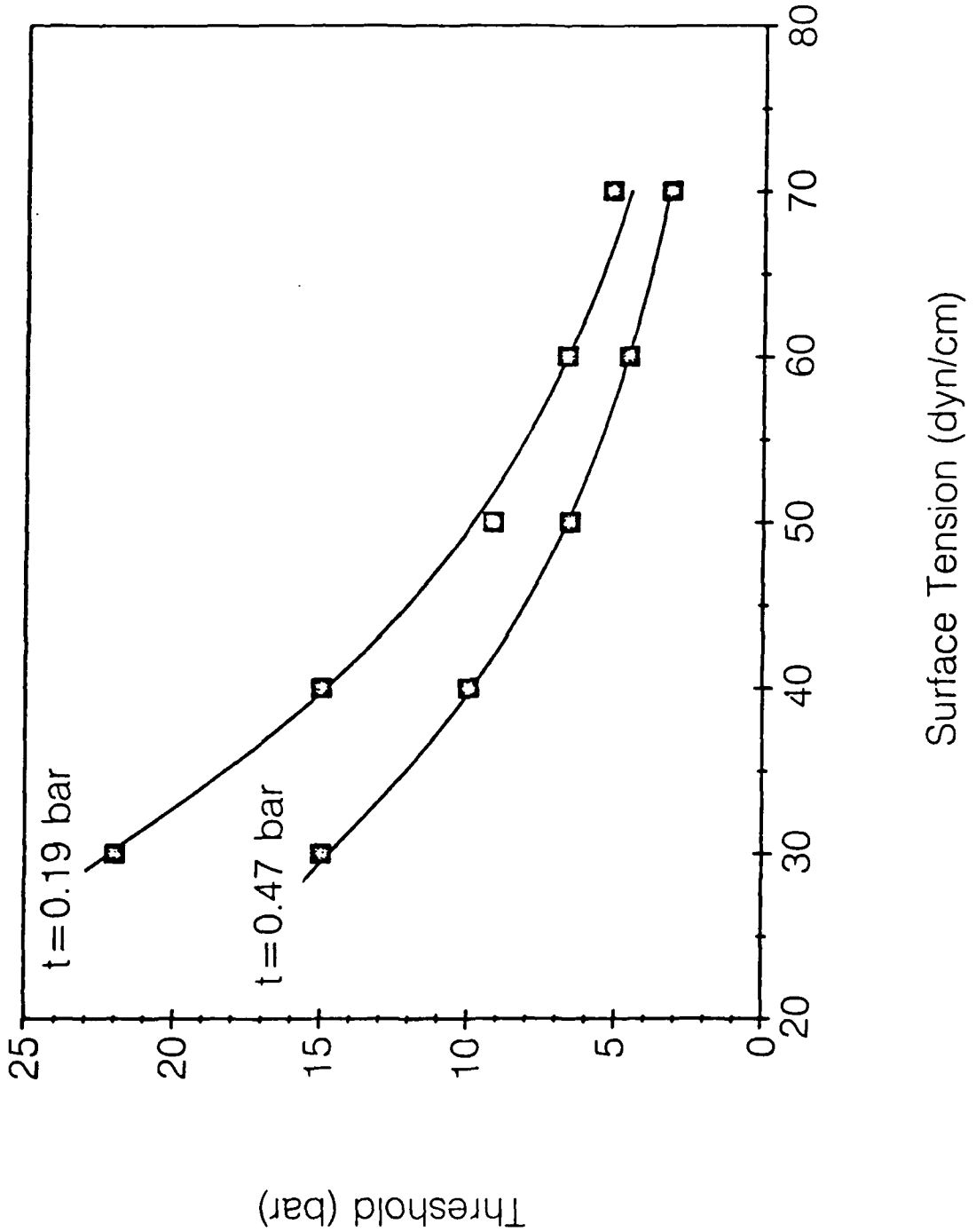
t=0.19 bar
t=0.47 bar
Threshold (bar)
Surface Tension (dyn/cm)
0
5
10
15
20
25
20
30
40
50
60
70
80

Figure 1-10

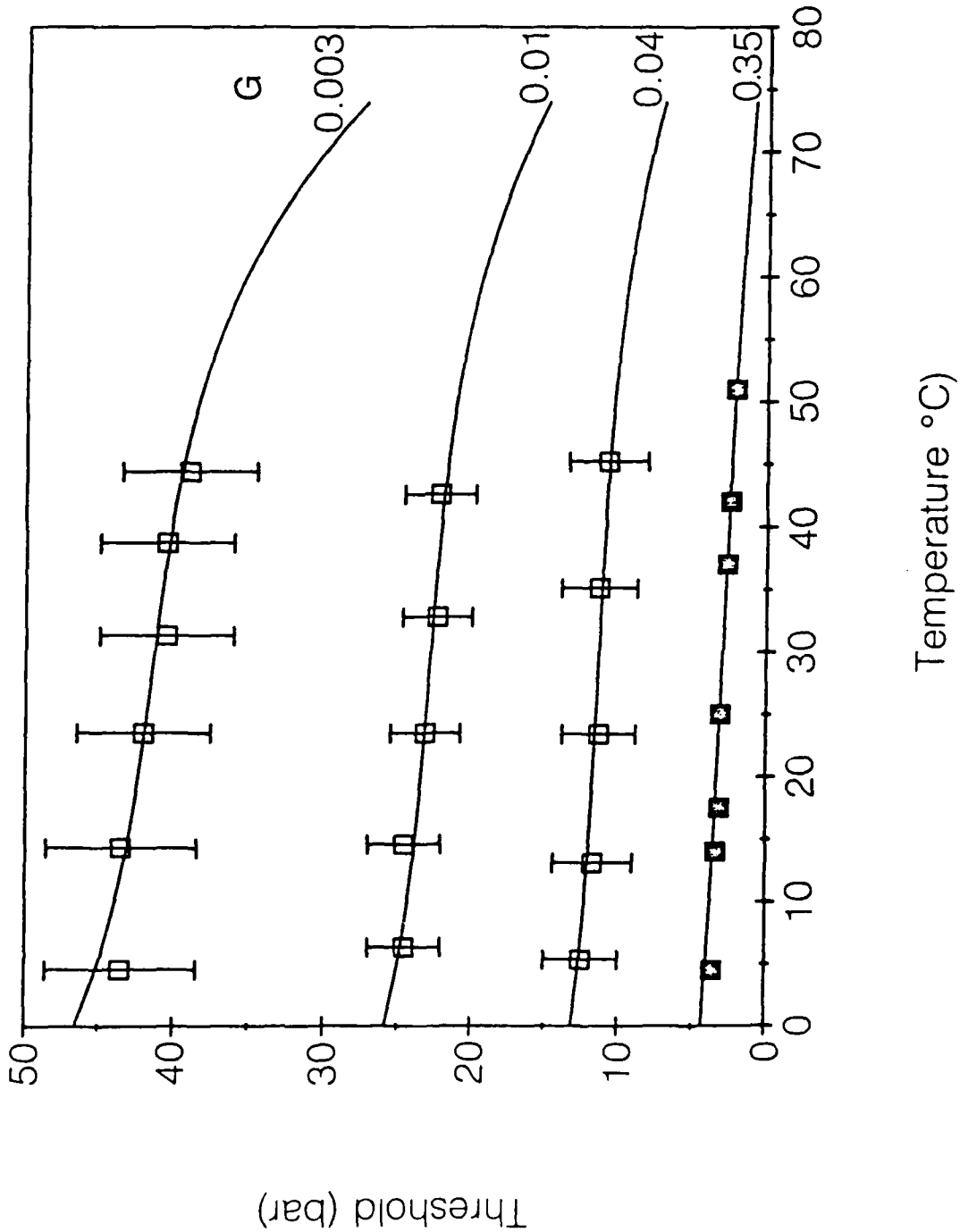
G
0.003
0.01
0.04
0.35
50
40
30
20
10
0
0
10
20
30
40
50
60
70
80
Threshold (bar)
Temperature °C)

Figure 1-11

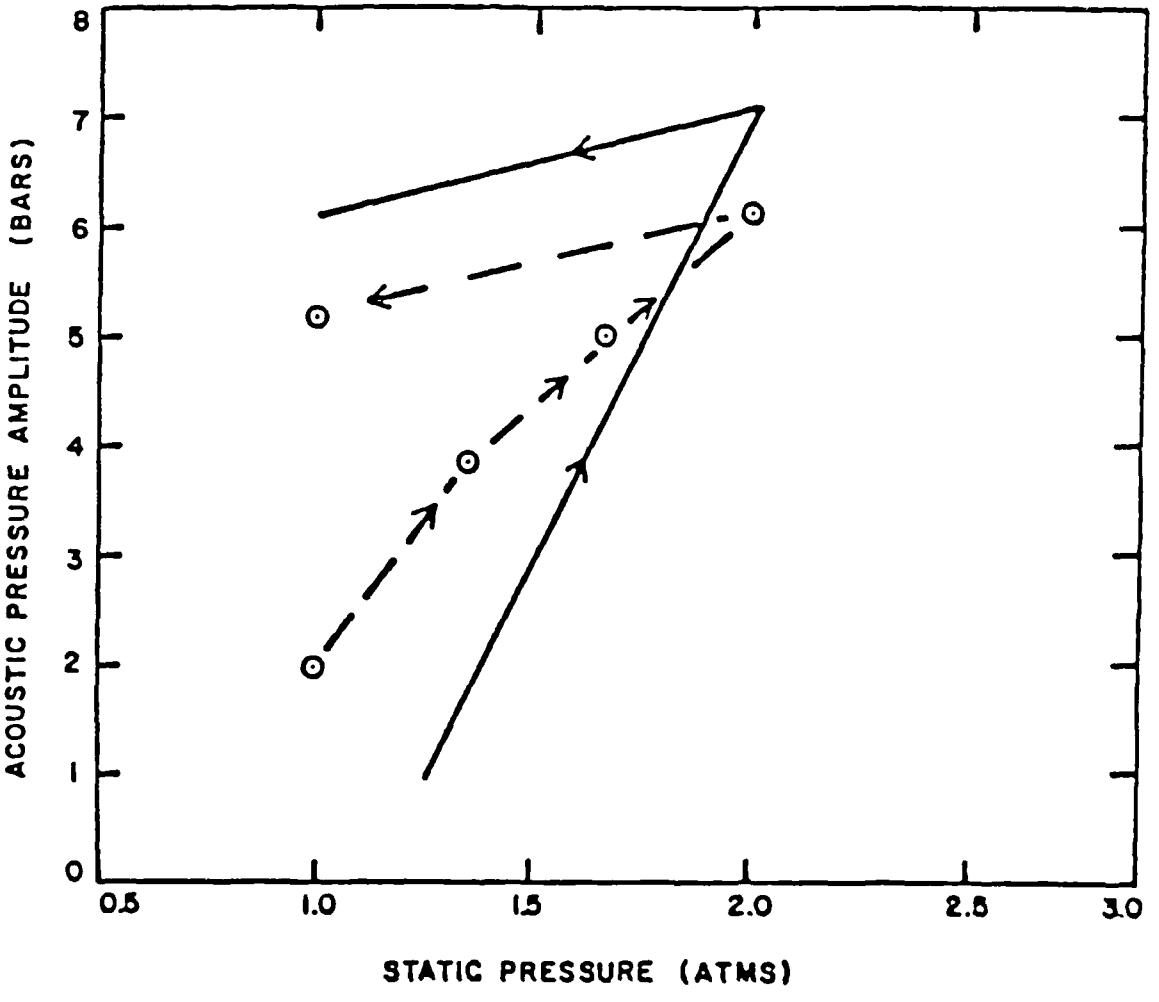
ACOUSTIC PRESSURE AMPLITUDE (BARS)
0
1
2
3
4
5
6
7
8
0.5
1.0
1.5
2.0
2.5
3.0
STATIC PRESSURE (ATMS)

Figure 1-12

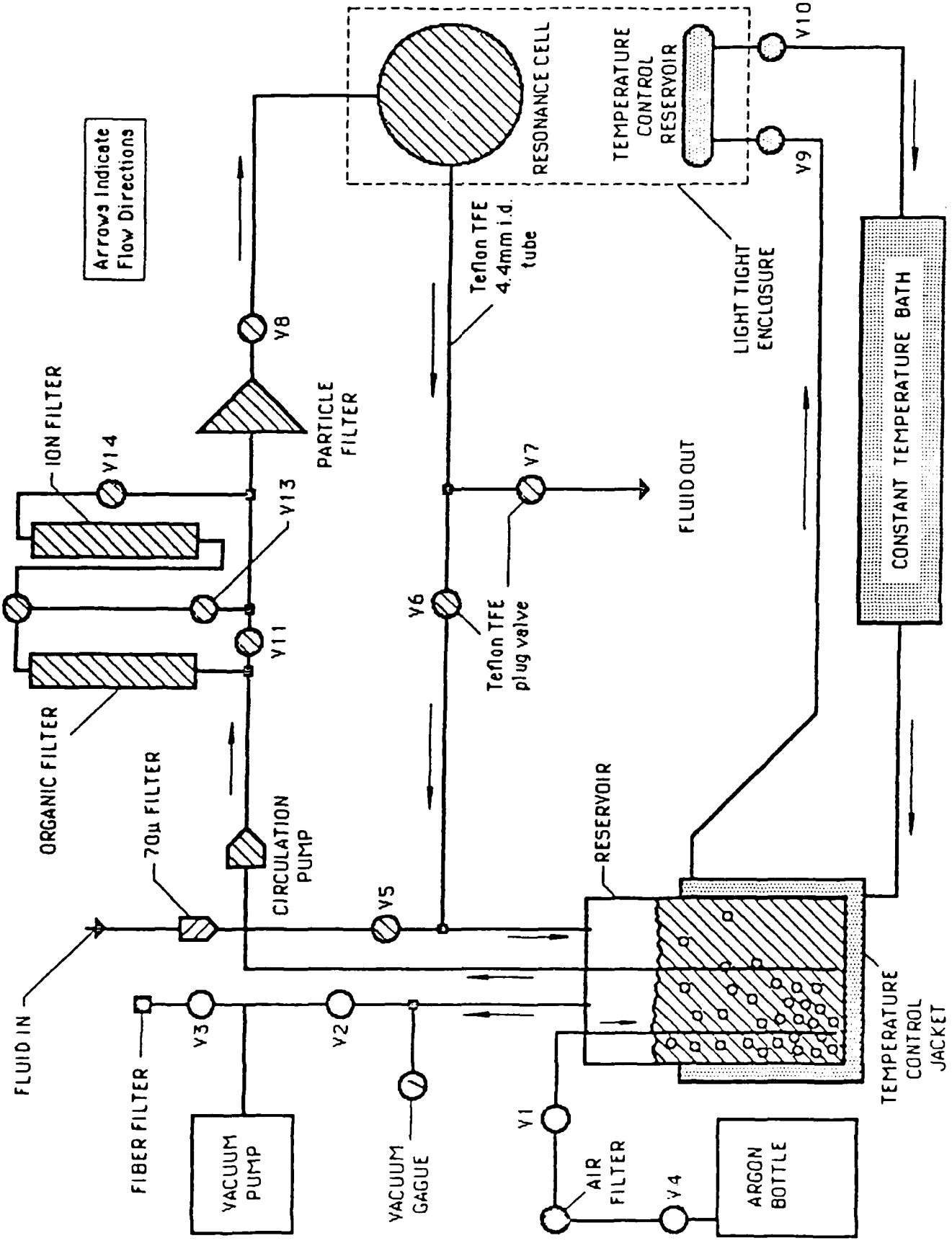
Arrows Indicate Flow Directions
RESONANCE CELL
TEMPERATURE CONTROL RESERVOIR
V10
V9
Teflon TFE 4.4mm i.d. tube
LIGHT TIGHT ENCLOSURE
CONSTANT TEMPERATURE BATH
V8
PARTICLE FILTER
ION FILTER
V14
V13
V12
V11
ORGANIC FILTER
V7
FLUID OUT
V6
Teflon TFE plug valve
70μ FILTER
CIRCULATION PUMP
V5
RESERVOIR
FLUID IN
V3
V2
FIBER FILTER
VACUUM PUMP
VACUUM GAGUE
V1
AIR FILTER
V4
ARGON BOTTLE
TEMPERATURE CONTROL JACKET

Figure 1-13

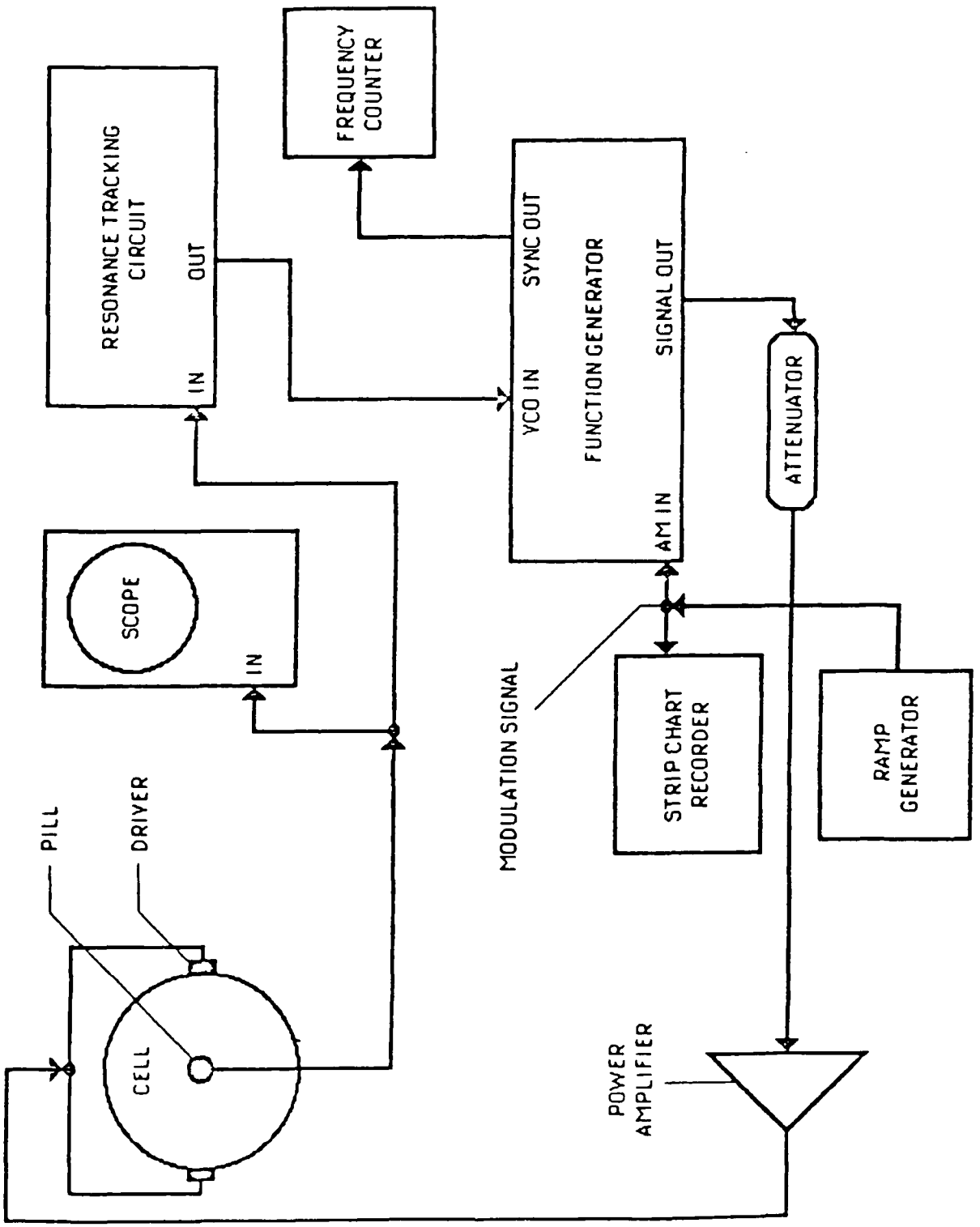
FREQUENCY COUNTER
RESONANCE TRACKING CIRCUIT
OUT
IN
SYNC OUT
FUNCTION GENERATOR
VCO IN
SIGNAL OUT
AM IN
ATTENUATOR
SCOPE
IN
MODULATION SIGNAL
STRIP CHART RECORDER
RAMP GENERATOR
PILL
DRIVER
CELL
POWER AMPLIFIER

Figure 1-14

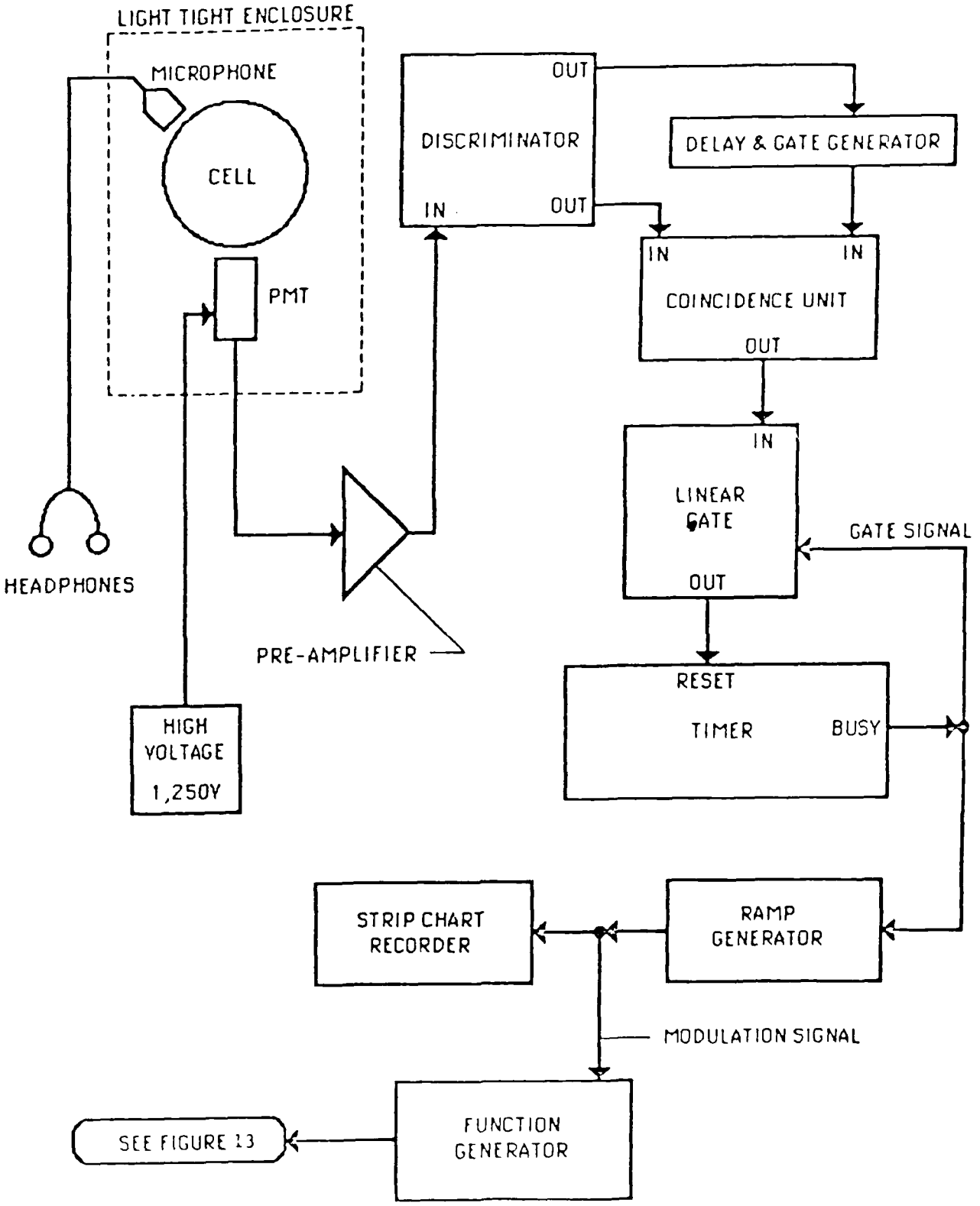
LIGHT TIGHT ENCLOSURE
MICROPHONE
CELL
PMT
HEADPHONES
HIGH VOLTAGE 1,250V
PRE-AMPLIFIER
DISCRIMINATOR
OUT
IN
OUT
DELAY & GATE GENERATOR
IN
IN
COINCIDENCE UNIT
OUT
IN
LINEAR GATE
OUT
GATE SIGNAL
RESET
TIMER
BUSY
STRIP CHART RECORDER
RAMP GENERATOR
MODULATION SIGNAL
FUNCTION GENERATOR
SEE FIGURE 13

Figure 1-28

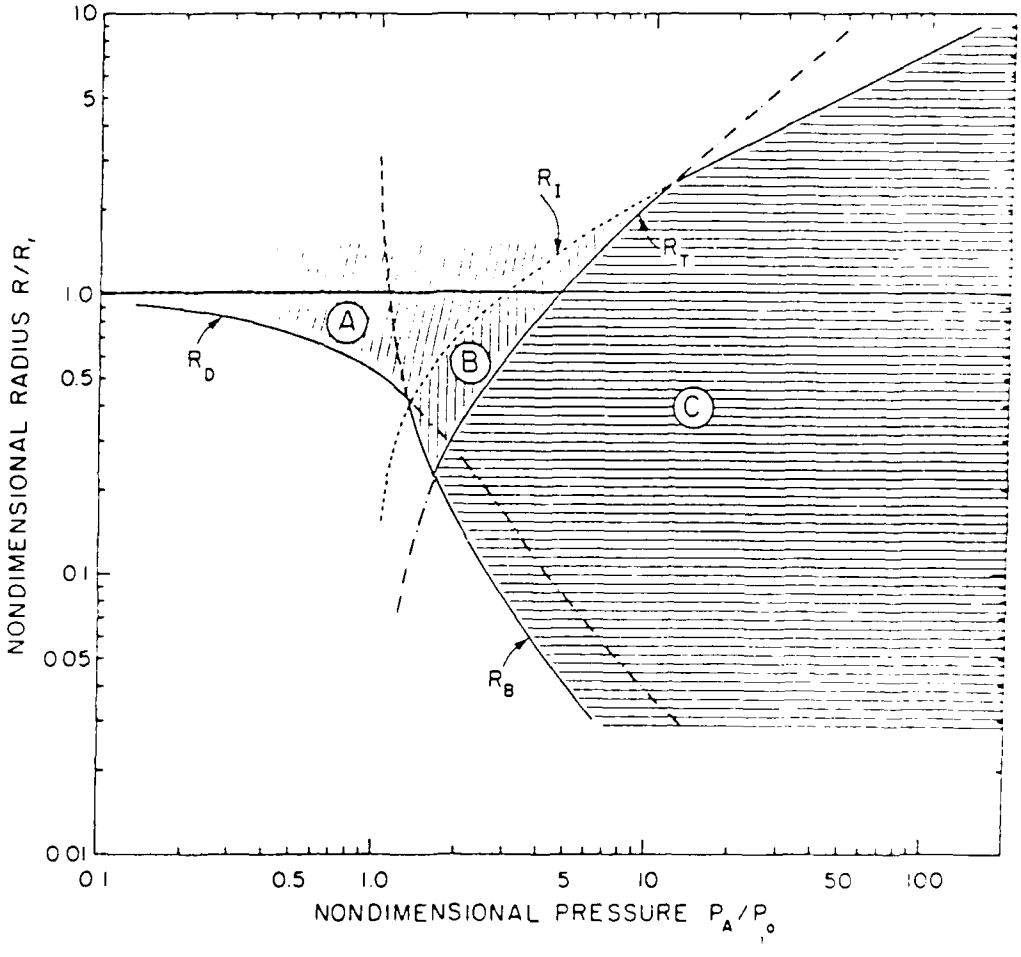
10
5
1.0
0.5
0.1
0.05
0.01
0.1
0.5
1.0
5
10
50
100
NONDIMENSIONAL RADIUS R/R,
NONDIMENSIONAL PRESSURE P_A/P_o
R_I
R_T
R_D
R_B
A
B
C

Figure 1-27

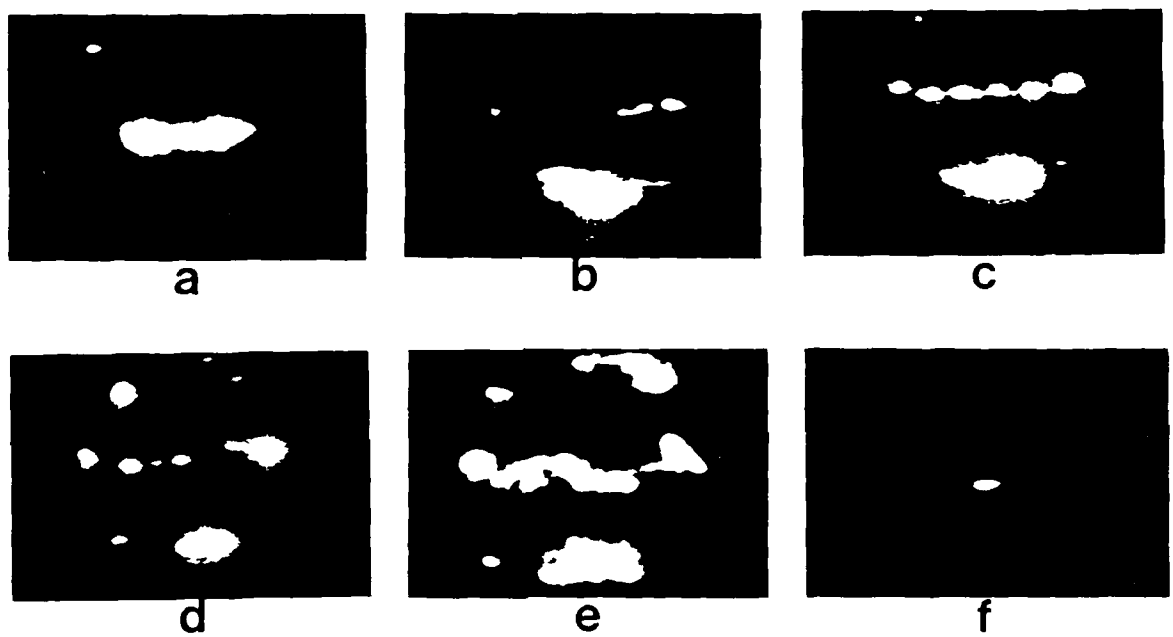

Figure 1-26

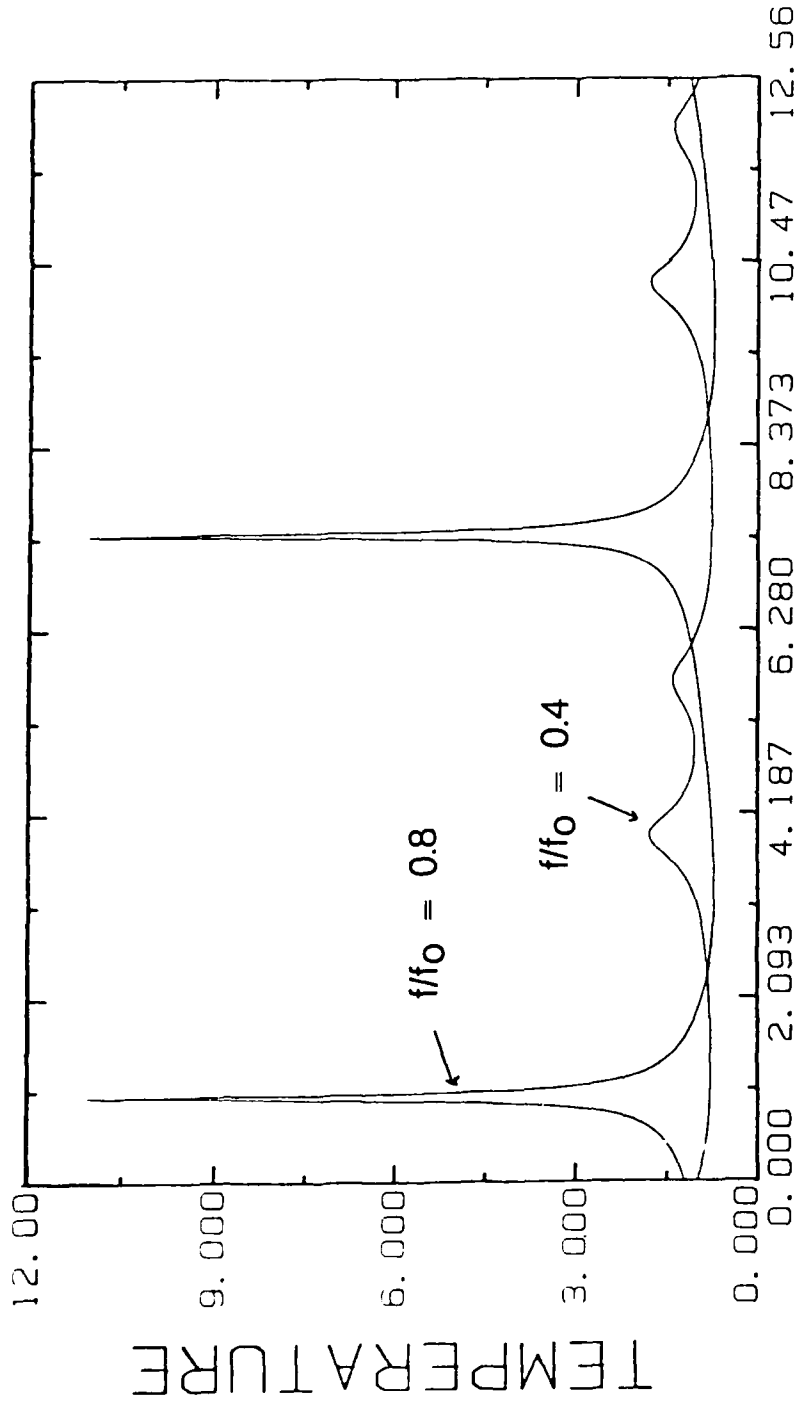
TEMPERATURE
12.00
9.000
6.000
3.000
0.000
0.000
2.093
4.187
6.280
8.373
10.47
12.56
TIME
f/fo = 0.8
f/fo = 0.4

Figure 1-25

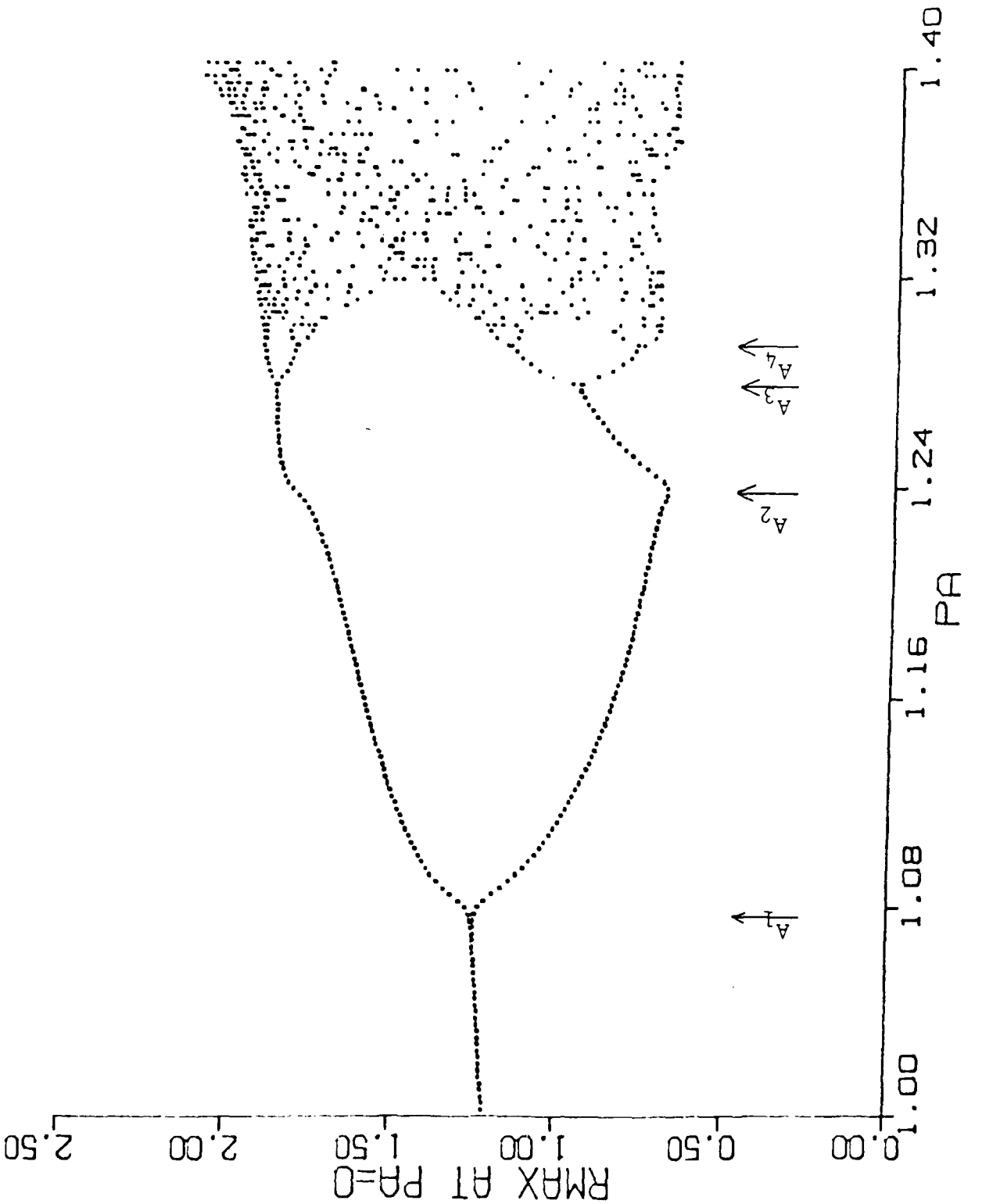
RMAX AT PA=0
0.00
0.50
1.00
1.50
2.00
2.50
1.00
1.08
1.16
1.24
1.32
1.40
PA
A1
A2
A3
A4

F/FO=0.500 RO=50.0 μM

PA=1.15 BAR FO=60.5 KHZ

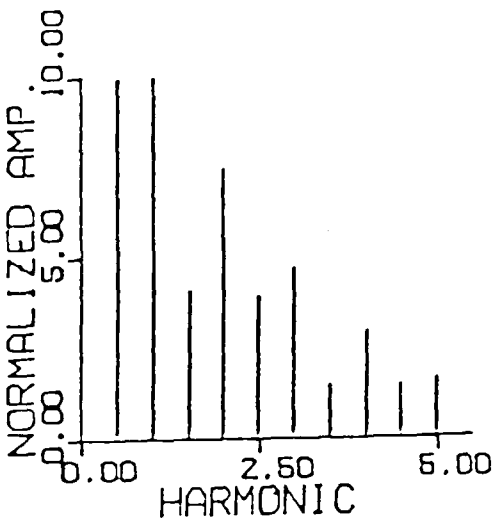

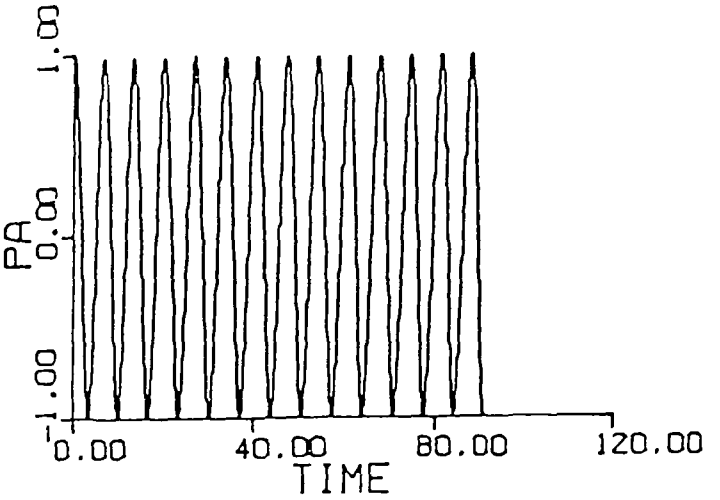

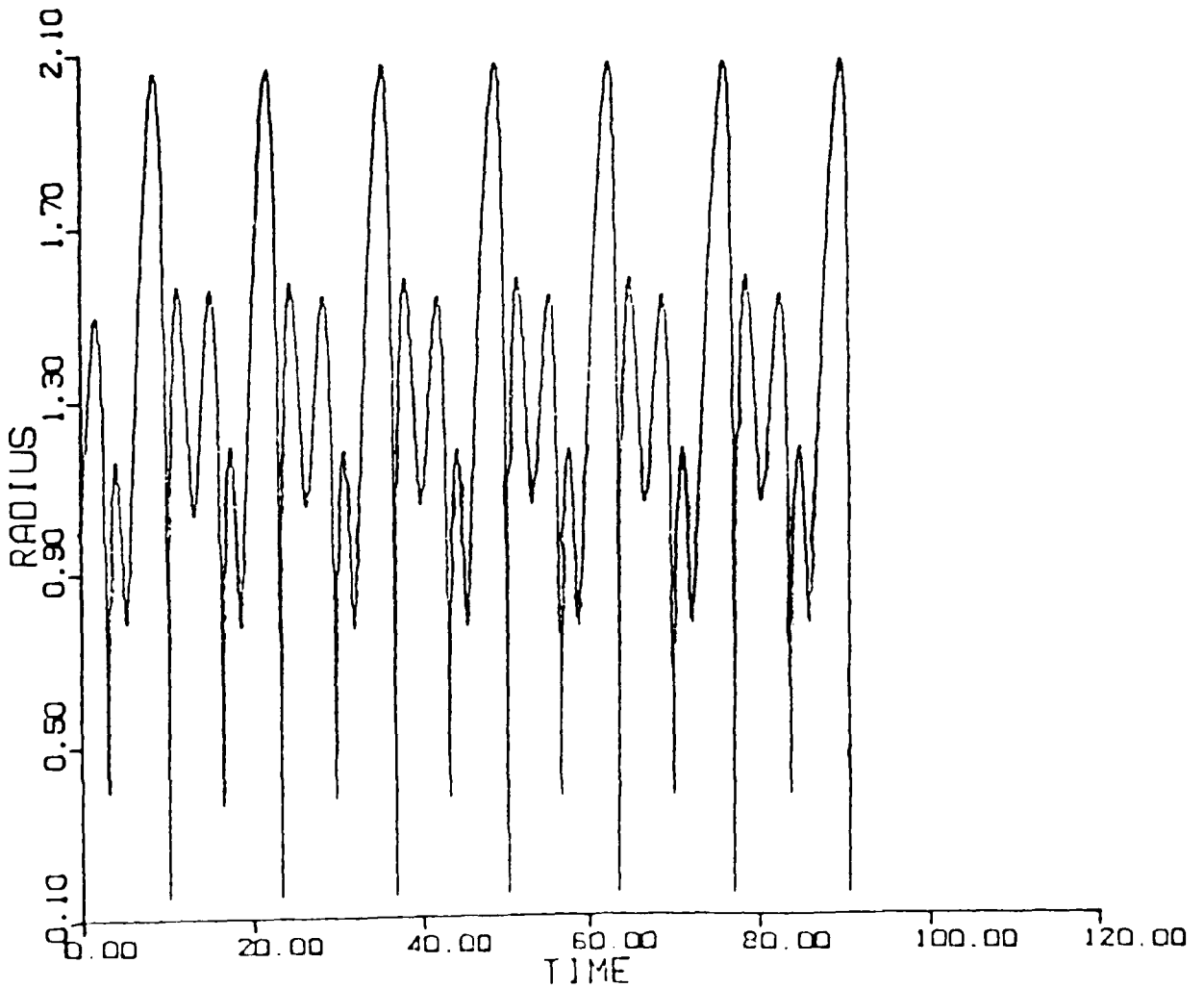

F/FO=0.500 RO=50.0 μM

PA=1.05 BAR FO=60.5 KHZ

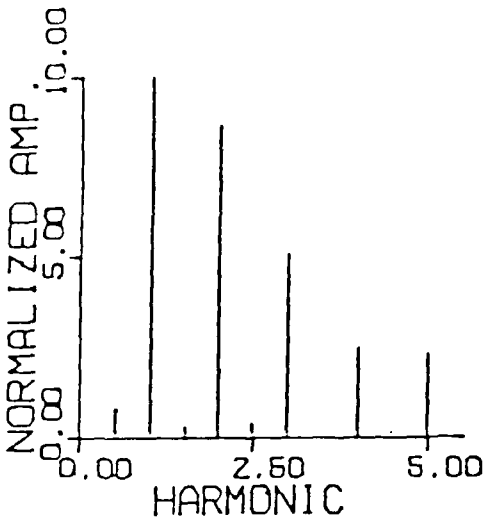

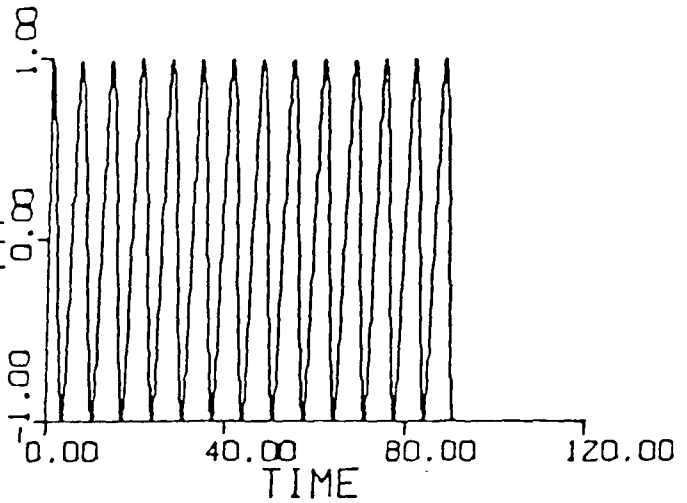

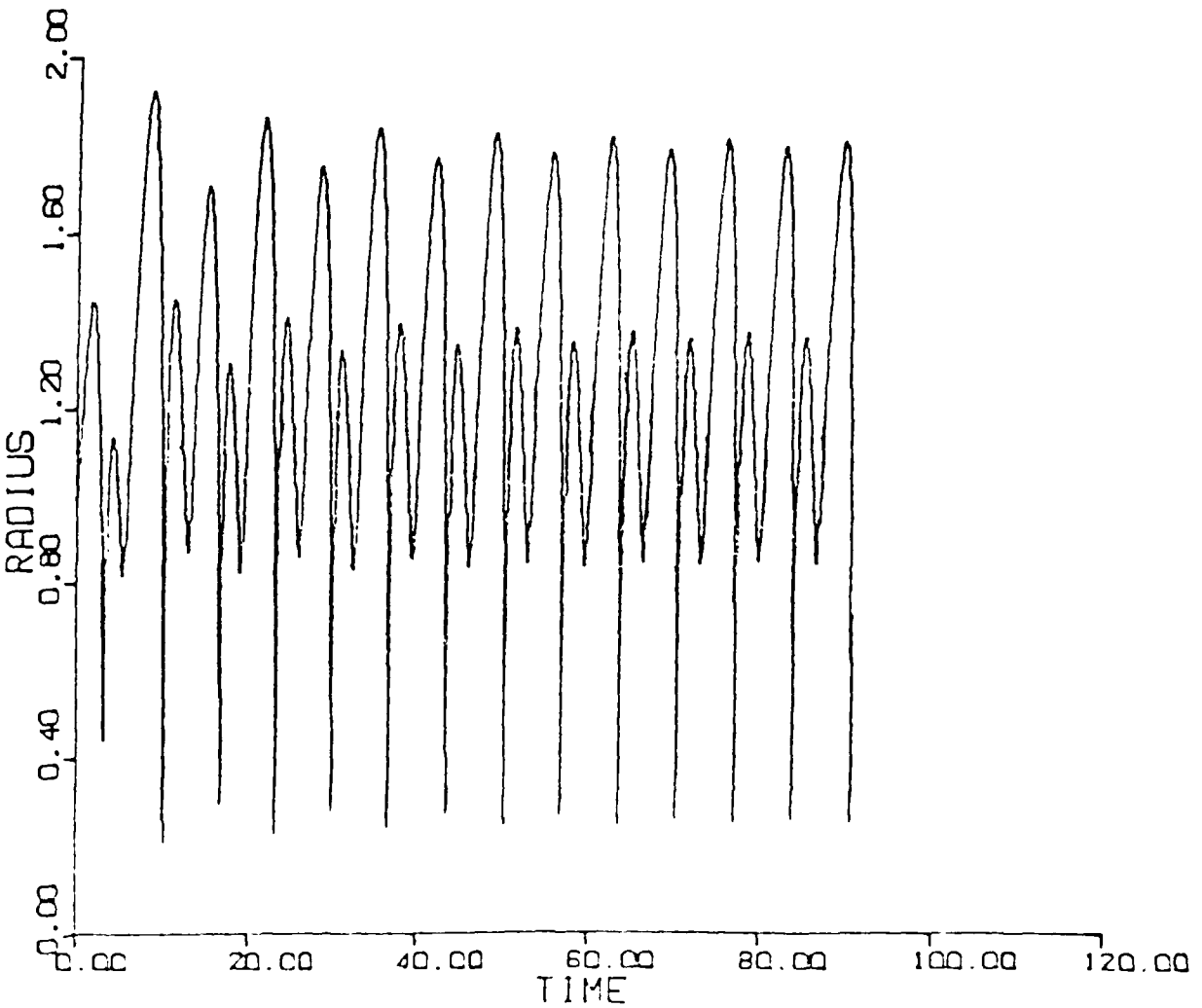

Figure 1-22

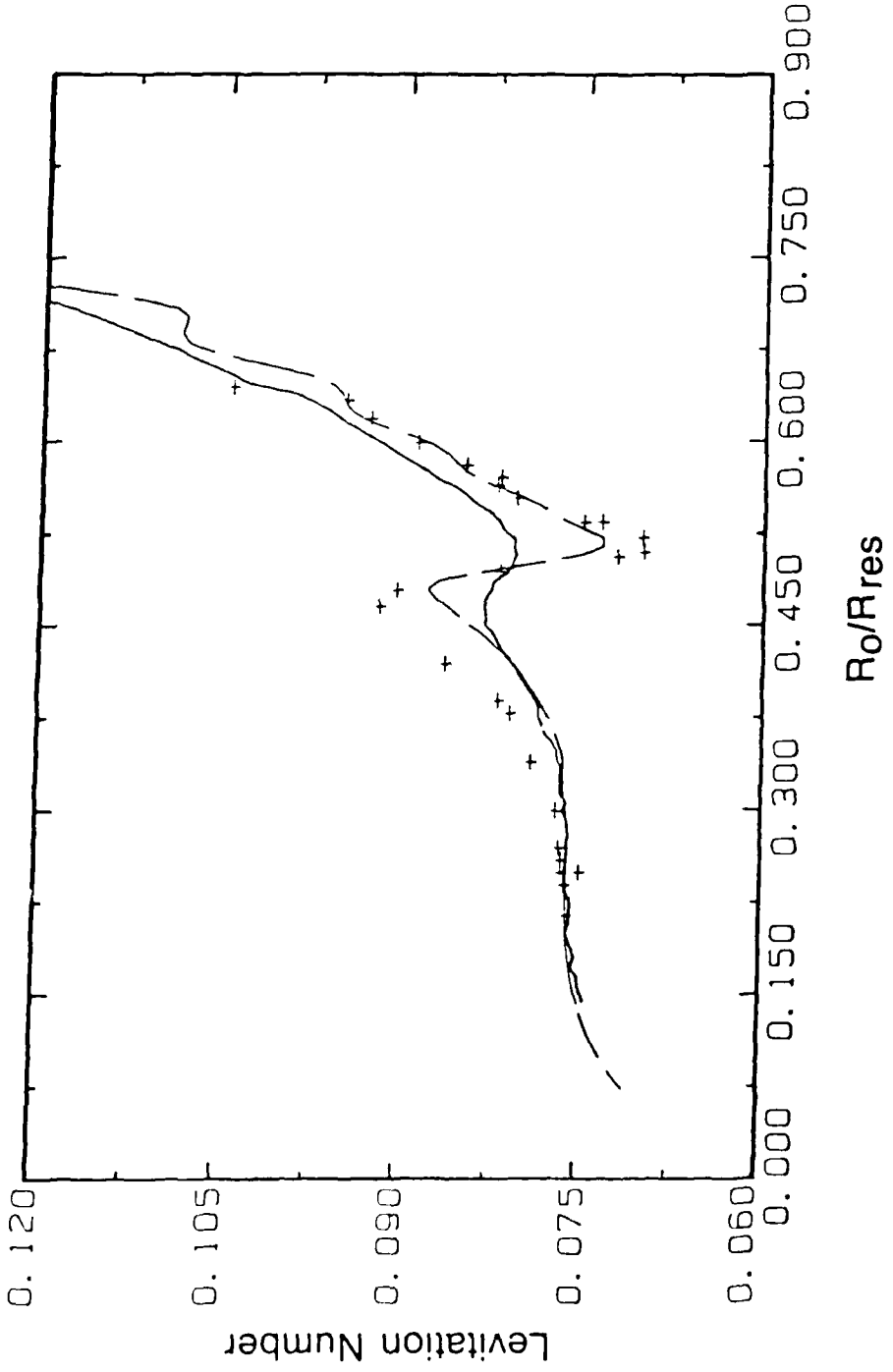
Levitation Number
0.120
0.105
0.090
0.075
0.060
0.000
0.150
0.300
0.450
0.600
0.750
0.900
Ro/Rres

Figure 1-21

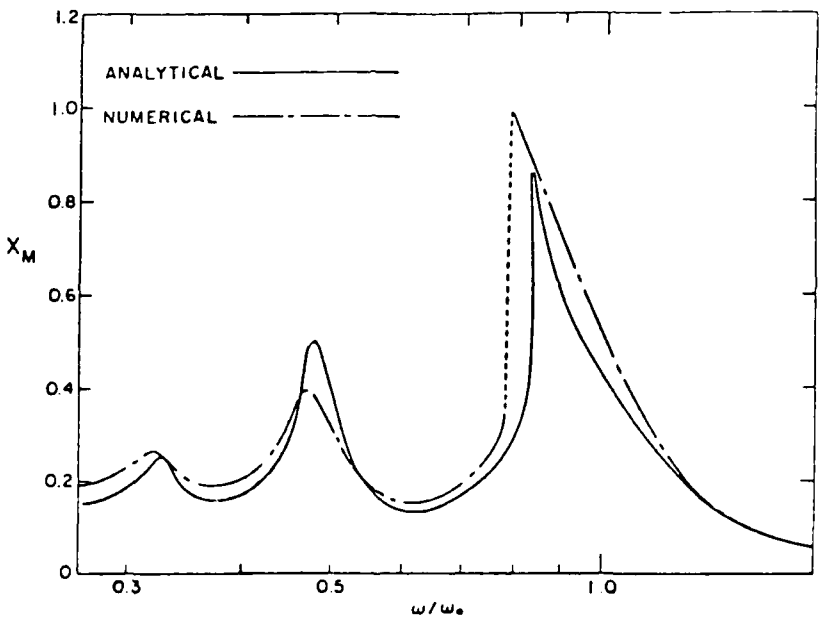
ANALYTICAL
NUMERICAL
X_M
1.2
1.0
0.8
0.6
0.4
0.2
0
0.3
0.5
1.0
ω/ω_e

Figure 1-20

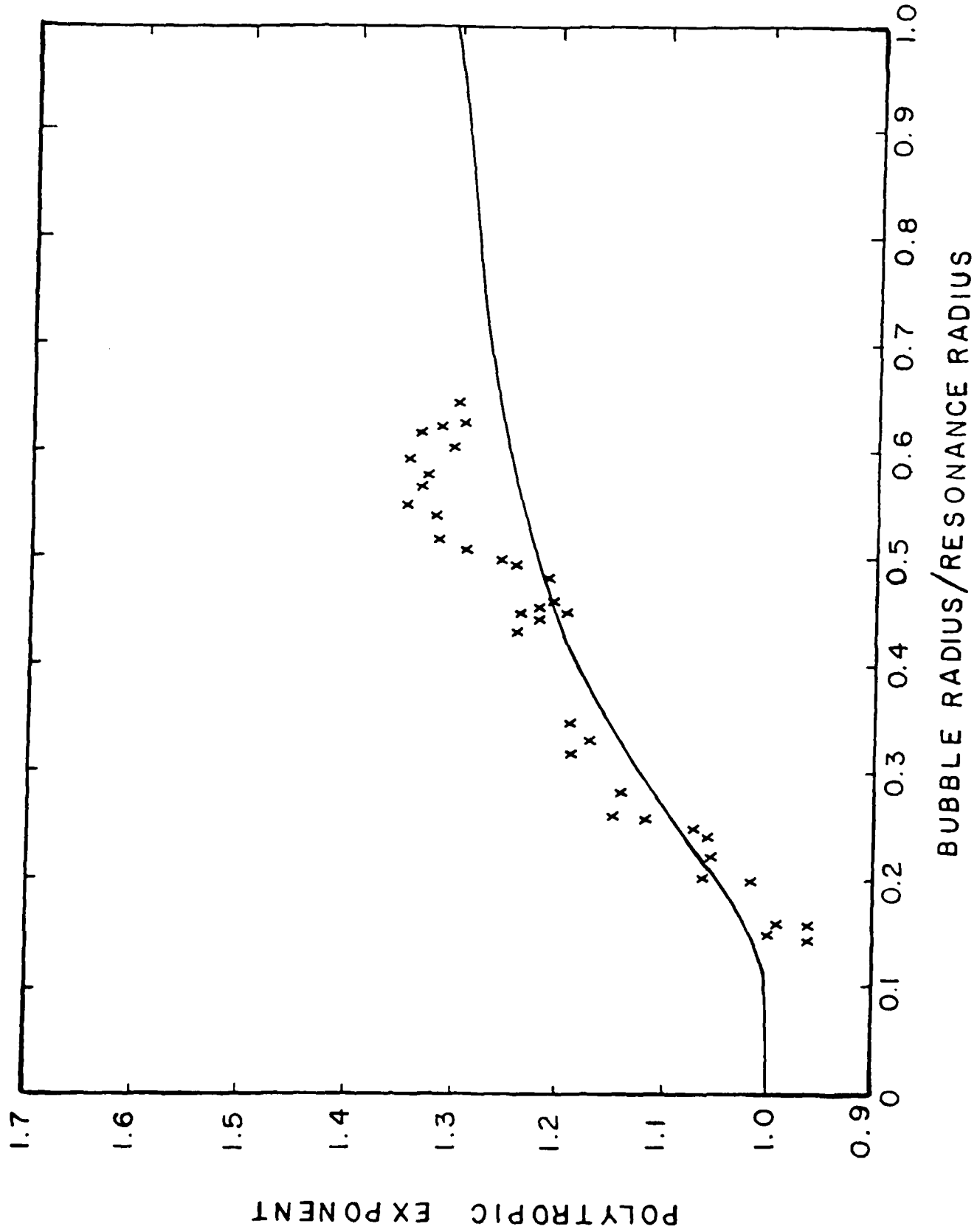
POLYTROPIC EXPONENT
1.7
1.6
1.5
1.4
1.3
1.2
1.1
1.0
0.9
0
0.1
0.2
0.3
0.4
0.5
0.6
0.7
0.8
0.9
1.0
BUBBLE RADIUS/RESONANCE RADIUS

Figure 1-19

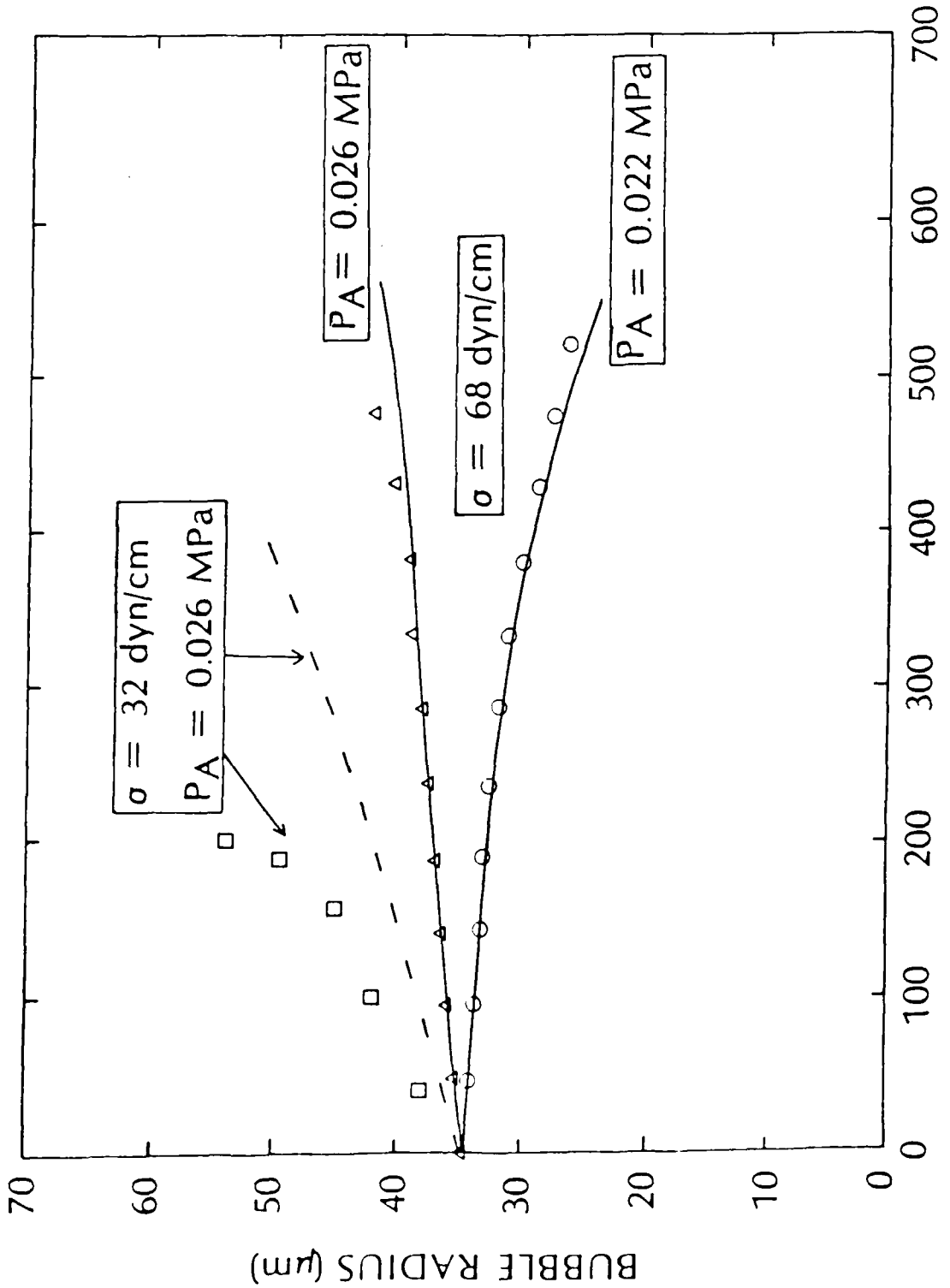
BUBBLE RADIUS (μm)
TIME (sec)
0
10
20
30
40
50
60
70
0
100
200
300
400
500
600
700
σ = 32 dyn/cm
PA = 0.026 MPa
PA = 0.026 MPa
σ = 68 dyn/cm
PA = 0.022 MPa

Figure I-18

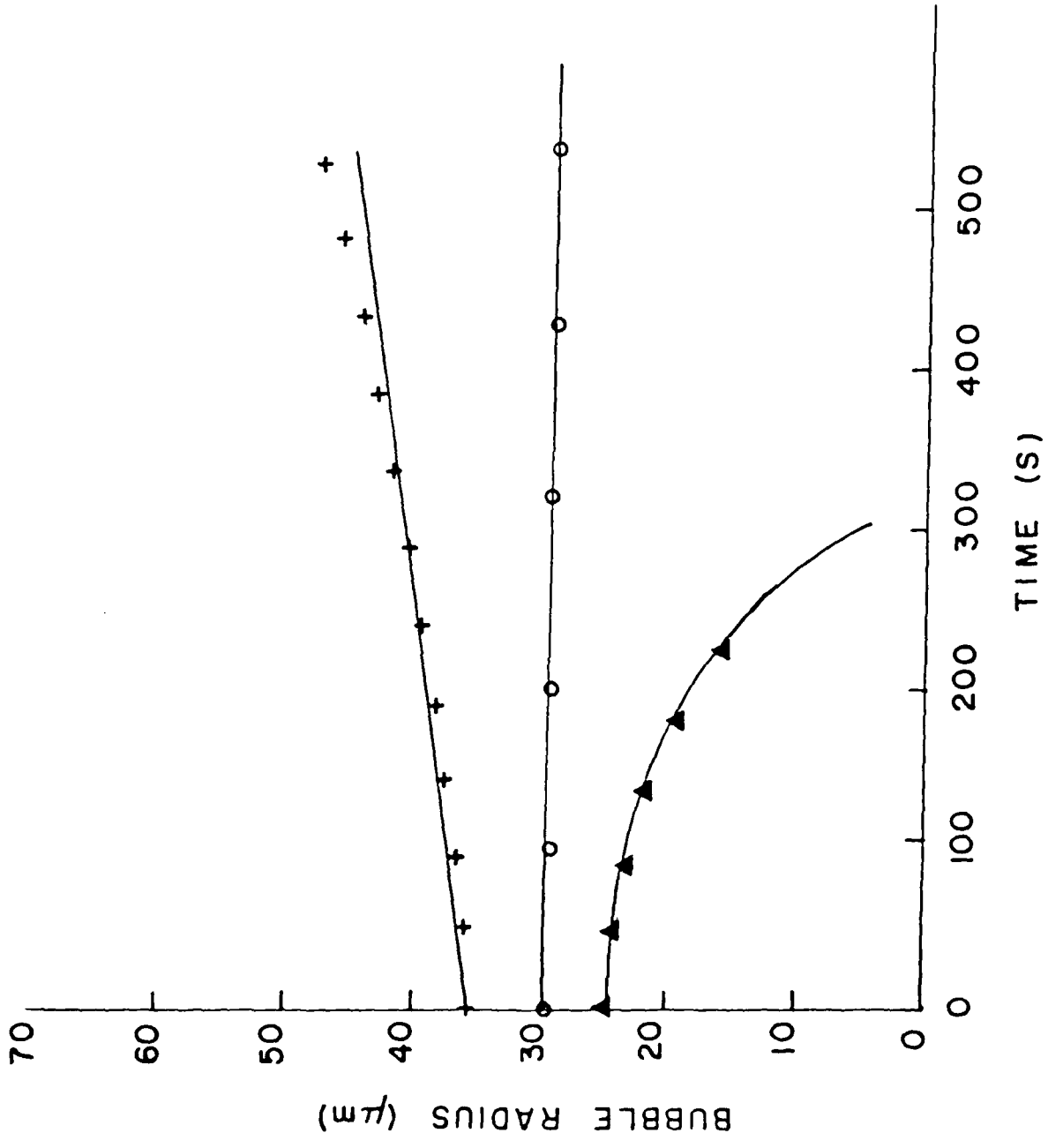
BUBBLE RADIUS (μm)
70
60
50
40
30
20
10
0
0
100
200
300
400
500
TIME (S)

Figure 1-17

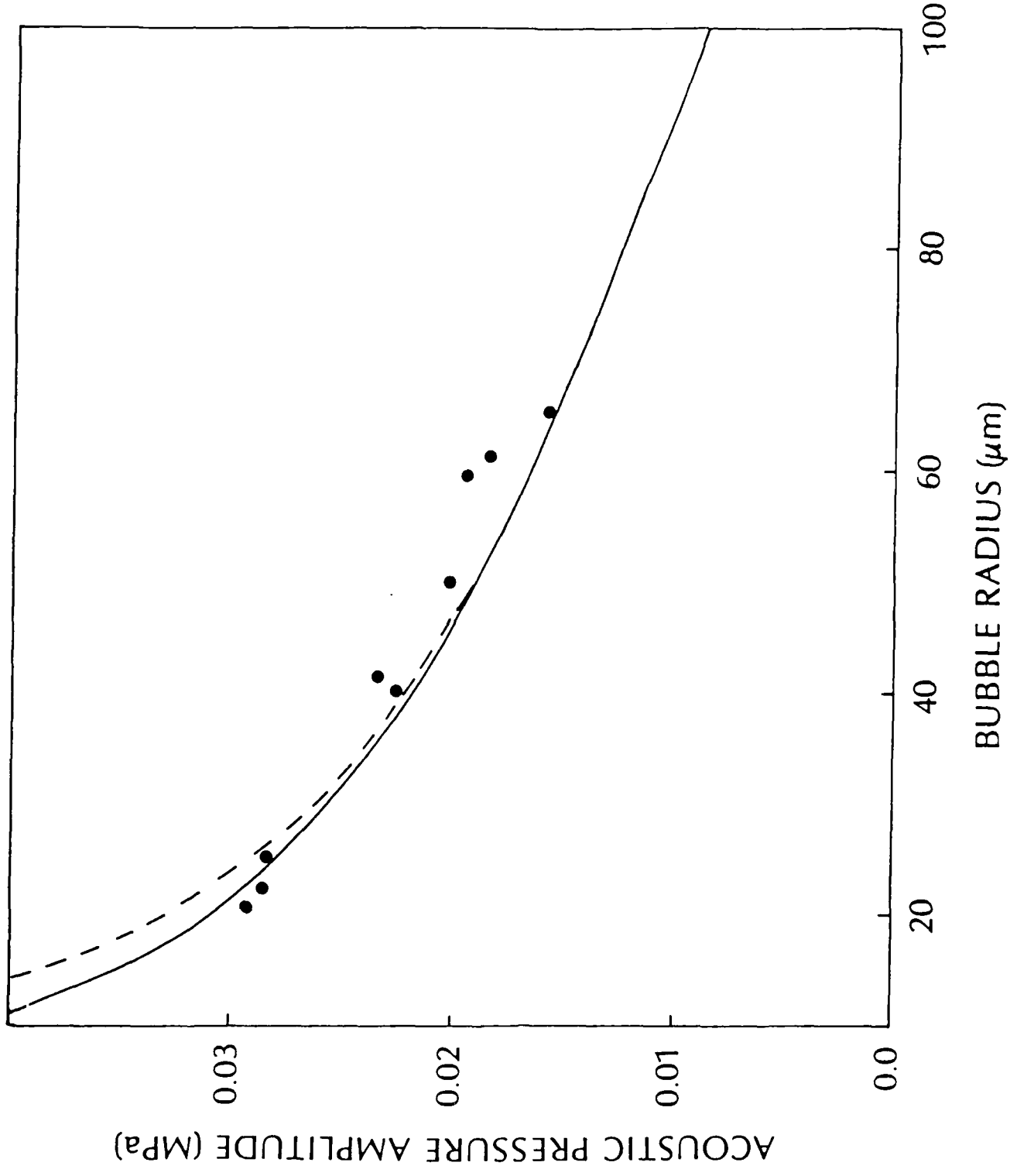
ACOUSTIC PRESSURE AMPLITUDE (MPa)
0.0
0.01
0.02
0.03
BUBBLE RADIUS (μm)
20
40
60
80
100

Figure 1-16

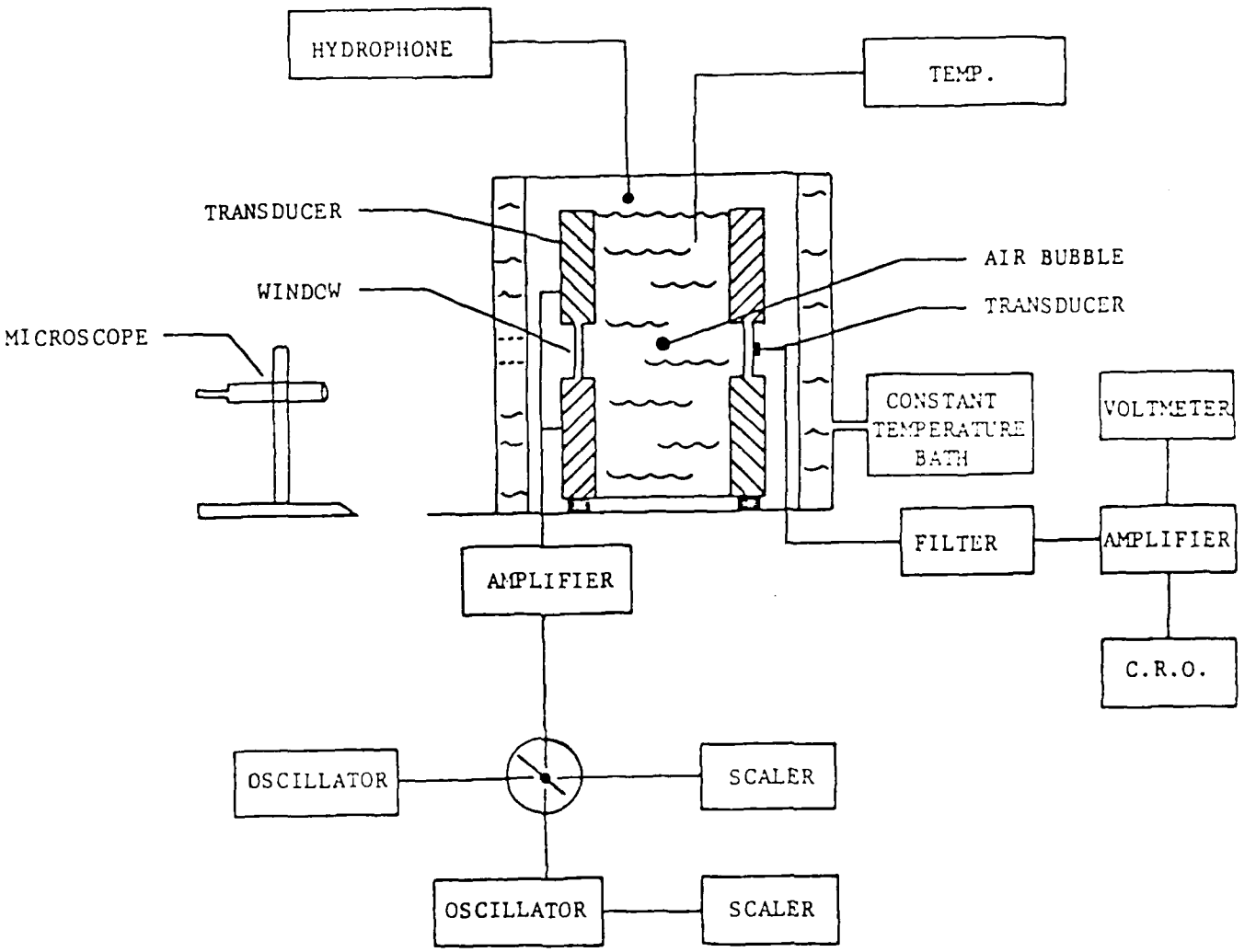
HYDROPHONE
TEMP.
TRANSDUCER
AIR BUBBLE
WINDOW
TRANSDUCER
MICROSCOPE
CONSTANT TEMPERATURE BATH
VOLTMETER
FILTER
AMPLIFIER
AMPLIFIER
C.R.O.
OSCILLATOR
SCALER
OSCILLATOR
SCALER

Figure 1-15

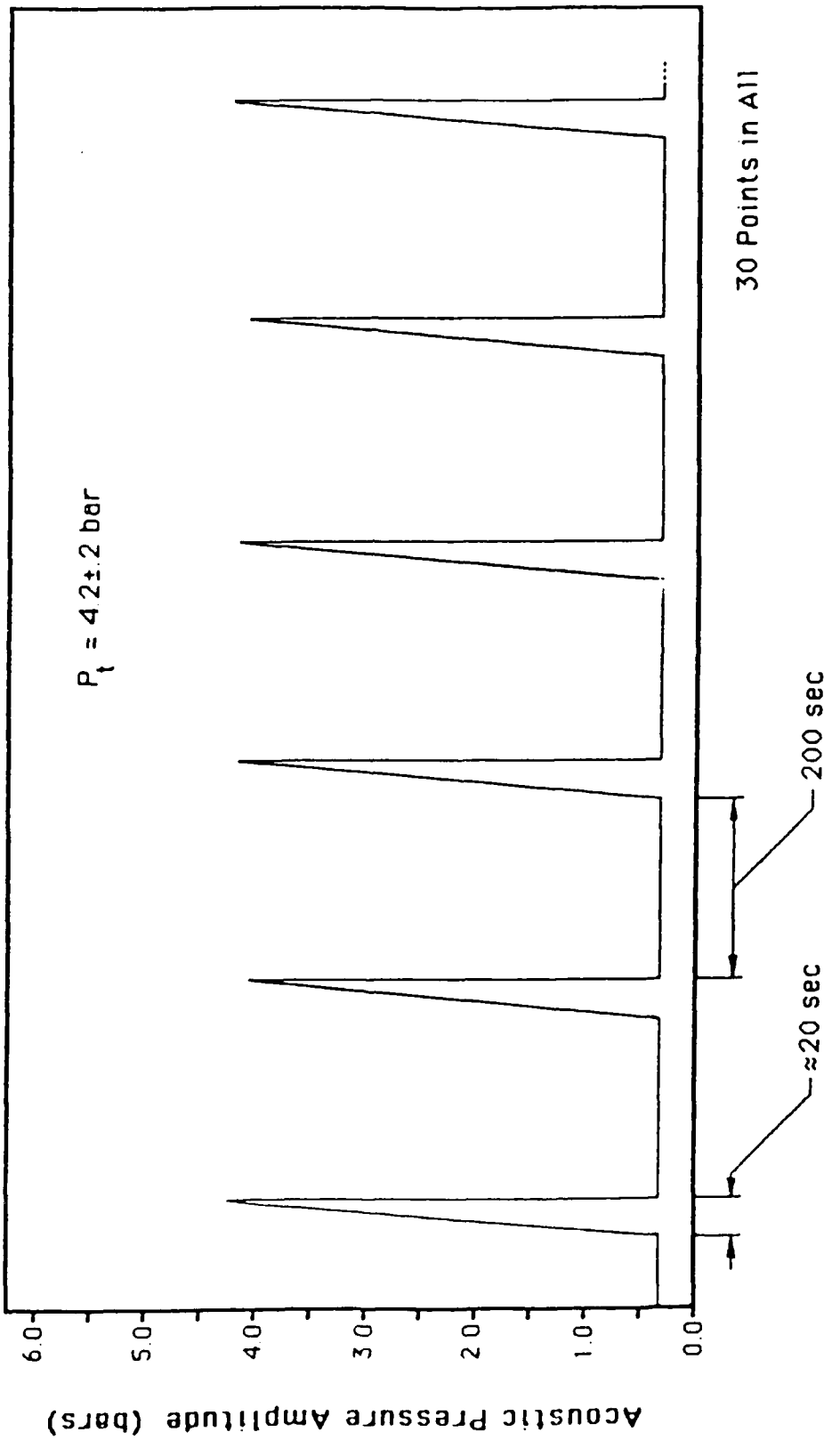
Acoustic Pressure Amplitude (bars)
6.0
5.0
4.0
3.0
2.0
1.0
0.0
P_t = 4.2±.2 bar
30 Points in All
200 sec
≈20 sec

Figure 1-29

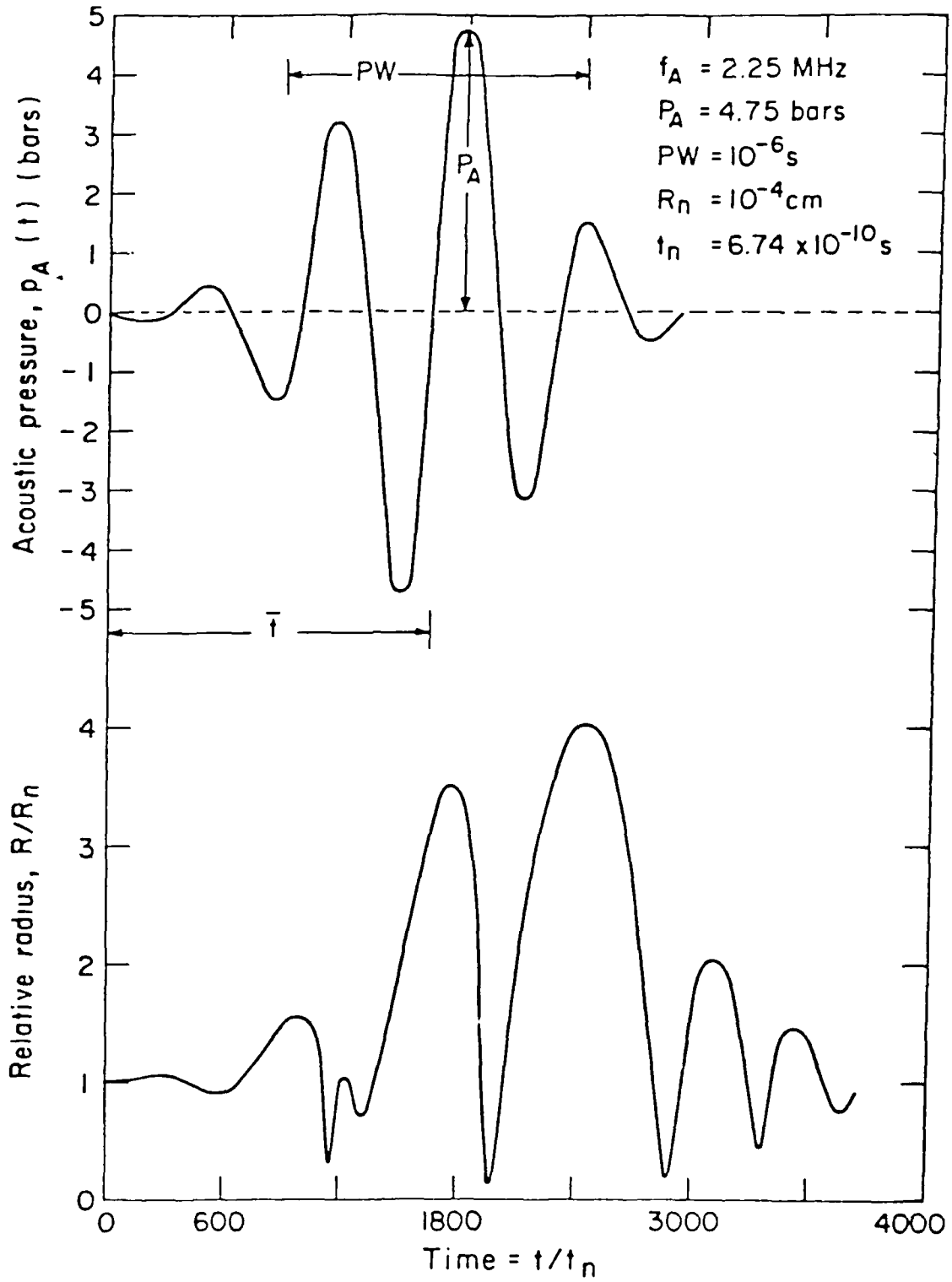
PW
P_A
f_A = 2.25 MHz
P_A = 4.75 bars
PW = 10^{-6}s
R_n = 10^{-4}cm
t_n = 6.74 x 10^{-10}s
$\bar{t}$
Acoustic pressure, p_A (t) (bars)
Relative radius, R/R_n
Time = t/t_n
5
4
3
2
1
0
-1
-2
-3
-4
-5
0
600
1800
3000
4000

Fgiure 1-30

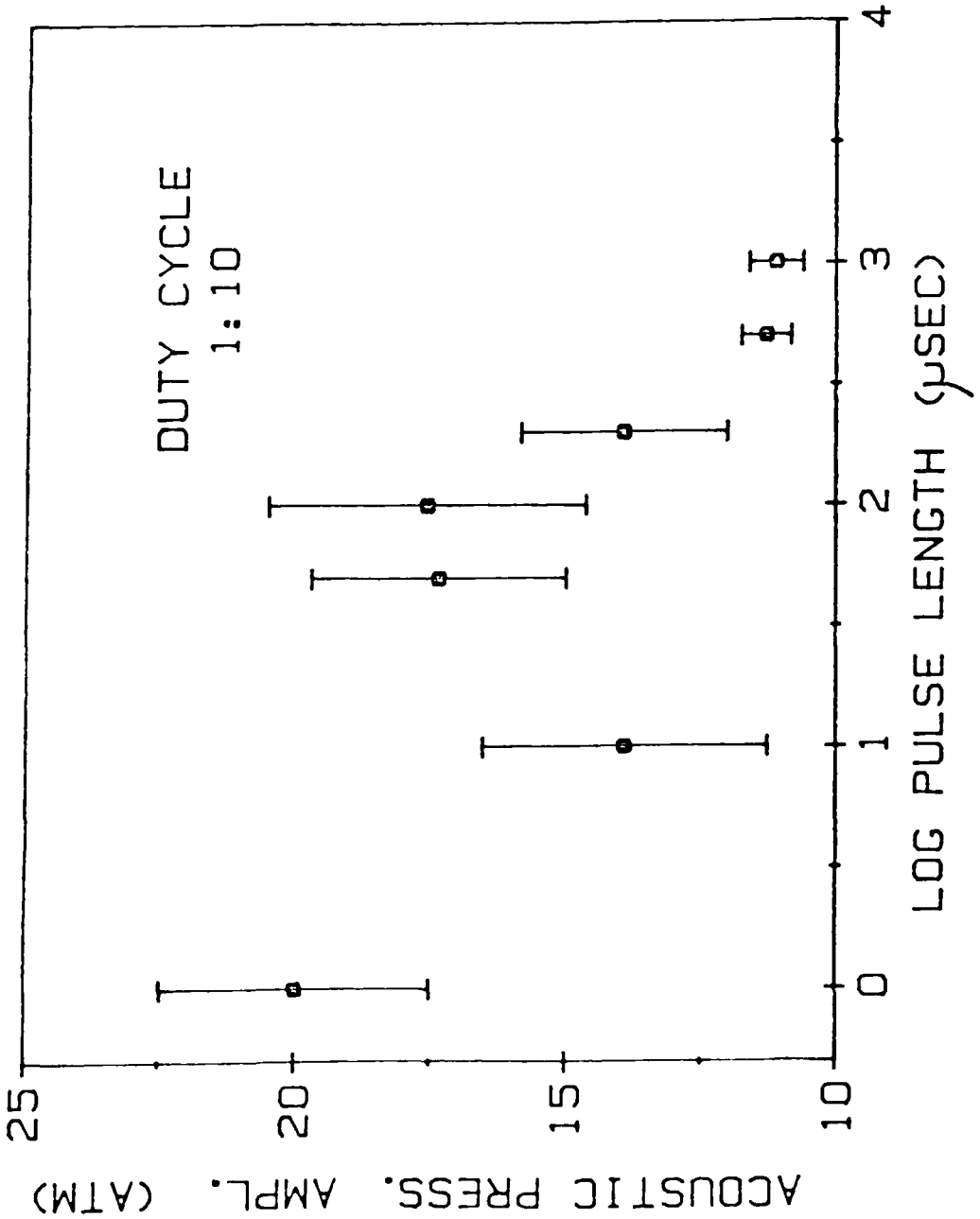
DUTY CYCLE
1:10
ACOUSTIC PRESS. AMPL. (ATM)
25
20
15
10
0
1
2
3
4
LOG PULSE LENGTH (μSEC)

Figure 1-31

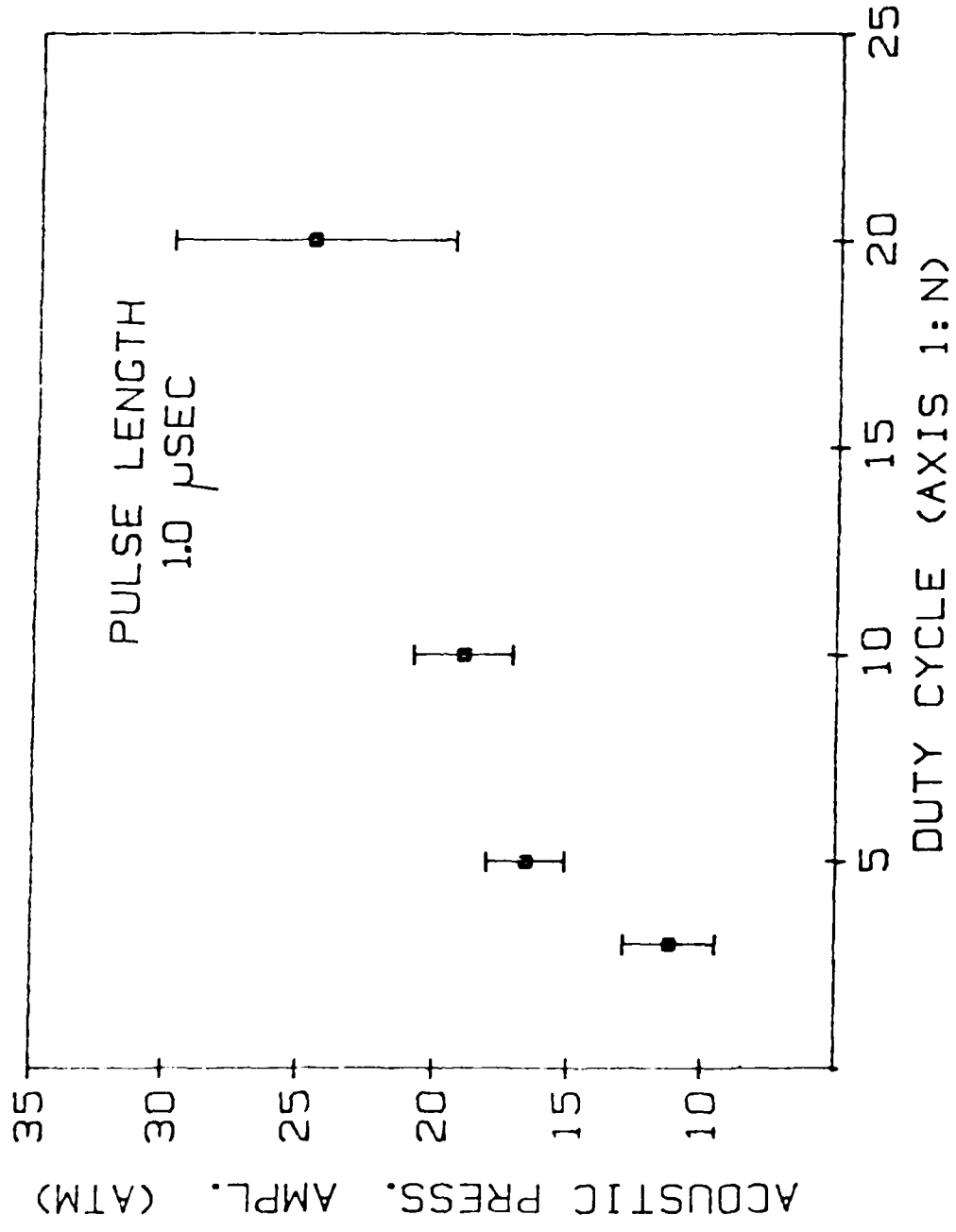
PULSE LENGTH
1.0 μSEC
ACOUSTIC PRESS. AMPL. (ATM)
35
30
25
20
15
10
5
10
15
20
25
DUTY CYCLE (AXIS 1:N)

END

FILMED

8-85

DTIC